2017

RF Superconductivity

Jean R. Delayen
Old Dominion University, jdelayen@odu.edu

Original Publication Citation
Delayen, J.R. (2017) *RF Superconductivity* [Tutorial presentation]. NAPAC2016: Proceedings of the North American Particle Accelerator Conference, Chicago, Illinois. https://accelconf.web.cern.ch/napac2016/talks/frb1tu01_talk.pdf

RF SUPERCONDUCTIVITY

Jean Delayen

Center for Accelerator Science
Old Dominion University
and
Thomas Jefferson National Accelerator Facility

Outline

- Fundamentals of rf superconductivity
  - Underlying physics
  - New developments
- Superconducting cavities
  - Various shapes
  - How they are made
- Limitations
  - Why SRF cavities aren't behaving (yet) according to theory

Why SRF?

- Normal Conductors
  - Skin depth proportional to $\omega^{-1/2}$
  - Surface resistance proportional to $\omega^{1/2 \rightarrow 2/3}$
  - Surface resistance independent of temperature (at low T)
  - For Cu at 300K and 1 GHz, R_s=8.3 mΩ

- Superconductors
  - Penetration depth independent of ω
  - Surface resistance proportional to ω^2
  - Surface resistance strongly dependent of temperature
  - For Nb at 2 K and 1 GHz, $R_s \approx 7$ nΩ

However: do not forget Carnot

Why are SC and NC Accelerators Different?

$$\frac{P}{L} \propto \frac{1}{\frac{R}{Q} Q R_S} \frac{E^2 R_S}{\omega}$$

For normal conductors $R_S \propto \omega^{1/2}$

$$\frac{P}{L} \propto \omega^{-\frac{1}{2}}$$

$$\frac{P}{A} \propto \omega^{\frac{1}{2}}$$

For superconductors $R_S \propto \omega^2$

$$\frac{P}{L} \propto \omega$$

$$\frac{P}{A} \propto \omega^2$$

SUPERCONDUCTIVITY FUNDAMENTALS

Jean Delayen

Center for Accelerator Science
Old Dominion University
and
Thomas Jefferson National Accelerator Facility

Historical Overview

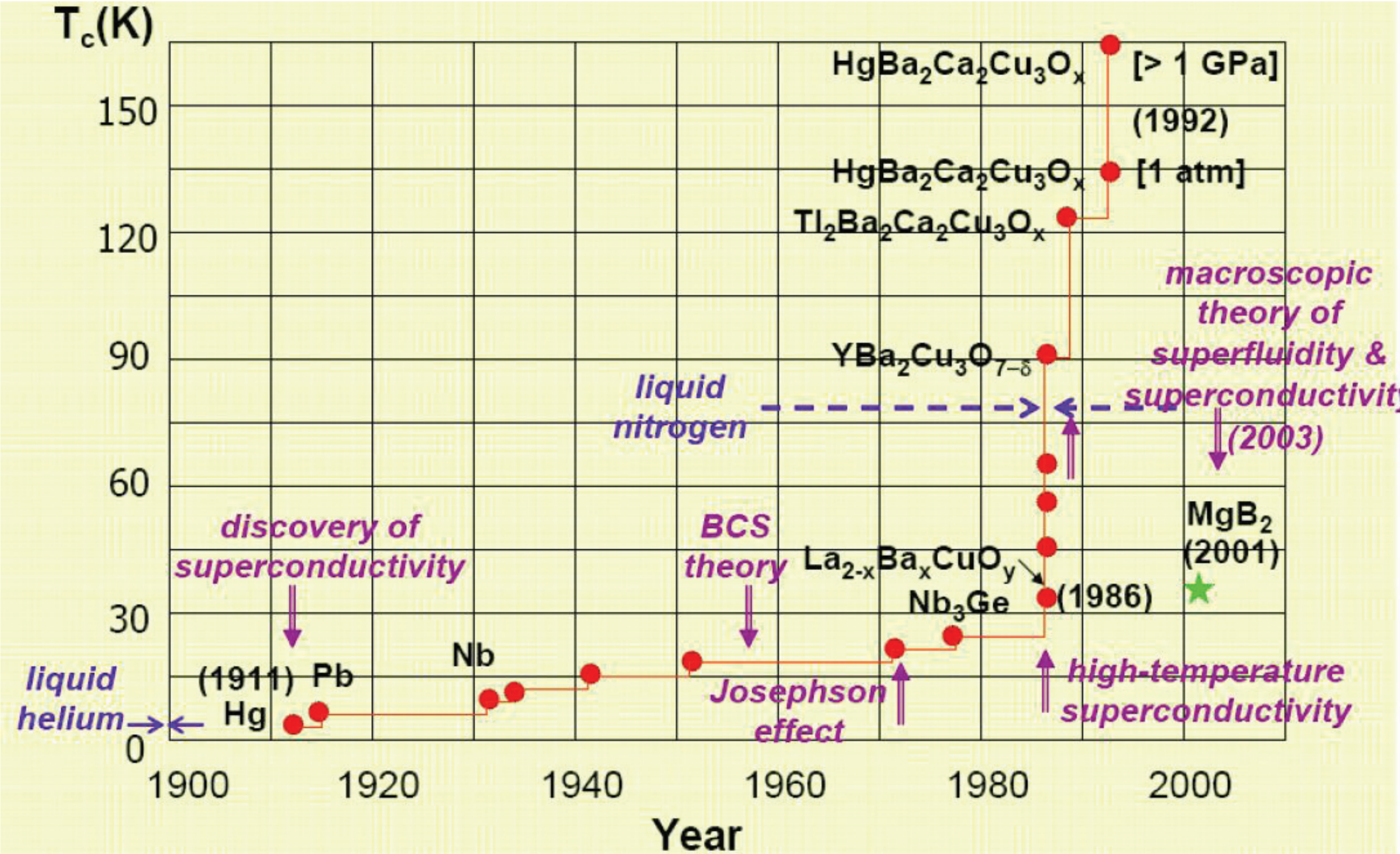

Perfect Conductivity

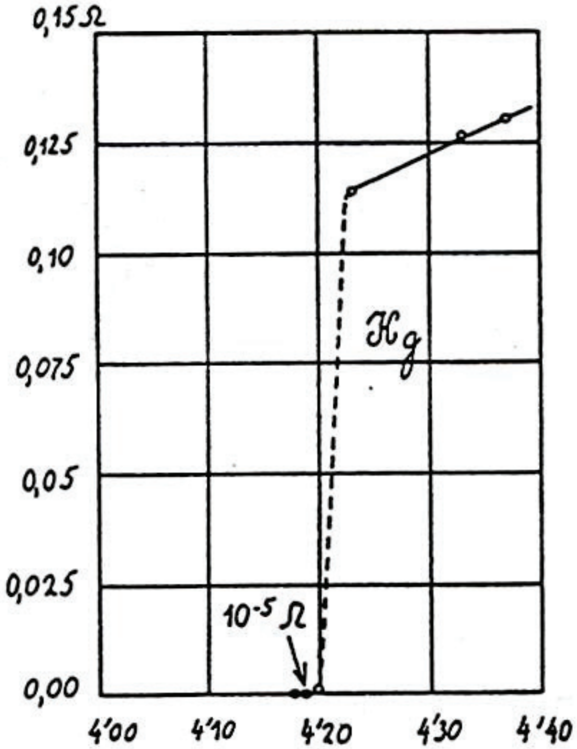

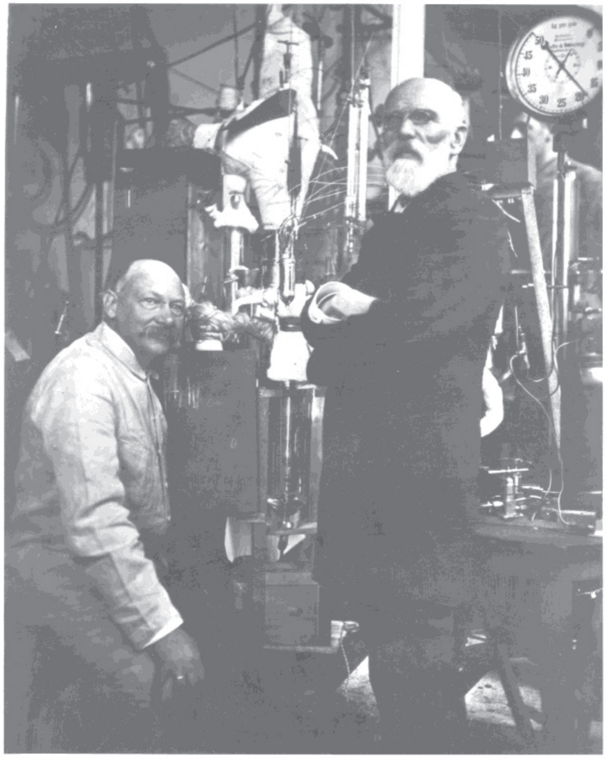

Kamerlingh Onnes and van der Waals in Leiden with the helium 'liquefactor' (1908)

Perfect Conductivity

Persistent current experiments on rings have measured

$$\frac{\sigma_s}{\sigma_n} > 10^{15}$$

Resistivity < 10^{-23} Ω.cm

Decay time > 10^{5} years

Perfect conductivity is not superconductivity

Superconductivity is a phase transition

A perfect conductor has an infinite relaxation time L/R

Perfect Diamagnetism (Meissner & Ochsenfeld 1933)

Perfect conductor

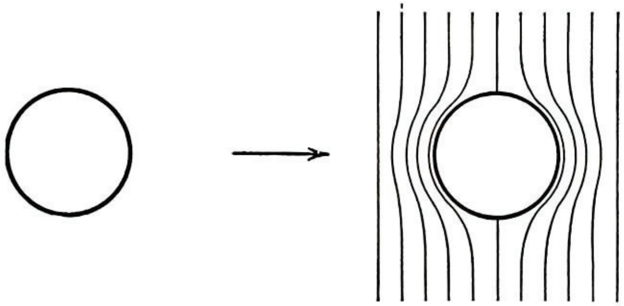

Case I. The specimen is first cooled below its transition temperature

and then brought into a magnetic field.

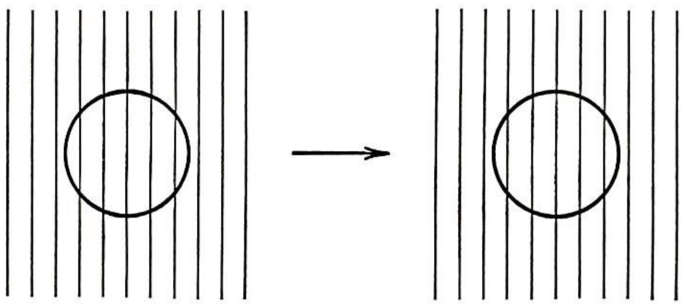

Case II. The specimen is brought into a magnetic field while it is in the normal state

and subsequently cooled below its transition temperature.

FIG. 3. The behavior expected for a transition into a state of *perfect conductivity*. The final state would depend on the *serial order* in which the specimen is brought into the same external conditions.

$$\frac{\partial B}{\partial t} = 0$$

Superconductor

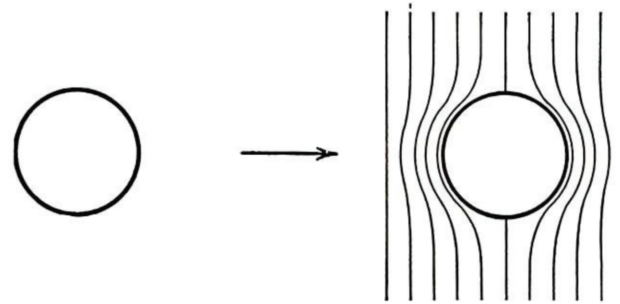

Case I. The specimen is first cooled below its transition temperature

and then brought into a magnetic field.

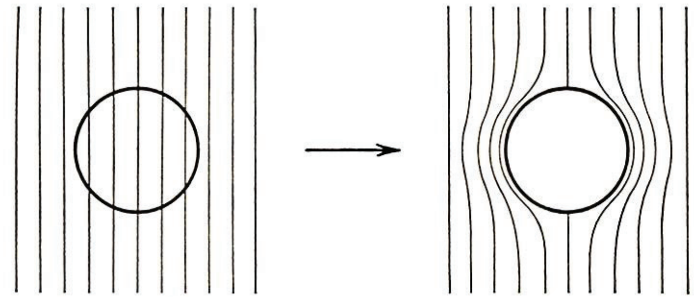

The magnetic field is applied while the specimen is in the normal state;

the field is pushed out when the specimen is cooled below its transition temperature.

FIG. 4. Case II of Fig. 3 according to Meissner. The *superconductor*, in contrast to the perfect conductor, has zero magnetic induction independently of the way in which the superconducting state has been reached.

$$B = 0$$

Critical Field (Type I)

Superconductivity is destroyed by the application of a magnetic field

$$H_c(T) \simeq H_c(0)\left[1-\left(\frac{T}{T_c}\right)^2\right]$$

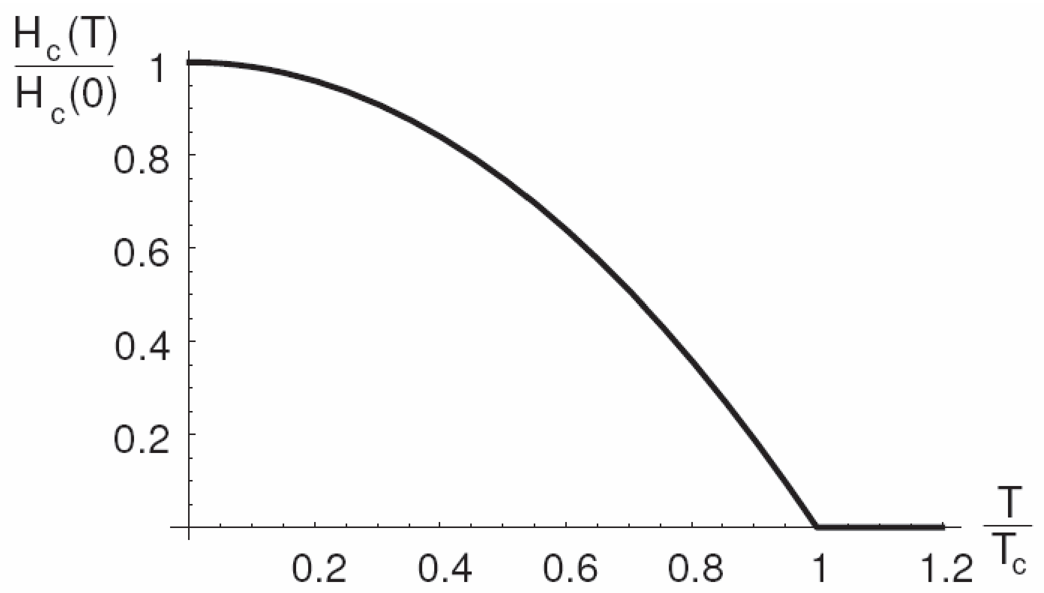

Type I or "soft" superconductors

Critical Field (Type II or "hard" superconductors)

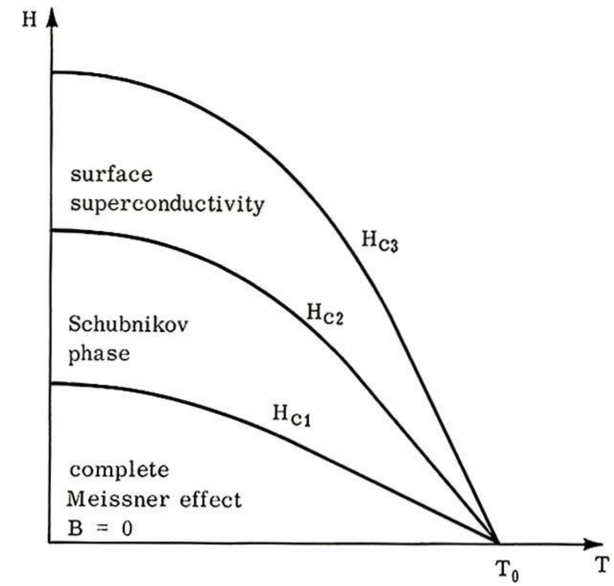

Figure 3-1
Phase diagram for a long cylinder of a Type II superconductor.

Expulsion of the magnetic field is complete up to H_{c1}, and partial up to H_{c2}

Between H_{c1} and H_{c2} the field penetrates in the form if quantized vortices or fluxoids

$$\phi_0 = \frac{\pi\hbar}{e}$$

Thermodynamic Properties

Entropy

Specific Heat

Energy

Free Energy

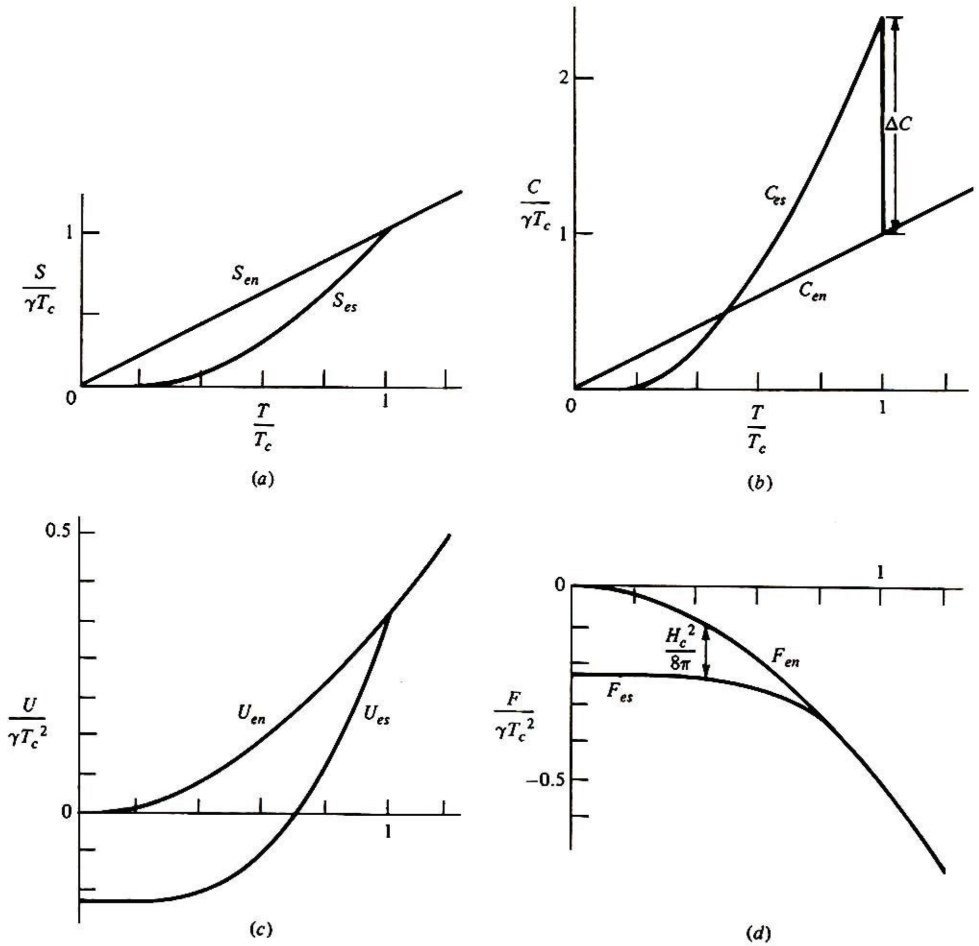

FIGURE 2-3
Comparison of thermodynamic quantities in superconducting and normal states. $U_{en}(0)$ is chosen as the zero of ordinates in (c) and (d). Because the transition is of second order, the quantities S, U, and F are continuous at T_c. Moreover, the slope of F_{es} joins continuously to that of F_{en} at T_c, since $\partial F/\partial T = -S$.

Thermodynamic Properties

When $T < T_c$ phase transition at $H = H_c(T)$ is of 1^{st} order $\Rightarrow$ latent heat

At $T = T_c$ transition is of 2^{nd} order $\Rightarrow$ no latent heat

jump in specific heat

$$C_{es}(T_c) \sim 3C_{en}(T_c)$$

$C_{en}(T) = \gamma T$ electronic specific heat

$C_{es}(T) \approx \alpha T^3$ reasonable fit to experimental data

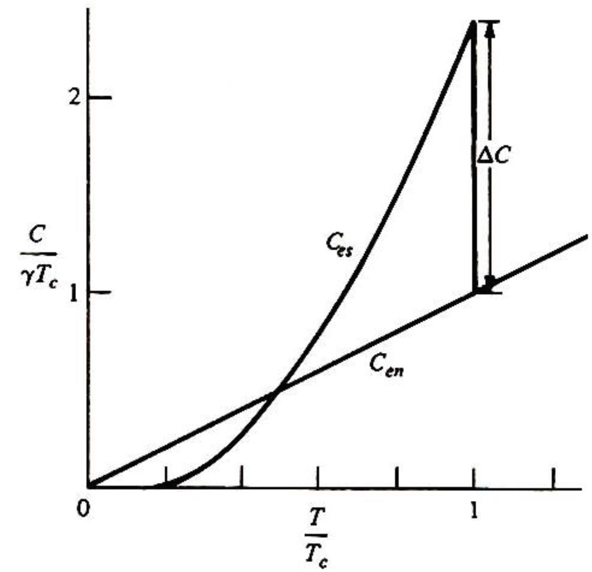

(b)

Isotope Effect (Maxwell 1950)

The critical temperature and the critical field at 0K are dependent on the mass of the isotope

$$T_c \sim H_c(0) \sim M^{-\alpha} \qquad \text{with } \alpha \simeq 0.5$$

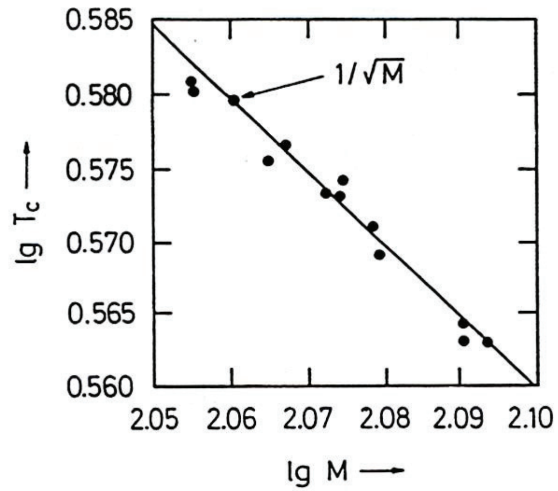

Figure 26: The critical temperature of various tin isotopes.

Energy Gap (1950s)

At very low temperature the specific heat exhibits an exponential behavior

$$c_s \propto e^{-bT_c/T} \qquad \text{with } b \simeq 1.5$$

Electromagnetic absorption shows a threshold

Tunneling between 2 superconductors separated by a thin oxide film shows the presence of a gap

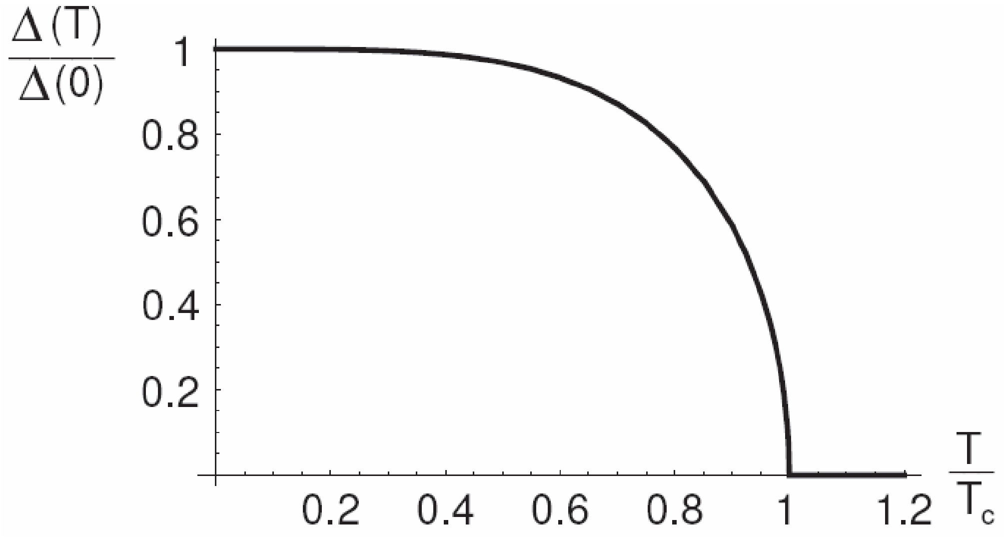

Two Fundamental Lengths

- London penetration depth λ
  - Distance over which magnetic fields decay in superconductors
- Pippard coherence length ξ
  - Distance over which the superconducting state decays

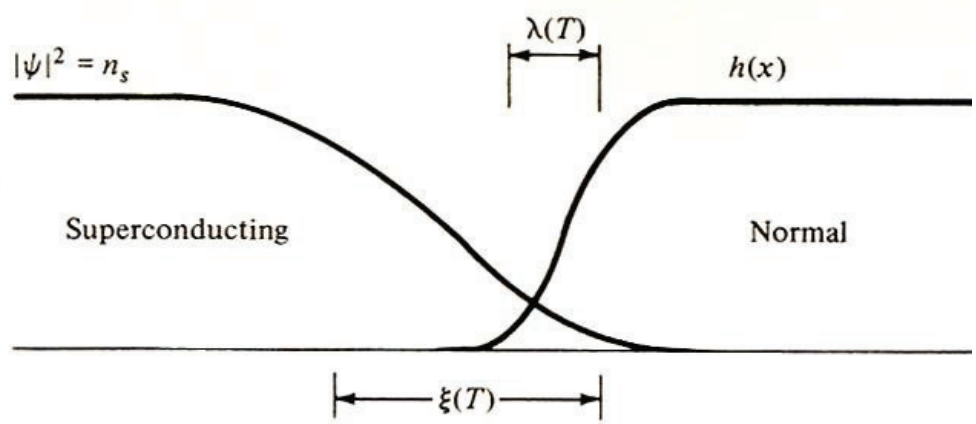

FIGURE 1-4
Interface between superconducting and normal domains in the intermediate sta

Two Types of Superconductors

- London superconductors (Type II)
  - $\lambda >> \xi$
  - Impure metals
  - Alloys
  - Local electrodynamics

- Pippard superconductors (Type I)
  - $\xi >> \lambda$
  - Pure metals
  - Nonlocal electrodynamics

Material Parameters for Some Superconductors

Superconductor	λ_L (0) (nm)	ξ_0 (nm)	κ	$2\Delta(0)/kT_c$	T_c(K)
Al	16	1500	0.011	3.40	1.18
In	25	400	0.062	3.50	3.3
Sn	28	300	0.093	3.55	3.7
Pb	28	110	0.255	4.10	7.2
Nb	32	39	0.82	3.5-3.85	8.95-9.2
Ta	35	93	0.38	3.55	4.46
Nb_3Sn	50	6	8.3	4.4	18
NbN	50	6	8.3	4.3	≤ 17
$Yba_2Cu_3o_x$	140	1.5	93	4.5	90

Phenomenological Models (1930s to 1950s)

Phenomenological model:
Purely descriptive
Everything behaves as though…..

A finite fraction of the electrons form some kind of condensate that behaves as a macroscopic system (similar to superfluidity)

At 0K, condensation is complete

At T_c the condensate disappears

Two Fluid Model – Gorter and Casimir

$T < T_c$ $\quad x =$ fraction of "normal" electrons

$(1-x)$: fraction of "condensed" electrons (zero entropy)

Assume: $\quad F(T) = x^{1/2} f_n(T) + (1-x) f_s(T)$ $\qquad$ free energy

Minimization of $F(T)$ gives $\boxed{x = \left(\frac{T}{T_C}\right)^4}$ $\qquad C_{es} = 3\gamma \frac{\mathrm{T}^3}{\mathrm{T}_\mathrm{C}^2}$

$$\boxed{\frac{H_c(T)}{H_c(0)} = 1 - \left(\frac{T}{T_C}\right)^2}$$

The Gorter-Casimir model is an "ad hoc" model (there is no physical basis for the assumed expression for the free energy) but provides a fairly accurate representation of experimental results

Model of F & H London (1935)

Proposed a 2-fluid model with a normal fluid and superfluid components

***n_s* : density of the superfluid component of velocity v_s**
***n_n* : density of the normal component of velocity v_n**

$$m\frac{\partial \vec{\upsilon}}{\partial t} = -e\vec{E}$$

superelectrons are accelerated by E

$$\overrightarrow{J_s} = -en_s\,\vec{\upsilon}$$

$$\frac{\partial \vec{J}_s}{\partial t} = \frac{n_s e^2}{m}\vec{E}$$

superelectrons

$$\vec{J}_n = \sigma_n \vec{E}$$

normal electrons

Model of F & H London (1935)

$$\frac{\partial \vec{J}_s}{\partial t} = \frac{n_s e^2}{m} \vec{E}$$

Maxwell: $$\vec{\nabla} \times \vec{E} = -\frac{\partial \vec{B}}{\partial t}$$

$$\Rightarrow \frac{\partial}{\partial t}\left(\frac{m}{n_s e^2} \vec{\nabla} \times \vec{J}_s + \vec{B} \right) = 0 \qquad \Rightarrow \frac{m}{n_s e^2} \vec{\nabla} \times \vec{J}_s + \vec{B} = \text{Constant}$$

F&H London postulated: $$\boxed{\frac{m}{n_s e^2} \vec{\nabla} \times \vec{J}_s + \vec{B} = 0}$$

Model of F & H London (1935)

combine with $\vec{\nabla} \times \vec{B} = \mu_0 \vec{J}_s$

$$\boxed{\nabla^2 \vec{B} - \frac{\mu_0 n_s e^2}{m} \vec{B} = 0}$$

$$B(x) = B_o \exp\left[-x / \lambda_L\right]$$

$$\lambda_L = \left[\frac{m}{\mu_0 n_s e^2}\right]^{\frac{1}{2}}$$

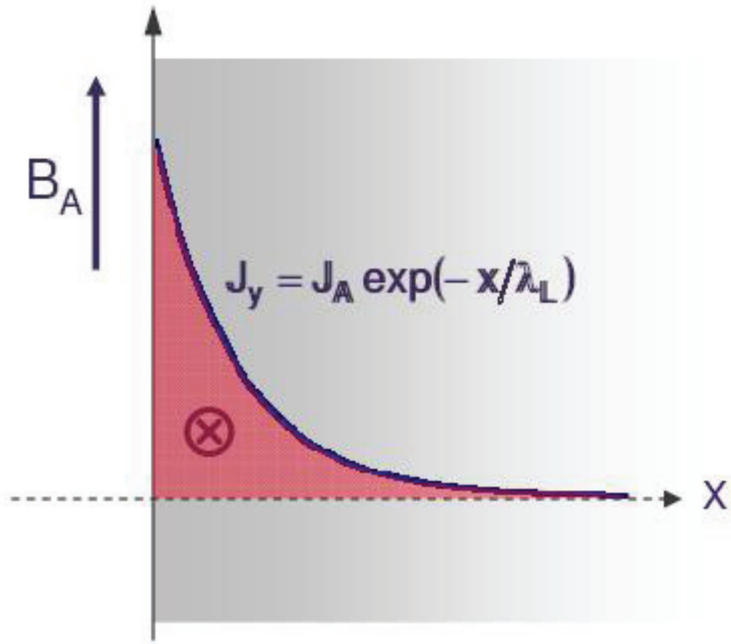

The magnetic field, and the current, decay exponentially over a distance λ (a few 10s of nm)

Model of F & H London (1935)

$$\lambda_L = \left[\frac{m}{\mu_0 n_s e^2}\right]^{\frac{1}{2}}$$

From Gorter and Casimir two-fluid model

$$n_s \propto \left[1 - \left(\frac{T}{T_C}\right)^4\right]$$

$$\lambda_L(T) = \lambda_L(0)\frac{1}{\left[1 - \left(\frac{T}{T_C}\right)^4\right]^{\frac{1}{2}}}$$

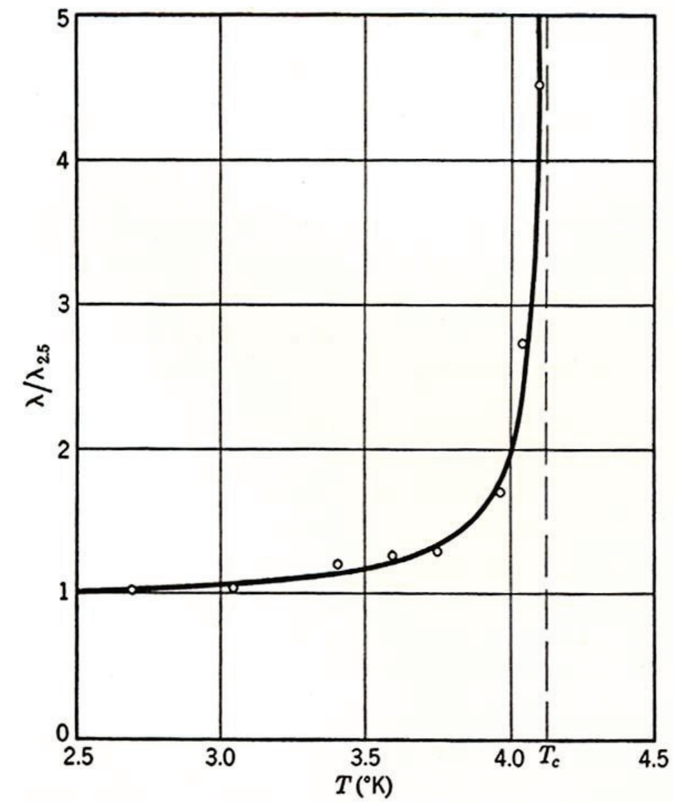

FIG. 21. Penetration depth as a function of temperature. (After Shoenberg, *Nature*, **43**, 433, 1939.)

Model of F & H London (1935)

London Equation: $\lambda^2 \nabla \times \vec{J}_s = -\frac{\vec{B}}{\mu_0} = -\vec{H}$

$$\nabla \times \vec{A} = \vec{H}$$

choose $\nabla \bullet \vec{A} = 0,$ $A_n = 0$ on sample surface (London gauge)

$$\boxed{\vec{J}_s = -\frac{1}{\lambda^2}\vec{A}}$$

Note: Local relationship between $\vec{J}_s$ and $\vec{A}$

Penetration Depth in Thin Films

Very thin films

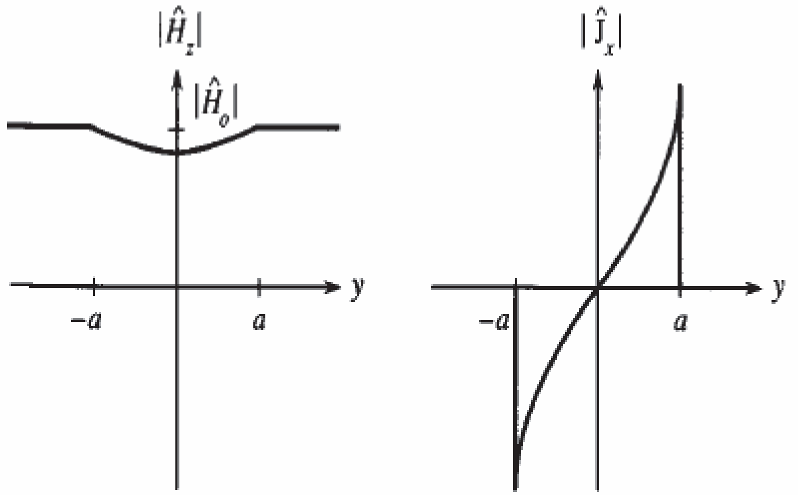

Very thick films

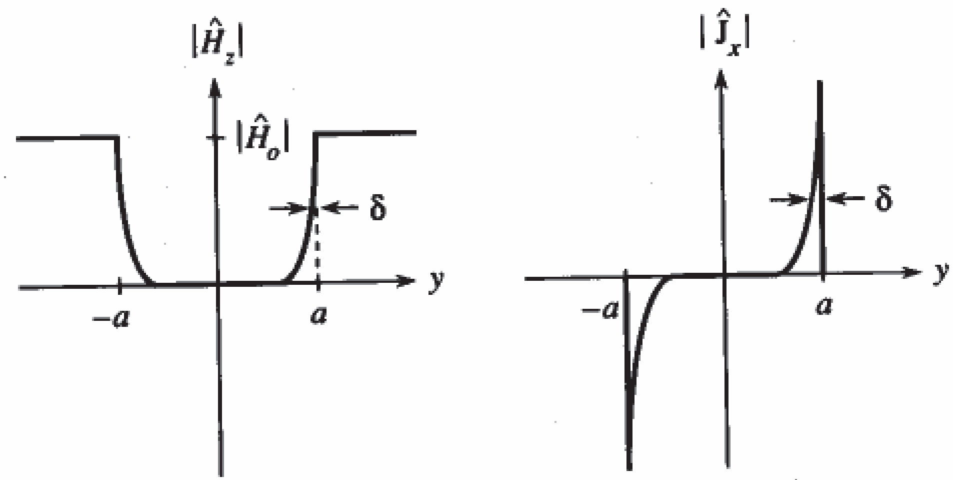

Pippard's Extension of London's Model

Observations:

-Penetration depth increased with reduced mean free path

- H_c and T_c did not change

-Need for a positive surface energy over 10^{-4} cm to explain existence of normal and superconducting phase in intermediate state

Non-local modification of London equation

Local: $$\vec{J} = -\frac{1}{c\lambda}\vec{A}$$

Non local: $$\vec{J}(r) = -\frac{3\sigma}{4\pi\xi_0\lambda c}\int \frac{\vec{R}\left[\vec{R}\bullet\vec{A}(r')\right]e^{-\frac{R}{\xi}}}{R^4}d\upsilon$$

$$\frac{1}{\xi} = \frac{1}{\xi_0} + \frac{1}{\ell}$$

London Electrodynamics

Linear London equations

$$\frac{\partial \vec{J}_s}{\partial t} = -\frac{\vec{E}}{\lambda^2 \mu_0} \qquad \nabla^2 \vec{H} - \frac{1}{\lambda^2}\vec{H} = 0$$

together with Maxwell equations

$$\nabla \times \vec{H} = \vec{J}_s \qquad \nabla \times \vec{E} = -\mu_0 \frac{\partial \vec{H}}{\partial t}$$

describe the electrodynamics of superconductors at all T if:

- The superfluid density n_s is spatially uniform
- The current density J_s is small

Ginzburg-Landau Theory

- Many important phenomena in superconductivity occur because n_s is not uniform
  - Interfaces between normal and superconductors
  - Trapped flux
  - Intermediate state

- London model does not provide an explanation for the surface energy (which can be positive or negative)

- GL is a generalization of the London model but it still retain the local approximation of the electrodynamics

Ginzburg-Landau Theory

- Ginzburg-Landau theory is a particular case of Landau's theory of second order phase transition
- Formulated in 1950, before BCS
- Masterpiece of physical intuition
- Grounded in thermodynamics
- Even after BCS it still is very fruitful in analyzing the behavior of superconductors and is still one of the most widely used theory of superconductivity

Ginzburg-Landau Theory

- Theory of second order phase transition is based on an order parameter which is zero above the transition temperature and non-zero below
- For superconductors, GL use a complex order parameter $\Psi(r)$ such that $|\Psi(r)|^2$ represents the density of superelectrons
- The Ginzburg-Landau theory is strictly valid close to T_c but useful and applied over a wide range of temperature

Ginzburg-Landau Equation for Free Energy

- Assume that Ψ(r) is small and varies slowly in space

- Expand the free energy in powers of Ψ(r) and its derivative

$$f = f_{n0} + \alpha|\psi|^2 + \frac{\beta}{2}|\psi|^4 + \frac{1}{2m^*}\left|\left(\frac{\hbar}{i}\nabla - \frac{e^*}{c}\mathbf{A}\right)\psi\right|^2 + \frac{h^2}{8\pi}$$

Field-Free Uniform Case

Identify the order parameter with the density of superelectrons

$$n_s = |\Psi|^2 \sim \frac{1}{\lambda_L^2(T)} \Rightarrow \frac{\lambda_L^2(0)}{\lambda_L^2(T)} = \frac{|\Psi(T)|^2}{|\Psi(0)|^2} = -\frac{1}{n}\frac{\alpha(T)}{\beta}$$

The parameters α and β are related to measurable quantities

$$n\alpha(T) = -\frac{H_c^2(T)}{4\pi}\frac{\lambda_L^2(T)}{\lambda_L^2(0)} \quad \text{and} \quad n^2\beta = \frac{H_c^2(T)}{4\pi}\frac{\lambda_L^4(T)}{\lambda_L^4(0)}$$

Field-Free Nonuniform Case

Equation of motion in the absence of electromagnetic field

$$-\frac{1}{2m^*}\nabla^2\psi + \alpha(T)\psi + \beta|\psi|^2\psi = 0$$

Look at solutions close to the constant one

$$\psi = \psi_\infty + \delta \quad \text{where} \quad |\psi_\infty|^2 = -\frac{\alpha(T)}{\beta}$$

To first order: $$\frac{1}{4m^*|\alpha(T)|}\nabla^2\delta - \delta = 0$$

Which leads to $$\delta \approx e^{-\sqrt{2}\,r/\xi(T)}$$

Field-Free Nonuniform Case

$$\delta \approx e^{-\sqrt{2}r/\xi(T)}$$ where $$\xi(T) = \frac{1}{\sqrt{2m^*|\alpha(T)|}} = \sqrt{\frac{2\pi n}{m^* H_c^2(T)}} \frac{\lambda_L(0)}{\lambda_L(T)}$$

is the Ginzburg-Landau coherence length.

It is different from, but related to, the Pippard coherence length. $$\xi(T) \simeq \frac{\xi_0}{\left(1-t^2\right)^{1/2}}$$

GL parameter: $$\kappa(T) = \frac{\lambda_L(T)}{\xi(T)}$$

Both $\lambda_L(T)$ and $\xi(T)$ diverge as $T \to T_c$ but their ratio remains finite

$\kappa(T)$ is almost constant over the whole temperature range

2 Fundamental Lengths

London penetration depth: length over which magnetic field decay

$$\lambda_L(T) = \left(\frac{m^*\beta}{2e^2\alpha'}\right)^{1/2}\sqrt{\frac{T_c}{T_c - T}}$$

Coherence length: scale of spatial variation of the order parameter (superconducting electron density)

$$\xi(T) = \left(\frac{\hbar^2}{4m^*\alpha'}\right)^{1/2}\sqrt{\frac{T_c}{T_c - T}}$$

The critical field is directly related to those 2 parameters

$$H_c(T) = \frac{\phi_0}{2\sqrt{2}\,\xi(T)\,\lambda_L(T)}$$

Surface Energy

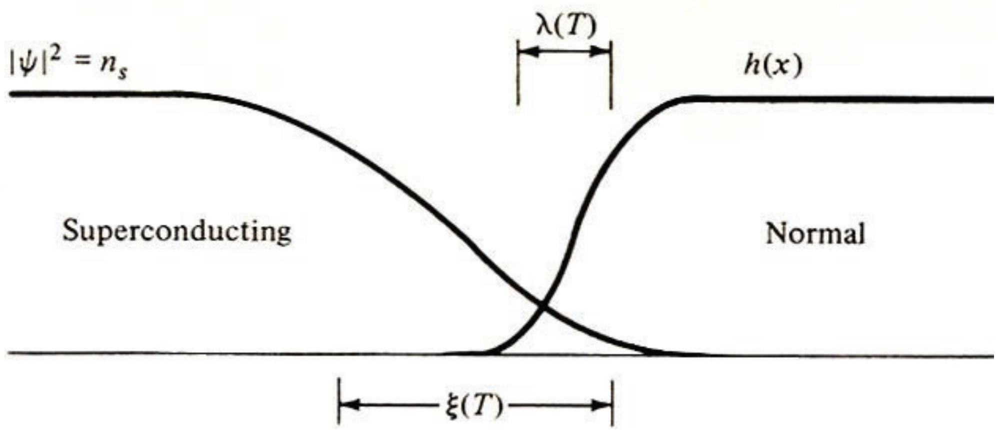

$$\sigma \simeq \frac{1}{8\pi}\left[H_c^2\xi - H^2\lambda\right]$$

$\dfrac{H^2\lambda}{8\pi}$: Energy that can be gained by letting the fields penetrate

$\dfrac{H_c^2\xi}{8\pi}$: Energy lost by "damaging" superconductor

Surface Energy $\sigma \simeq \frac{1}{8\pi}\left[H_c^2\xi - H^2\lambda\right]$

Interface is stable if σ>0

If $\xi >> \lambda$ σ>0

Superconducting up to H_c where superconductivity is destroyed globally

If λ >>ξ σ<0 for $H^2 > H_c^2 \frac{\xi}{\lambda}$

Advantageous to create small areas of normal state with large area to volume ratio

$\rightarrow$ quantized fluxoids

More exact calculation (from Ginzburg-Landau):

$\kappa = \frac{\lambda}{\xi} < \frac{1}{\sqrt{2}}$: Type I

$\kappa = \frac{\lambda}{\xi} > \frac{1}{\sqrt{2}}$: Type II

Critical Fields

Even though it is more energetically favorable for a type I superconductor to revert to the normal state at H_c, the surface energy is still positive up to a superheating field $H_{sh}>H_c$ → metastable superheating region in which the material may remain superconducting for short times.

Type I $\quad H_c \quad$ Thermodynamic critical field

$$H_{sh} \simeq \frac{H_c}{\sqrt{\kappa}}$$ Superheating critical field

Field at which surface energy is

Type II $\quad H_c \quad$ Thermodynamic critical field

$$H_{c2} = \sqrt{2}\ \kappa\ H_c$$

$$H_{c1} \simeq \frac{H_c^2}{H_{c2}}$$

$$\simeq \frac{1}{2\kappa}(\ln\kappa + .008)H_c \qquad (\text{for } \kappa \gg 1)$$

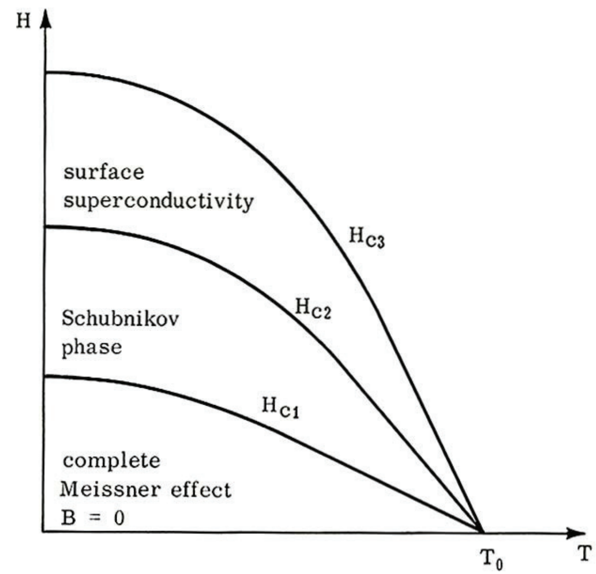

Figure 3-1
Phase diagram for a long cylinder of a Type II superconductor.

Superheating Field

Ginsburg-Landau:

$$H_{sh} \sim \frac{0.9H_c}{\sqrt{\kappa}} \quad \text{for } \kappa \ll 1$$

$$\sim 1.2\ H_c \quad \text{for } \kappa \sim 1$$

$$\sim 0.75\ H_c \quad \text{for } \kappa \gg 1$$

The exact nature of the rf critical field of superconductors is still an open question

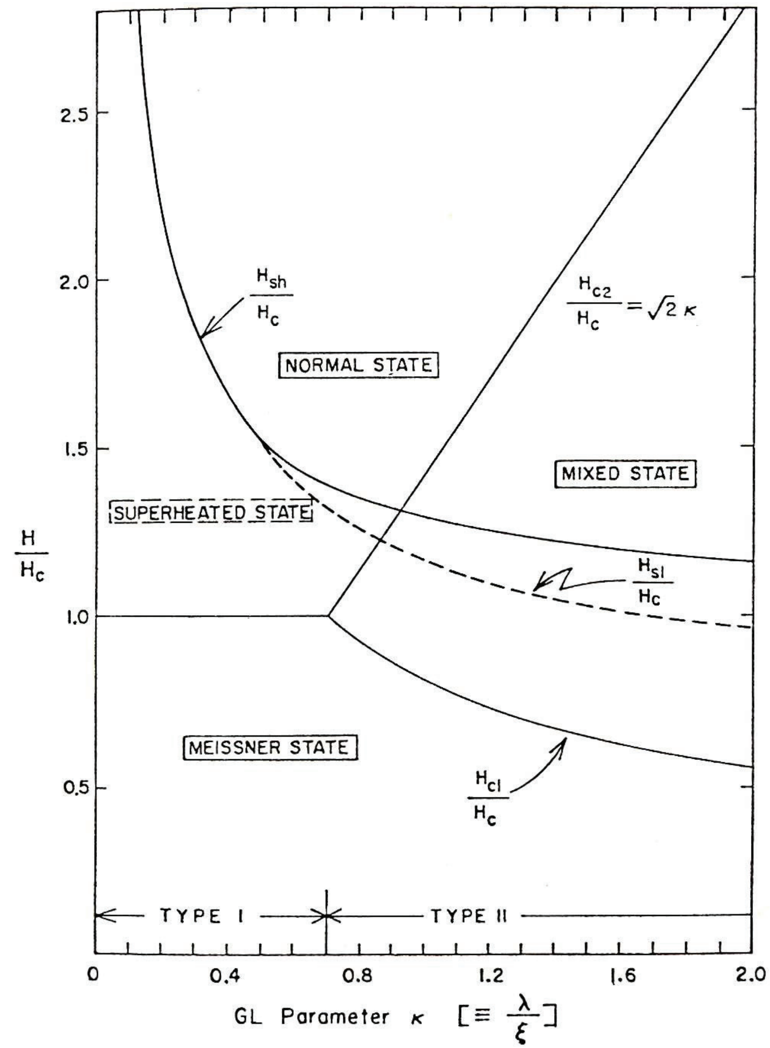

Fig. 13: Phase diagram of superconductors[42] in the transition regime of type I and II. The normalized critical fields are shown as a function of κ.

Material Parameters for Some Superconductors

Superconductor	λ_L (0) (nm)	ξ_0 (nm)	κ	$2\Delta(0)/kT_c$	T_c(K)
Al	16	1500	0.011	3.40	1.18
In	25	400	0.062	3.50	3.3
Sn	28	300	0.093	3.55	3.7
Pb	28	110	0.255	4.10	7.2
Nb	32	39	0.82	3.5-3.85	8.95-9.2
Ta	35	93	0.38	3.55	4.46
Nb_3Sn	50	6	8.3	4.4	18
NbN	50	6	8.3	4.3	≤ 17
$Yba_2Cu_3o_X$	140	1.5	93	4.5	90

BCS

- What needed to be explained and what were the clues?
  - Energy gap (exponential dependence of specific heat)
  - Isotope effect (the lattice is involved)
  - Meissner effect

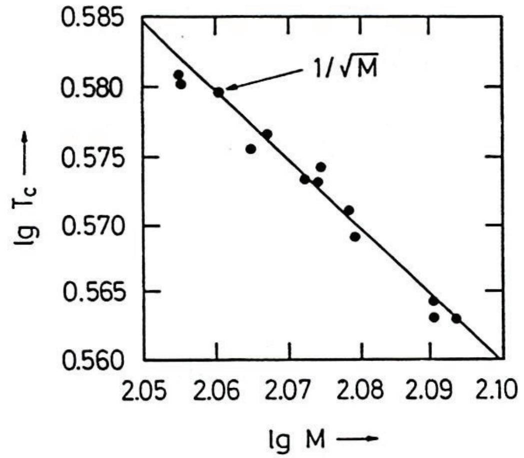

Figure 26: The critical temperature of various tin isotopes.

Cooper Pairs

Assumption: Phonon-mediated attraction between electron of equal and opposite momenta located within $\hbar\omega_D$ of Fermi surface

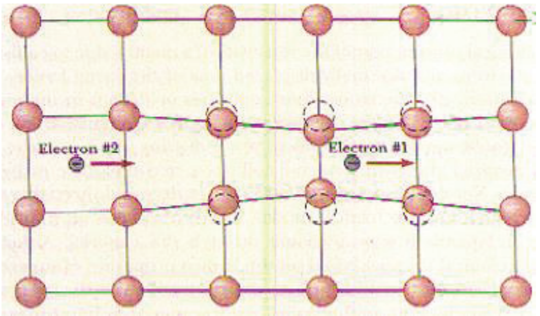

Moving electron distorts lattice and leaves behind a trail of positive charge that attracts another electron moving in opposite direction

Fermi ground state is unstable

Electron pairs can form bound states of lower energy

Bose condensation of overlapping Cooper pairs into a coherent Superconducting state

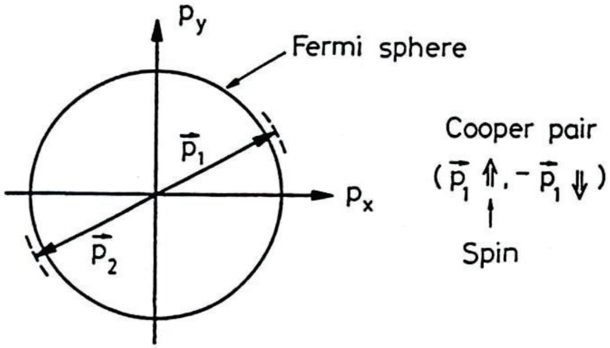

Figure 20: A pair of electrons of opposite momenta added to the full Fermi sphere.

BCS

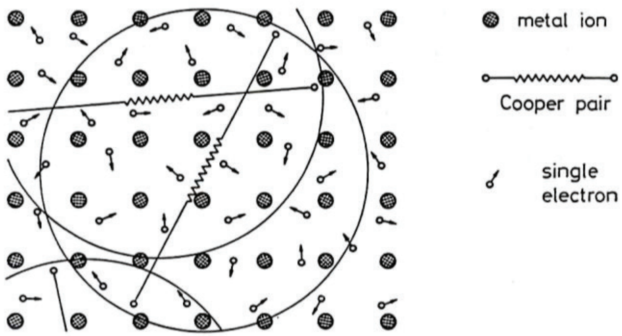

Figure 22: Cooper pairs and single electrons in the crystal lattice of a superconductor. (After Essmann and Träuble [12]).

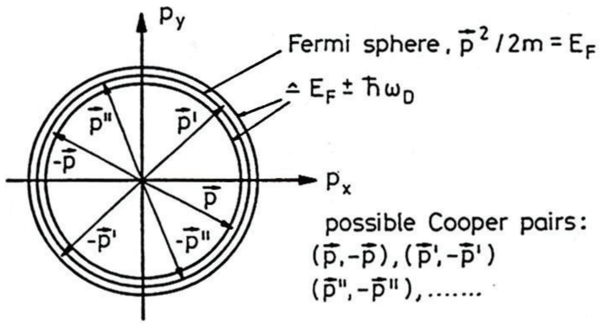

Figure 23: Various Cooper pairs $(\vec{p}, -\vec{p})$, $(\vec{p}', -\vec{p}')$, $(\vec{p}'', -\vec{p}'')$, ... in momentum space.

The size of the Cooper pairs is much larger than their spacing

They form a coherent state

BCS

- The BCS model is an extremely simplified model of reality
  - The Coulomb interaction between single electrons is ignored
  - Only the term representing the scattering of pairs is retained
  - The interaction term is assumed to be constant over a thin layer at the Fermi surface and 0 everywhere else
  - The Fermi surface is assumed to be spherical

- Nevertheless, the BCS results (which include only a very few adjustable parameters) are amazingly close to the real world

BCS

Critical temperature

$$kT_c = 1.14\,\hbar\omega_D \quad \exp\left[-\frac{1}{VN(E_F)}\right]$$

$$\Delta(0) = 1.76\,kT_c$$

element	Sn	In	Tl	Ta	Nb	Hg	Pb
$\Delta(0)/k_B T_c$	1.75	1.8	1.8	1.75	1.75	2.3	2.15

Coherence length (the size of the Cooper pairs)

$$\xi_0 = .18\frac{\hbar\upsilon_F}{kT_c}$$

BCS Energy Gap

At finite temperature:

Implicit equation for the temperature dependence of the gap:

$$\frac{1}{V\rho(0)} = \int_0^{\hbar\omega_D} \frac{\tanh\left[(\varepsilon^2+\Delta^2)^{1/2}/2kT\right]}{(\varepsilon^2+\Delta^2)^{1/2}}\,d\varepsilon$$

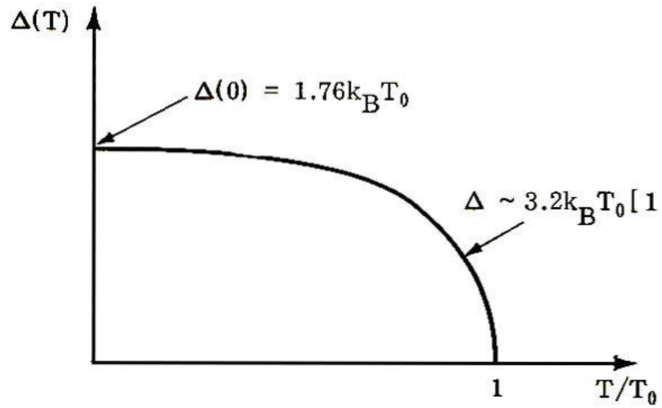

Figure 4-4
Variation of the order parameter Δ with temperature in the BCS approximation.

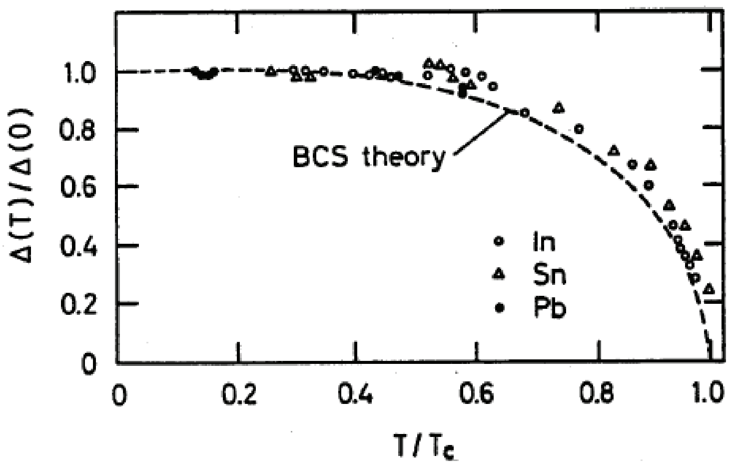

BCS Specific Heat

Specific heat

$$C_{es} \simeq \quad \exp\left(-\frac{\Delta}{kT}\right) \quad \text{for} \quad T < \frac{T_c}{10}$$

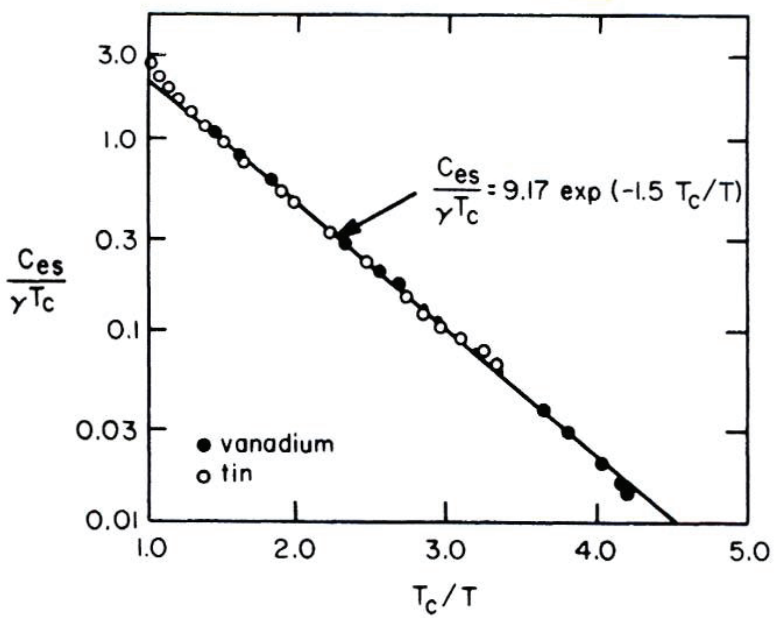

Fig. 22. Reduced electronic specific heat in superconducting vanadium and tin. [From Biondi et al., (*150*).]

Electrodynamics and Surface Impedance in BCS Model

$$H_0\phi + H_{ex}\ \phi = i\hbar\frac{\partial\phi}{\partial t}$$

$$H_{ex} = \frac{e}{mc}\sum A(r_i,t)\,p_i$$

H_{ex} is treated as a small perturbation

$$H_{rf} << H_c$$

There is, at present, no model for superconducting surface resistance at high rf field

$$J \propto \int \frac{R[R\cdot A]I(\omega,R,T)e^{-\frac{R}{l}}}{R^4}dr$$ similar to Pippard's model

$$J(k) = -\frac{c}{4\pi}K(k)A(k)$$

$K(0) \neq 0:$ Meissner effect

Penetration Depth

$$\lambda = \frac{2}{\pi}\int \frac{dk}{K(k)+k^2}\,dk \qquad \text{(specular)}$$

Represented accurately by $\lambda \sim \dfrac{1}{\sqrt{1-\left(\dfrac{T_c}{T}\right)^4}}$ near T_c

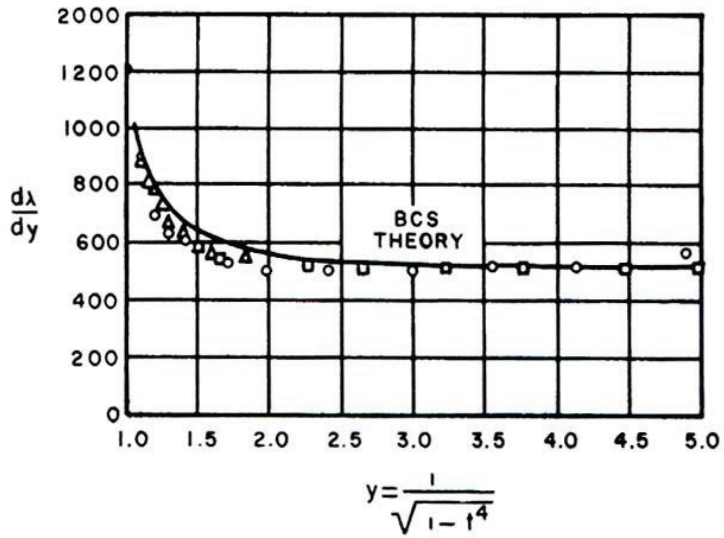

Fig. 30. Temperature dependence of $d\lambda/dy$ for tin obtained by Schawlow and Devlin (*207*) compared with the theoretical curve obtained from the BCS theory.

Surface Resistance of Superconductors

Superconductors are free of power dissipation in static fields.

In microwave fields, the time-dependent magnetic field in the penetration depth will generate an electric field.

$$\vec{\nabla} \times \vec{E} = -\frac{\partial \vec{B}}{\partial t}$$

The electric field will induce oscillations in the normal electrons, which will lead to power dissipation

Surface Impedance in the Two-Fluid Model

$$R_s \simeq \frac{1}{\lambda_L}\frac{\sigma_n}{\sigma_s^2}$$

$$\sigma_n = \frac{n_n e^2 l}{m_e v_F} \propto l \; \exp\left[-\frac{\Delta(T)}{kT}\right] \qquad \sigma_s = \frac{1}{\mu_0 \lambda_L^2 \omega}$$

$$\boxed{R_s \propto \lambda_L^3 \; \omega^2 \; l \exp\left[-\frac{\Delta(T)}{kT}\right]}$$

This assumes that the mean free path is much larger than the coherence length

For niobium we need to replace the London penetration depth with

$$\Lambda = \lambda_L \sqrt{1 + \xi / l}$$

As a result, the surface resistance shows a minimum when $\xi \approx l$

Surface Resistance of Niobium

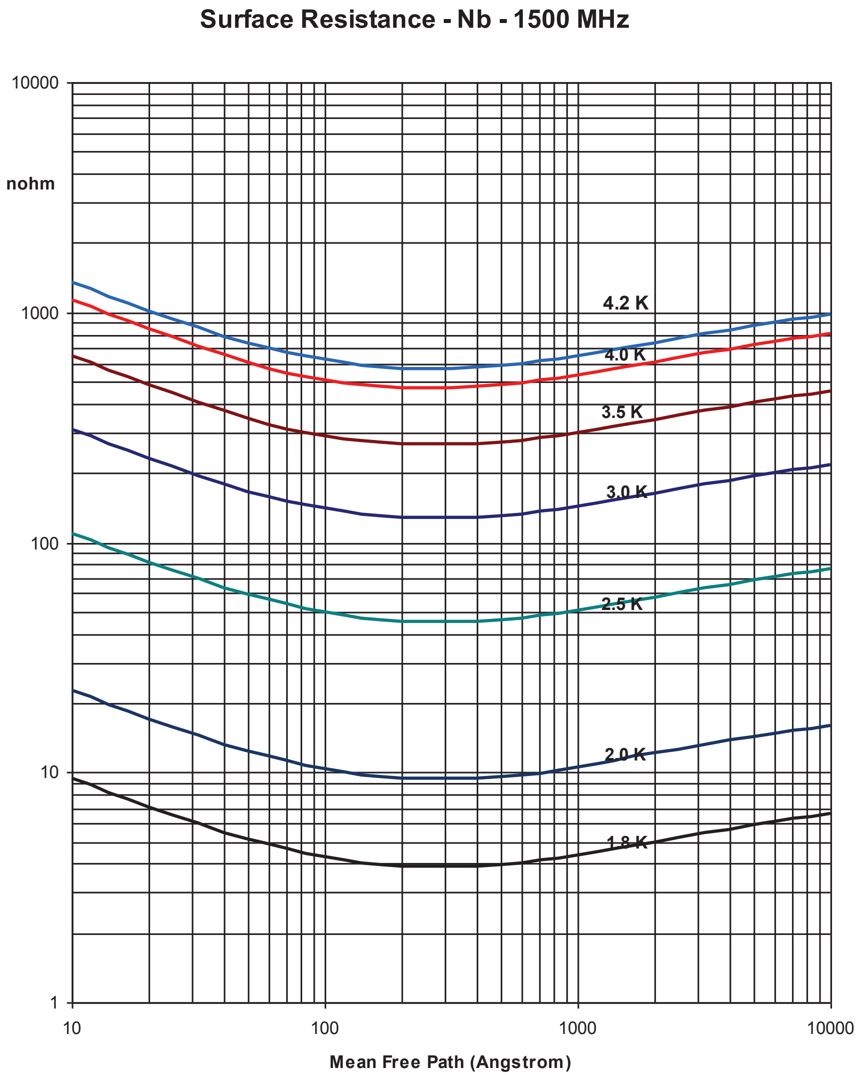

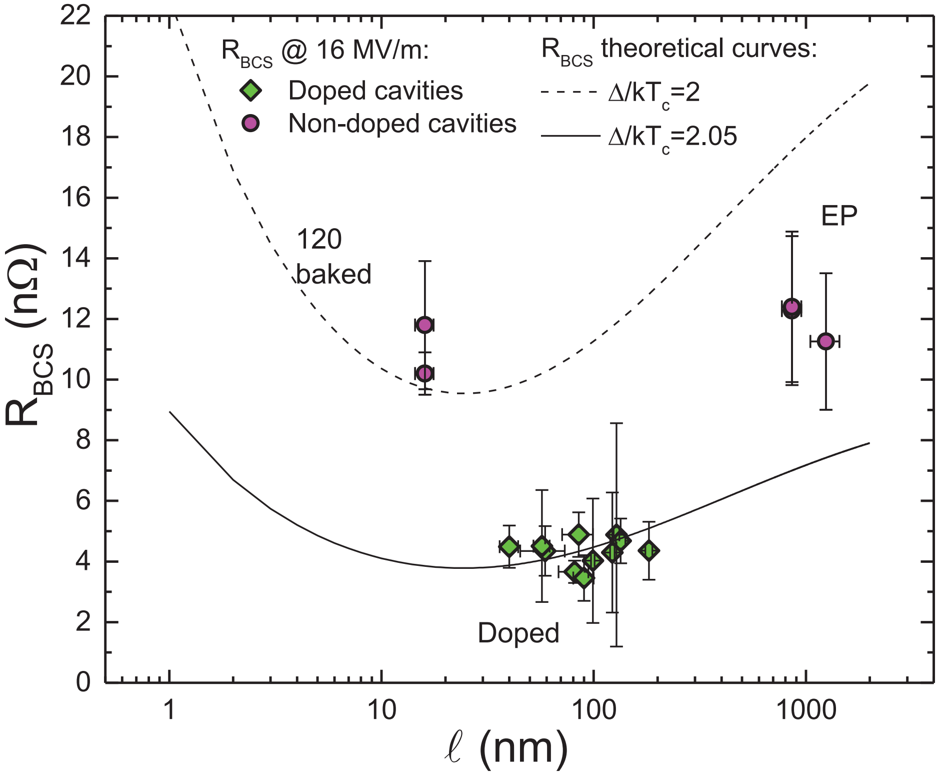

Surface Resistance of Superconductors

Temperature dependence

–close to T_c :

dominated by change in $\lambda(t)$ $\quad \dfrac{t^4}{\left(1-t^2\right)^{3/2}}$

–for $T < \dfrac{T_c}{2}$:

dominated by density of excited states $\sim e^{-\Delta/kT}$

$$R_s \sim \frac{A}{T}\omega^2 \exp\left(-\frac{\Delta}{kT}\right)$$

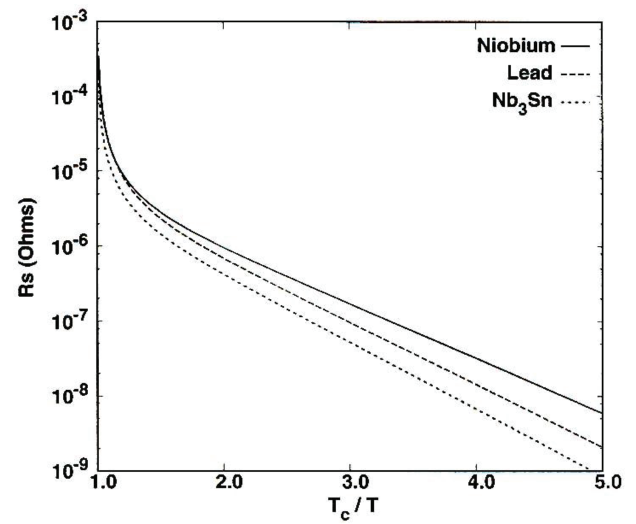

Figure 4.5: Theoretical surface resistance at 1.5 GHz of lead, niobium and Nb_3Sn as calculated from program [94]. The values given in Table 4.1 were used for the material parameters.

Frequency dependence

ω^2 is a good approximation

A reasonable formula for the BCS surface resistance of niobium is

$$R_{BCS} = 9\times 10^{-5}\frac{f^2(\text{GHz})}{T}\exp\left(-1.83\frac{T_c}{T}\right)$$

Surface Resistance of Superconductors

- The surface resistance of superconductors depends on the frequency, the temperature, and a few material parameters
  - Transition temperature
  - Energy gap
  - Coherence length
  - Penetration depth
  - Mean free path

- A good approximation for $T<T_c/2$ and $\omega<<\Delta/h$ is

$$R_s \sim \frac{A}{T}\omega^2 \exp\left(-\frac{\Delta}{kT}\right)+R_{res}$$

Surface Resistance of Superconductors

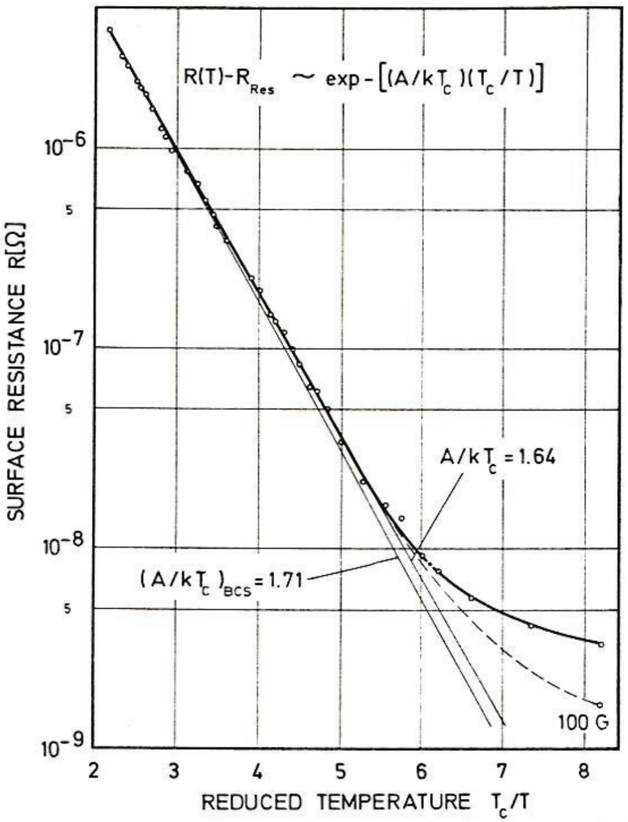

Fig. 2. Temperature dependence of surface resistance of niobium at 3.7 GHz measured in the TE_{011} mode at $H_{rf} \simeq 10$ G. The values computed with the BCS theory used the following material parameters:

$T_c = 9.25$ K; $\lambda_L(T=0, l=\infty) = 320$ Å;
$\Delta(0)/kT = 1.85$; $\xi_F(T=0, l=\infty) = 620$ Å; $l = 1000$ Å or 80 Å.

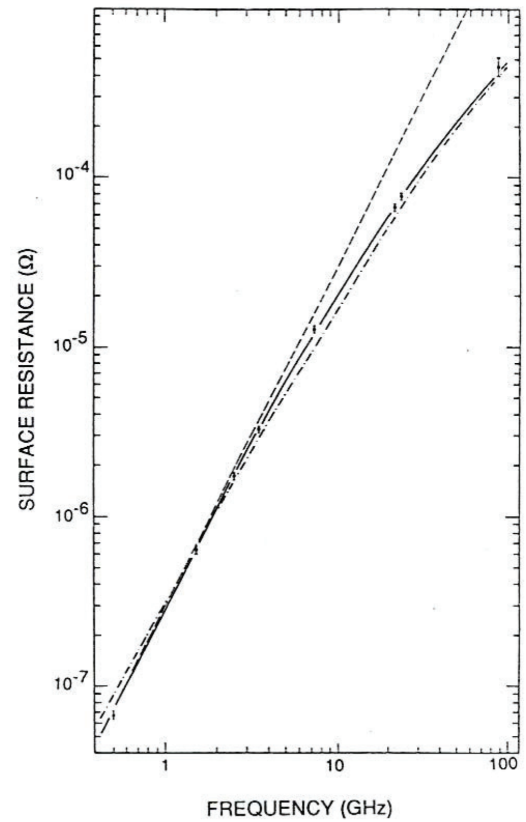

Fig. 5. The surface resistance of Nb at 4.2 K as a function of frequency [62,63]. Whereas the isotropic BCS surface resistance (– · – ·) resulted in $R \propto \omega^{1.8}$ around 1 GHz, the measurements fit better to ω^2 (– – –). The solid curve, which fits the data over the entire range, is a calculation based on the smearing of the BCS density-of-states singularity by the energy gap anisotropy in the presence of impurity scattering [61]. The authors thank G. Müller for providing this figure.

Super and Normal Conductors

- Normal Conductors
  - Skin depth proportional to $\omega^{-1/2}$
  - Surface resistance proportional to $\omega^{1/2 \rightarrow 2/3}$
  - Surface resistance independent of temperature (at low T)
  - For Cu at 300K and 1 GHz, R_s=8.3 mΩ

- Superconductors
  - Penetration depth independent of ω
  - Surface resistance proportional to ω^2
  - Surface resistance strongly dependent of temperature
  - For Nb at 2 K and 1 GHz, $R_s \approx 7$ nΩ

However: do not forget Carnot

SRF CAVITIES

Jean Delayen

Center for Accelerator Science
Old Dominion University
and
Thomas Jefferson National Accelerator Facility

Design Considerations

$\frac{H_{s,\max}}{E_{acc}}$	minimum	critical field
$\frac{E_{s,\max}}{E_{acc}}$	minimum	field emission
$\frac{< H_s^2 >}{E_{acc}^2}$	minimum	shunt impedance, current losses
$\frac{< E_s^2 >}{E_{acc}^2}$	minimum	dielectric losses
$\frac{U}{E_{acc}^2}$	minimum maximum	control of microphonics voltage drop for high charge per bunch

TM-CLASS CAVITIES

350 MHz, 4-cell, Nb on Cu

1500 MHz, 5-cell

1300 MHz 9-cell

Pill Box Cavity

Hollow right cylindrical enclosure

Operated in the TM$_{010}$ mode $H_z = 0$

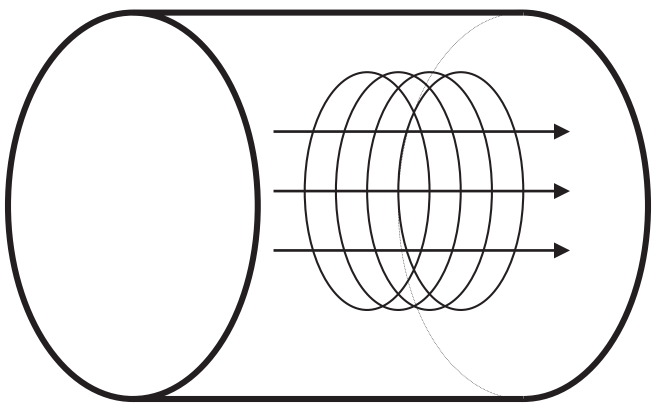

$$\frac{\partial^2 E_z}{\partial^2 r} + \frac{1}{r}\frac{\partial E_z}{\partial r} = \frac{1}{c^2}\frac{\partial^2 E_z}{\partial^2 t} \qquad \omega_0 = \frac{2.405c}{R}$$

$$E_z(r,z,t) = E_0 J_0\left(2.405\frac{r}{R}\right)e^{-i\omega_0 t}$$

$$H_\varphi(r,z,t) = -i\frac{E_0}{\mu_0 c} J_1\left(2.405\frac{r}{R}\right)e^{-i\omega_0 t}$$

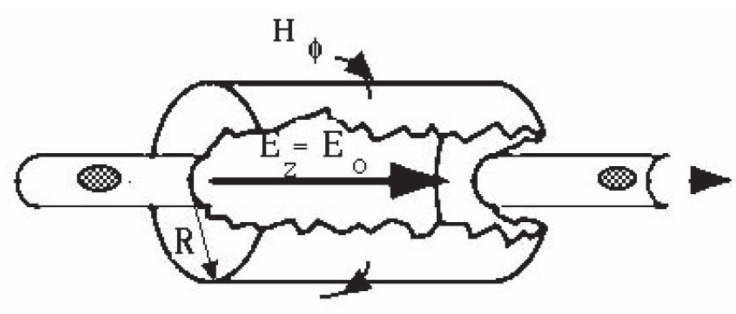

TM_{010} Mode in a Pill Box Cavity

$$E_r = E_\varphi = 0 \qquad E_z = E_0 J_0\left(x_{01}\frac{r}{R}\right)$$

$$H_r = H_z = 0 \qquad H_\varphi = -i\omega\varepsilon E_0 \frac{R}{x_{01}} J_1\left(x_{01}\frac{r}{R}\right)$$

$$\omega = x_{01}\frac{c}{R} \qquad x_{01} = 2.405$$

$$R = \frac{x_{01}}{2\pi}\lambda = 0.383\lambda$$

TM$_{010}$ Mode in a Pill Box Cavity

Energy content

$$U = \varepsilon_0 E_0^2 \frac{\pi}{2} J_1^2(x_{01}) L R^2$$

Power dissipation

$$P = E_0^2 \frac{R_s}{\eta^2} \pi J_1^2(x_{01})(R+L)R$$

$$x_{01} = 2.40483$$

$$J_1(x_{01}) = 0.51915$$

Geometrical factor

$$G = \eta \frac{x_{01}}{2} \frac{L}{(R+L)}$$

TM_{010} Mode in a Pill Box Cavity

Energy Gain

$$\Delta W = E_0 \frac{\lambda}{\pi} \sin \frac{\pi L}{\lambda}$$

Gradient

$$E_{acc} = \frac{\Delta W}{\lambda / 2} = E_0 \frac{2}{\pi} \sin \frac{\pi L}{\lambda}$$

Shunt impedance

$$R_{sh} = \frac{\eta^2}{R_s} \frac{1}{\pi^3 J_1^2(x_{01})} \frac{\lambda^2}{R(R+L)} \sin^2\left(\frac{\pi L}{\lambda}\right)$$

Real Cavities

Beam tubes reduce the electric field on axis

Gradient decreases

Peak fields increase

R/Q decreases

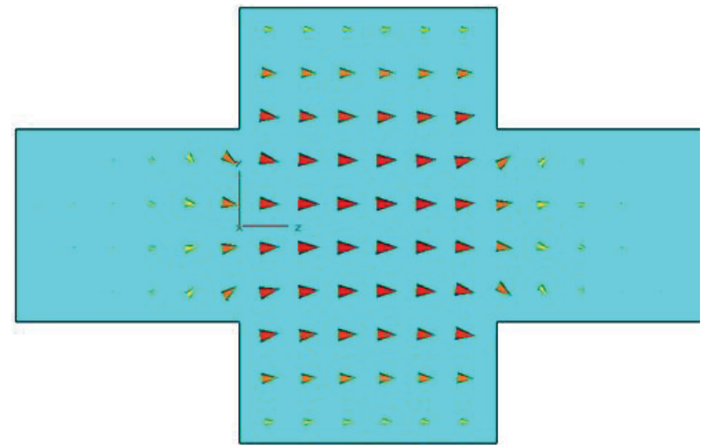

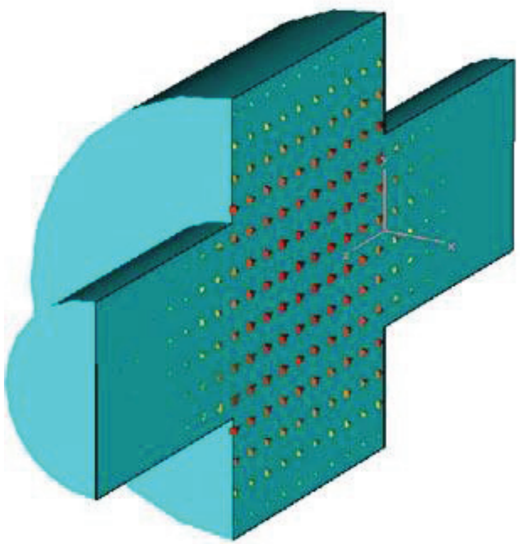

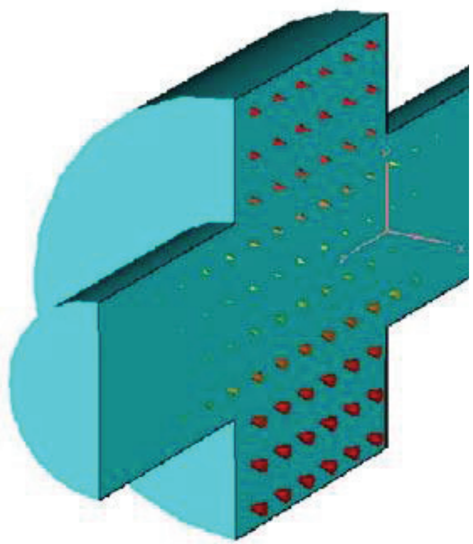

Real Cavities

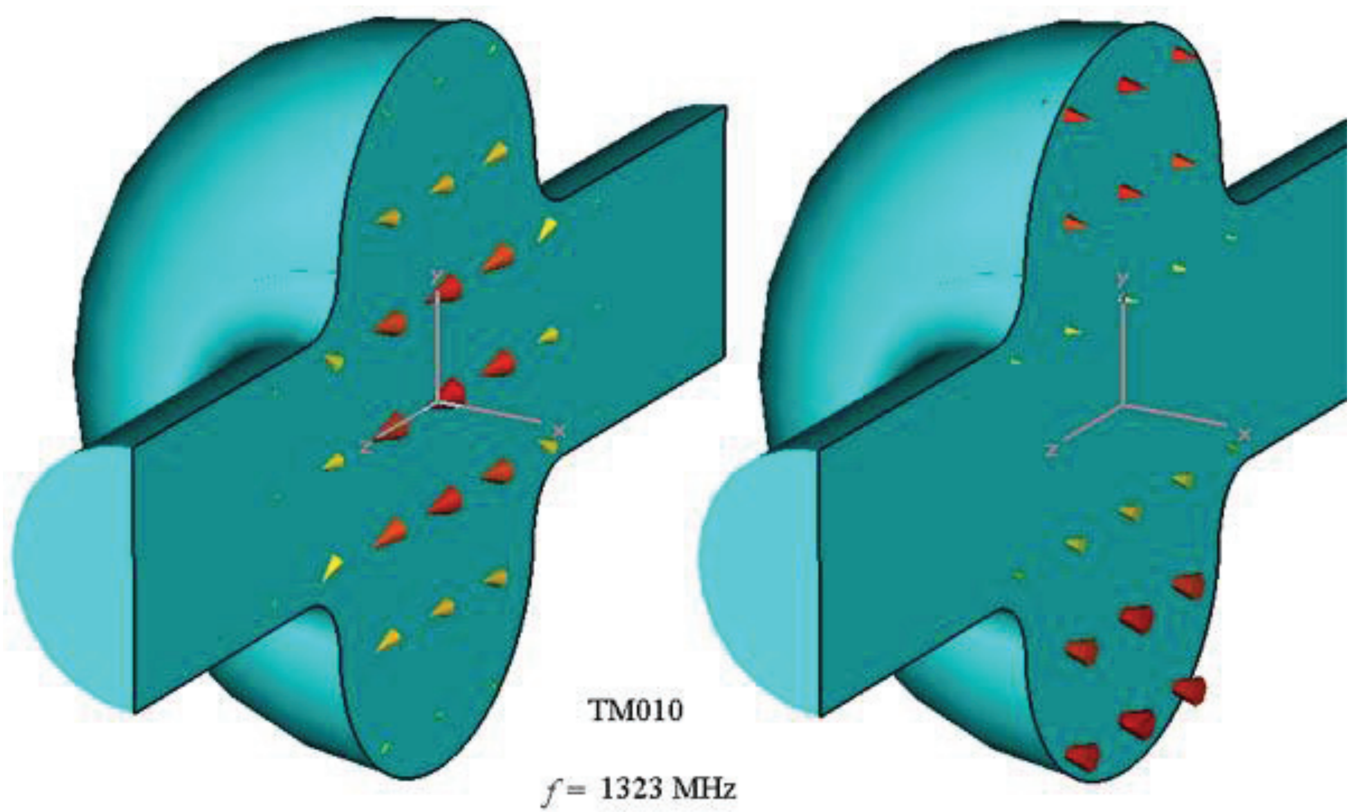

Single Cell Cavities

Electric field high at iris

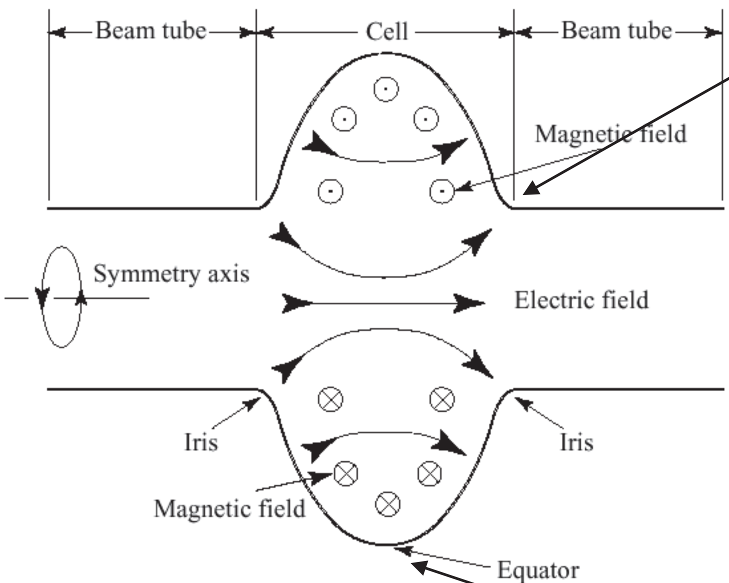

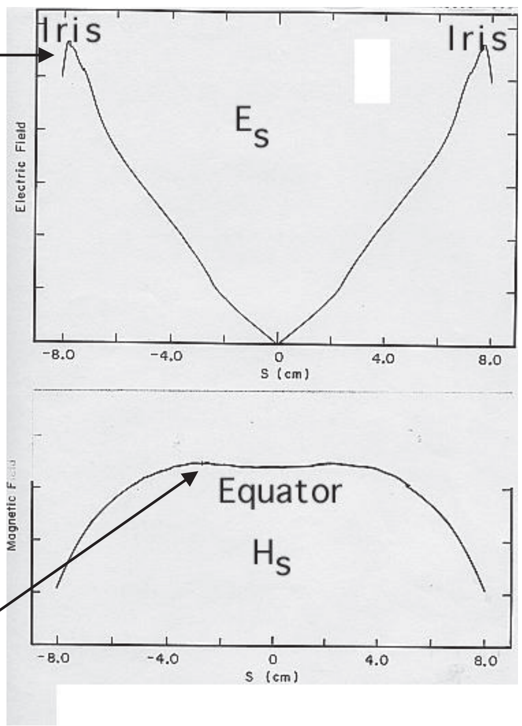

Magnetic field high at equator

Cell Shape Design

- What is the purpose of the cavity?
- What EM parameters should be optimized to meet the design specs?

The "perfect" shape does not exist, it all depends on your application

New Trend in TM-Cavity Design

- The **field emission is not a hard limit** in the performance of sc cavities if the surface preparation is done in the right way.

- **Magnetic flux on the wall** limits performance of a sc cavity (Q_0 decreases or/and quench). Hard limit **~180 mT** for Nb.

"Rule of thumb" for Optimizing Peak Surface Fields

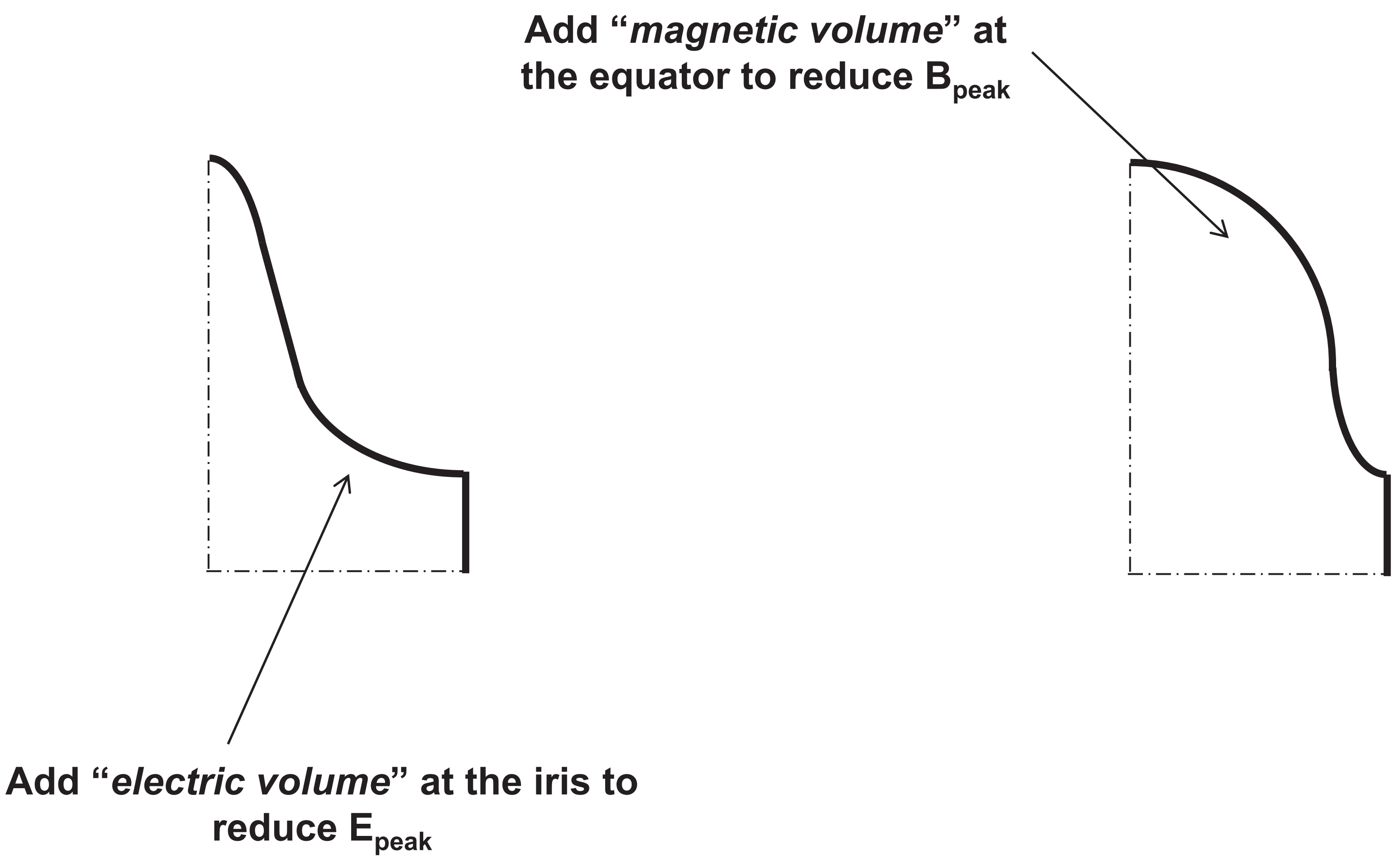

New Shapes for ILC

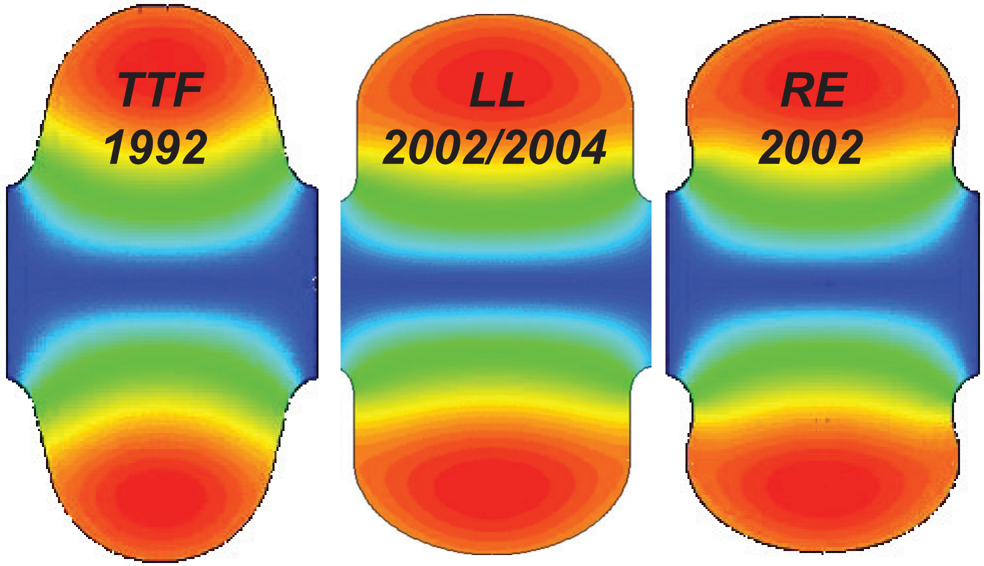

r_{iris}	[mm]	35	30	33
k_{cc}	[%]	1.9	1.52	1.8
E_{peak}/E_{acc}	-	1.98	2.36	2.21
B_{peak}/E_{acc}	[mT/(MV/m)]	4.15	3.61	3.76
R/Q	[Ω]	113.8	133.7	126.8
G	[Ω]	271	284	277
R/Q*G	[Ω*Ω]	30840	37970	35123

SUPERFISH

- Free, 2D finite-difference code to design cylindrically symmetric structures (monopole modes only)
- Use symmetry planes to reduce number of mesh points

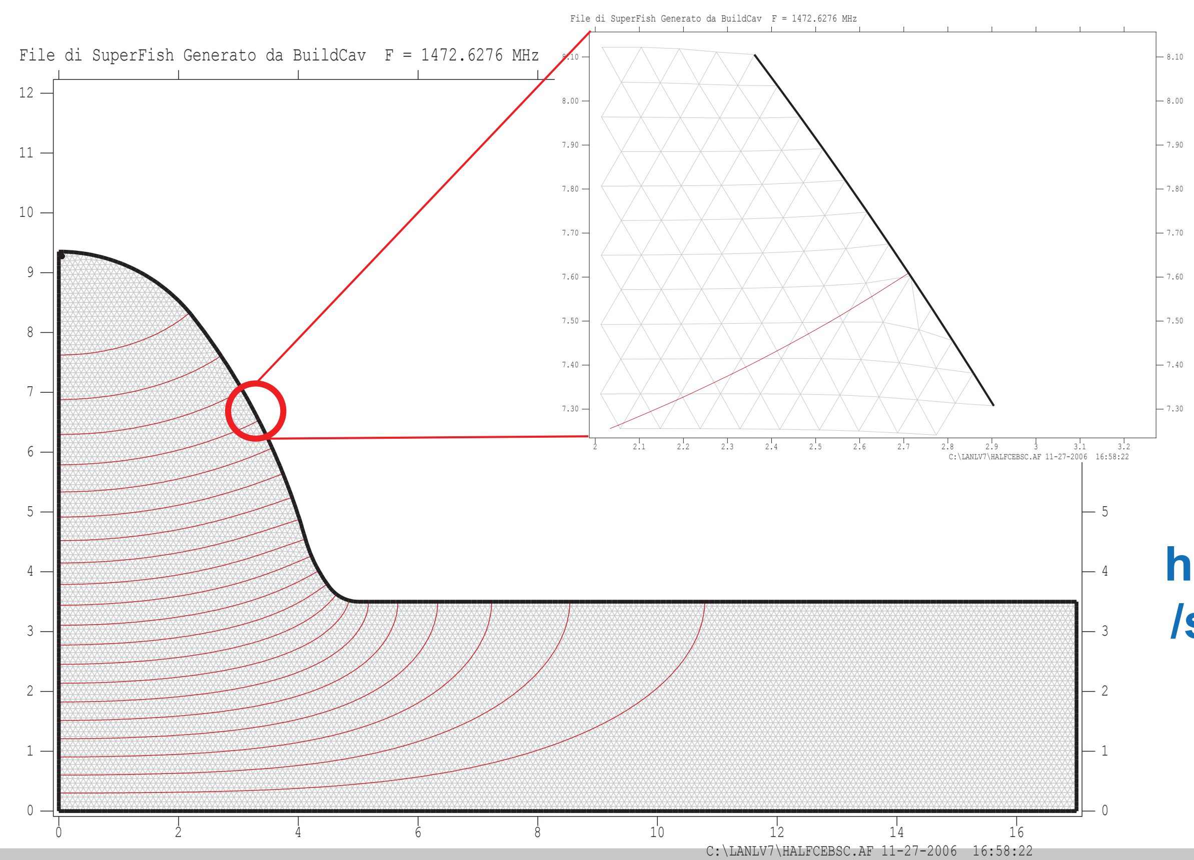

http://laacg1.lanl.gov/laacg/services/download_sf.phtml

CST Microwave Studio

- Expensive, 3D finite-element code, used to design complex RF structure.
  http://www.cst.com/Content/Products/MWS/Overview.aspx

- Runs on PC
- Perfect Boundary Approximation

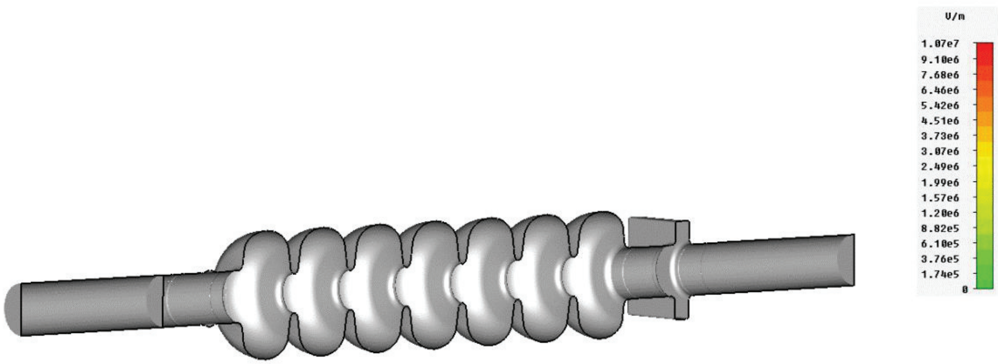

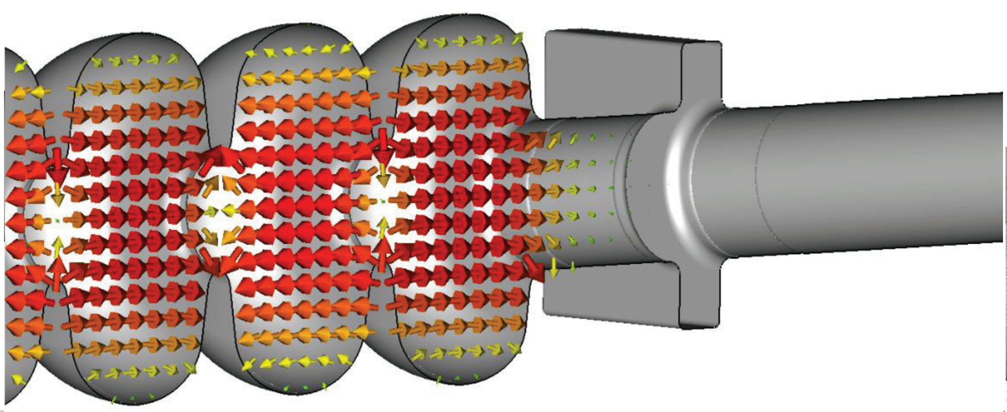

Hexahedral mesh

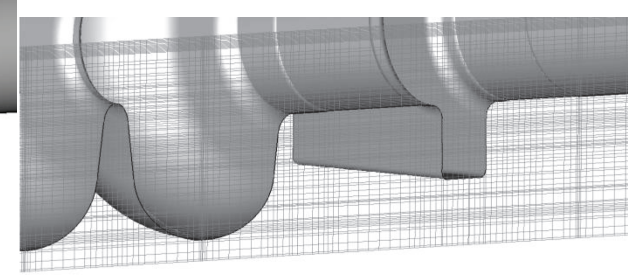

Omega3P

- SLAC, 3D code, high-order Parallel Finite Element (PFE) method
- Runs on Linux
- Tetrahedral conformal mesh
- High order finite elements (basis order p =1 – 6
- Separate software for user interface (CuBit)

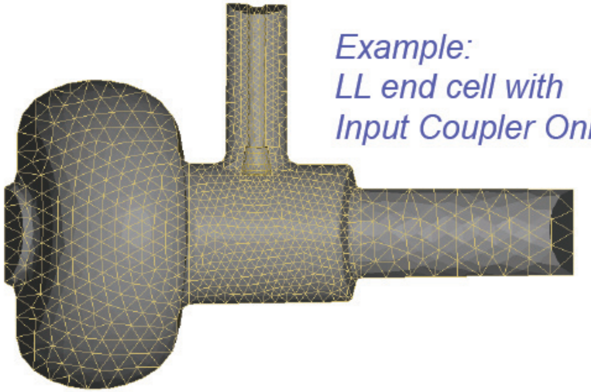

Example:
LL end cell with
Input Coupler Only

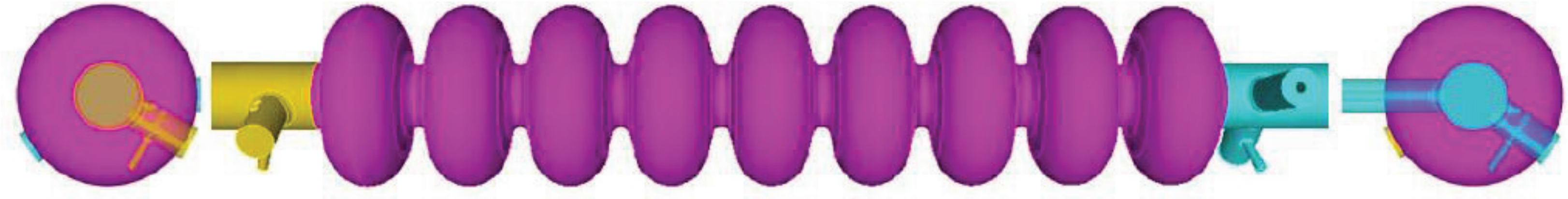

Multicell Cavities

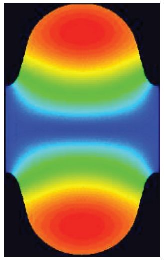

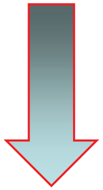

Single-cell is attractive from the RF-point of view:

- **Easier to manage HOM damping**
- **No field flatness problem.**
- **Input coupler transfers less power**
- **Easy for cleaning and preparation**

- ***But it is expensive to base even a small linear accelerator on the single cell. We do it only for very high beam current machines.***

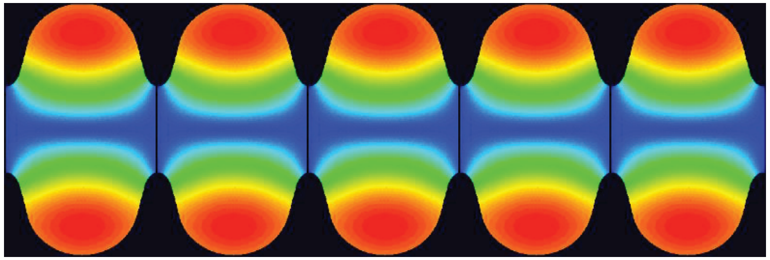

A multi-cell structure is less expensive and offers higher real-estate gradient but:

Field flatness (stored energy) in cells becomes sensitive to frequency errors of individual cells

- ***Other problems arise: HOM trapping…***

Velocity Acceptance

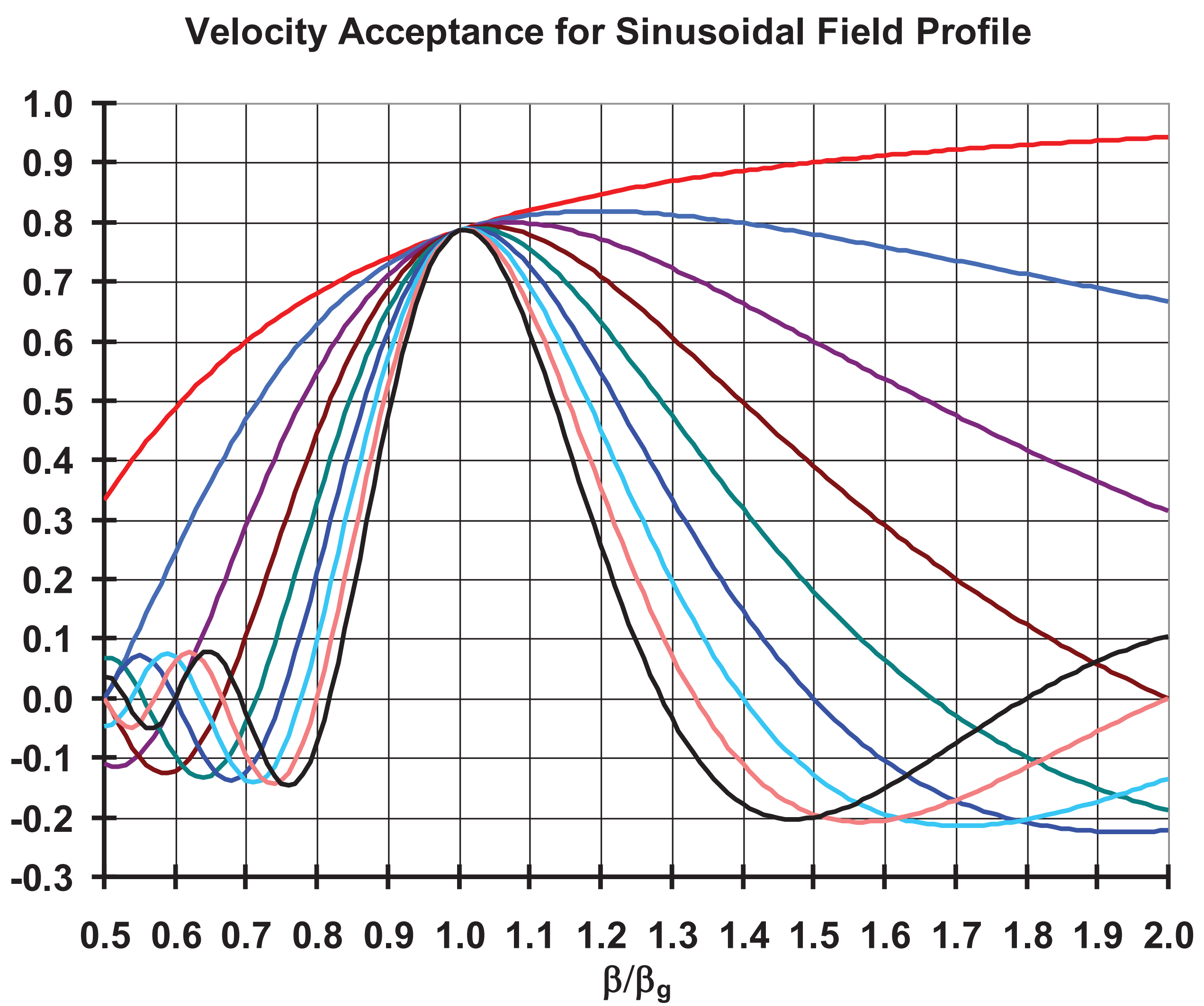

Pros and Cons of Multicells

- Cost of accelerators are lower (less auxiliaries: LHe vessels, tuners, fundamental power couplers, control electronics)
- Higher real-estate gradient (better fill factor)

- Field flatness vs. N
- HOM trapping vs. N
- Power capability of fundamental power couplers vs. N
- Chemical treatment and final preparation become more complicated
- The worst performing cell limits whole multi-cell structure

Coupling between cells

ω_o

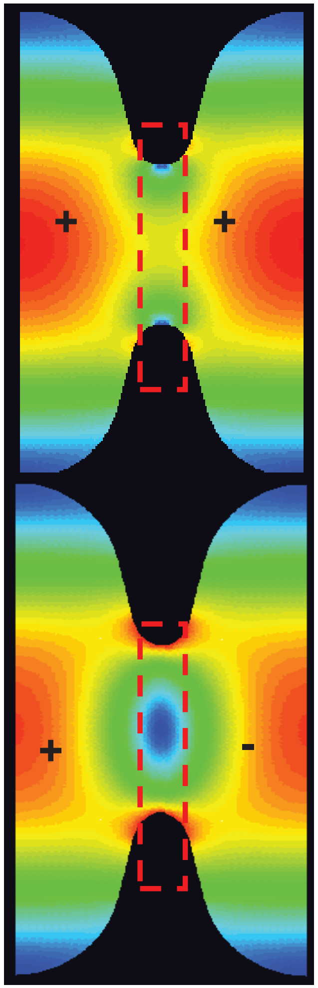

ω_π

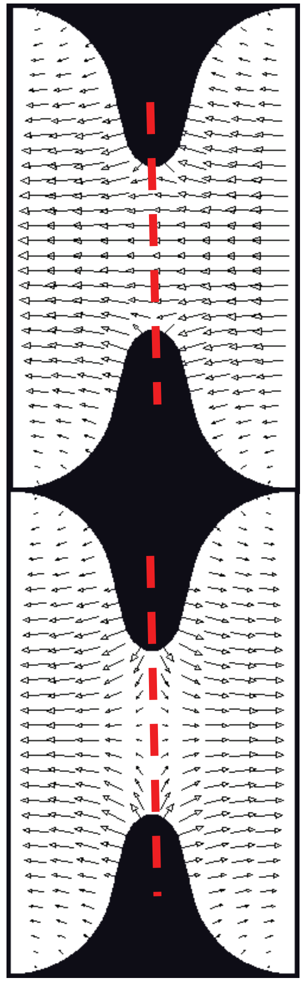

Symmetry plane for the H field

Symmetry plane for the E field which is an additional solution

The normalized difference between these frequencies is a measure of the energy flow via the coupling region

$$k_{cc} = \frac{\omega_\pi - \omega_0}{\frac{\omega_\pi + \omega_0}{2}}$$

Multi-Cell Cavities

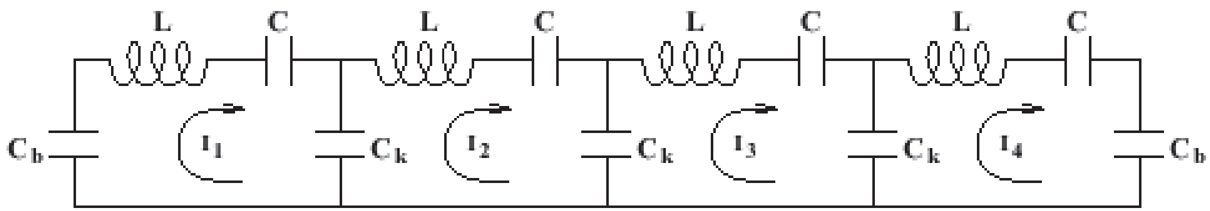

$$k = \frac{C}{C_k} \qquad C_b = C_k / 2$$

Mode frequencies:

$$\frac{\omega_m^2}{\omega_0^2} = 1 + 2k\left(1 - \cos\frac{\pi m}{n}\right)$$

$$\frac{\omega_n - \omega_{n-1}}{\omega_0} \simeq k\left(1 - \cos\frac{\pi}{n}\right) \simeq \frac{k}{2}\left(\frac{\pi}{n}\right)^2$$

Voltages in cells:

$$V_j^m = \sin\left(\pi m \frac{2j-1}{2n}\right)$$

Pass-Band Modes Frequencies

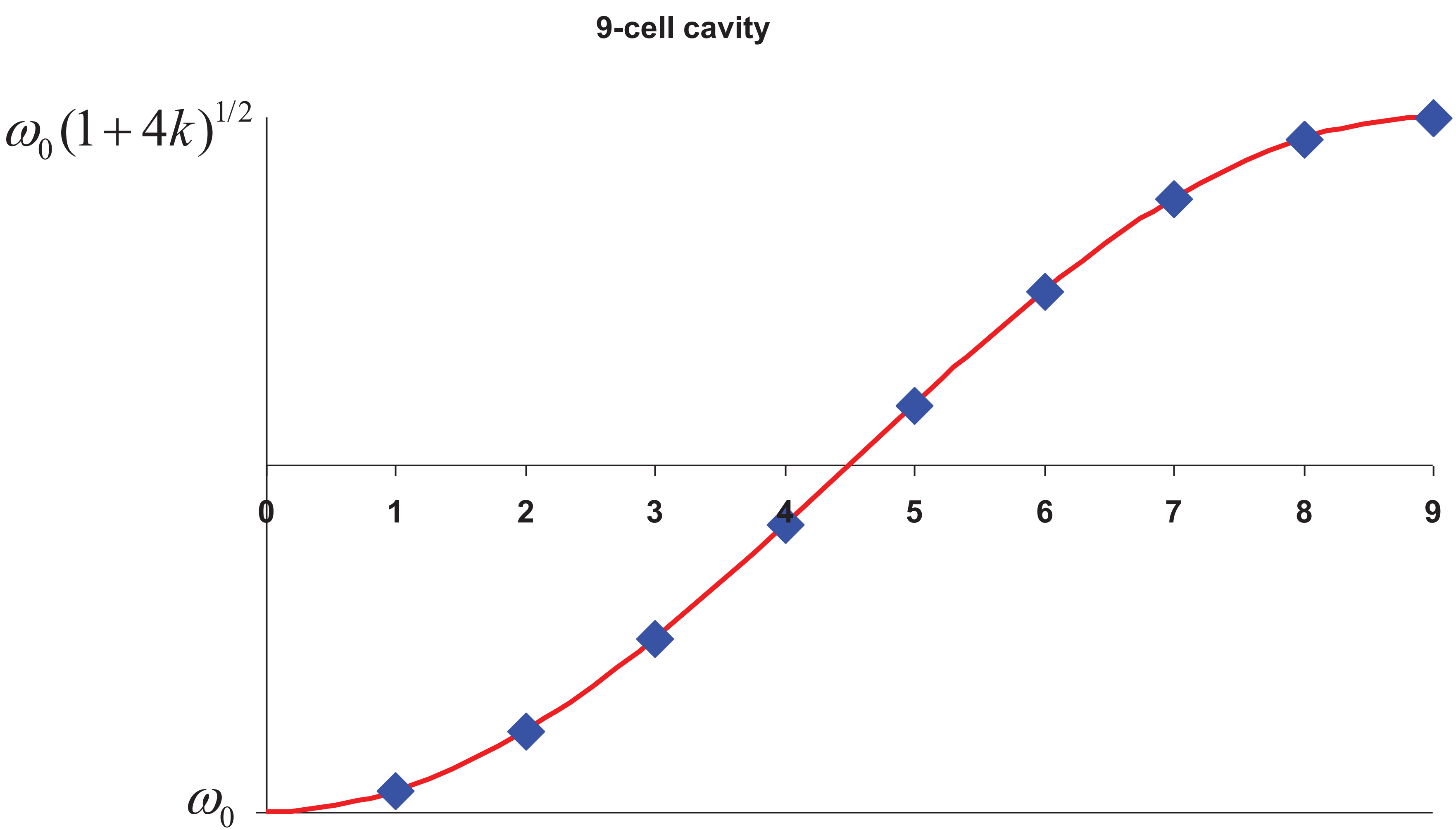

Cell Excitations in Pass-Band Modes

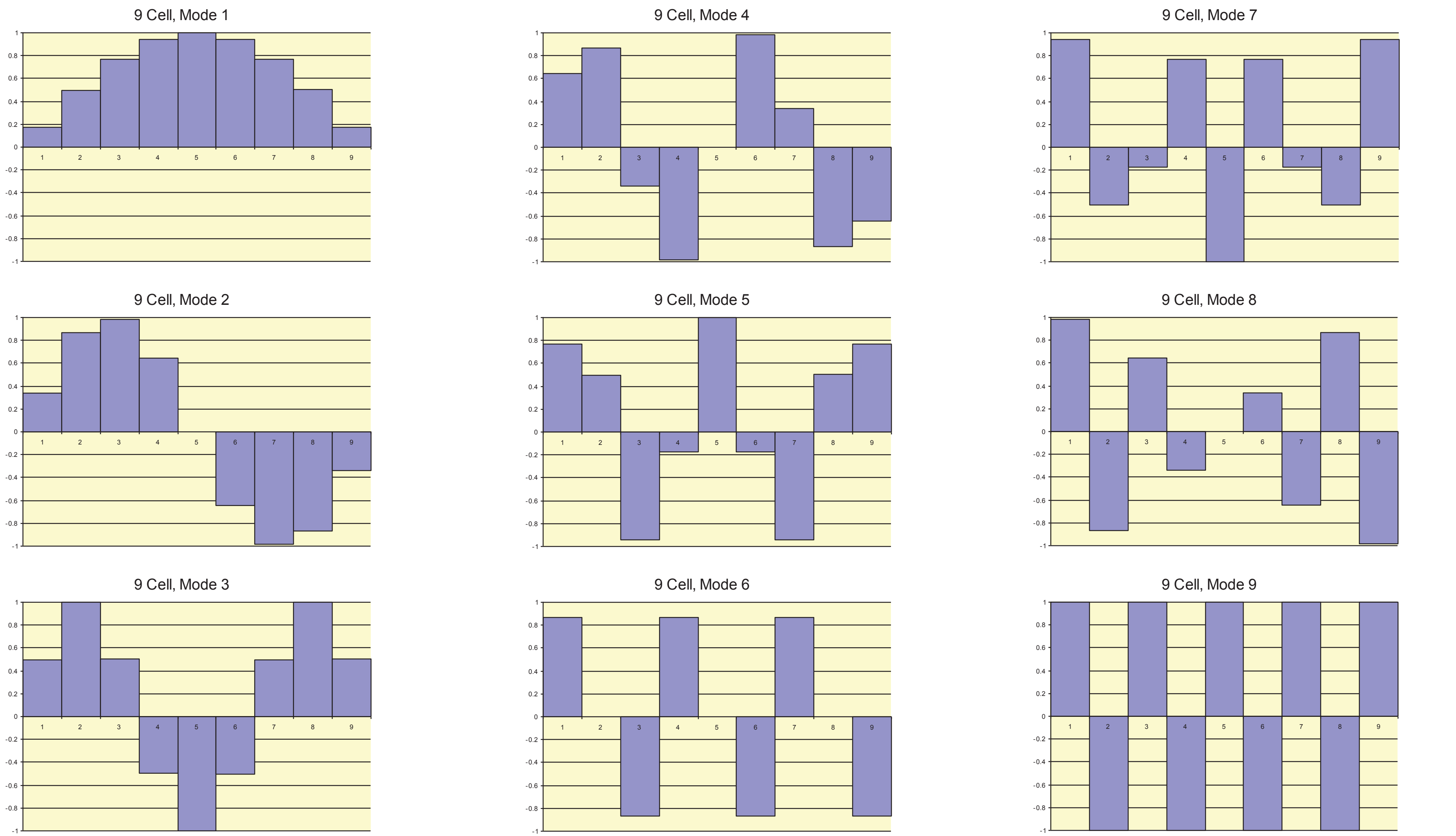

Multipacting Simulations

Once the cavity shape has been designed, multipacting simulations have to be done:

- get the fields on the contour
- electrons are launched from given initial sites at given phases of the RF field
- for a fixed field level the electron trajectories are calculated by integrating the equations of motion, until the electrons hit the wall
- record the location, phase, and impact energy
- the number of secondary electrons is determined, given the SEY function
- the trajectory calculation is continued if the field phase is such as secondary electrons leave the wall
- after a given number of impacts N the No. of free electrons and their avg. impact energy and the No. of secondary electrons is calculated

Counter function

Enhanced counter function

Counter function: field levels at which resonant conditions are satisfied

At field levels where Enhanced counter function > No. initial electrons: Multipacting

Example: Multipacting in SNS HOM Coupler

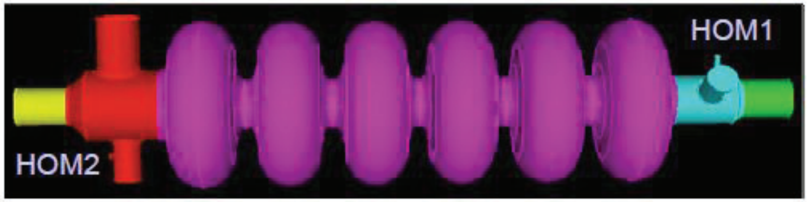

- SNS SCRF cavity experienced RF heating at HOM coupler
- 3D MP simulations showed MP barriers closed to measurements
- Similar analysis are carried out for ILC ICHIRO and crab cavity

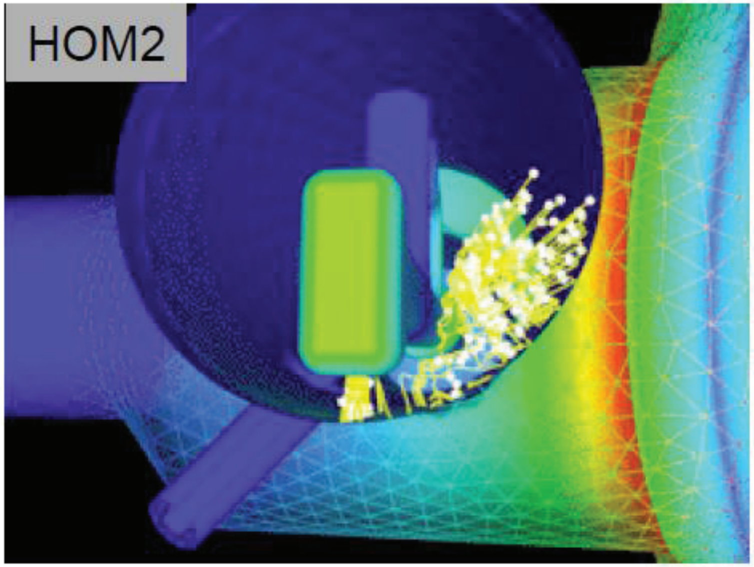

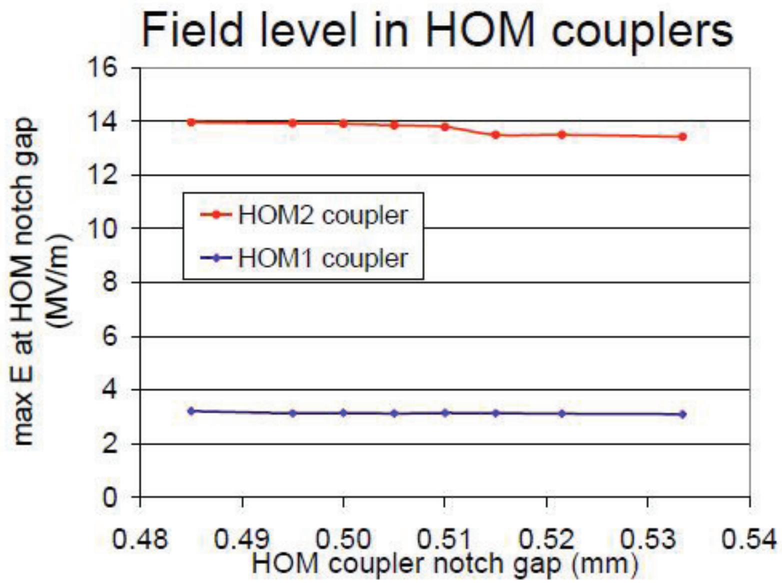

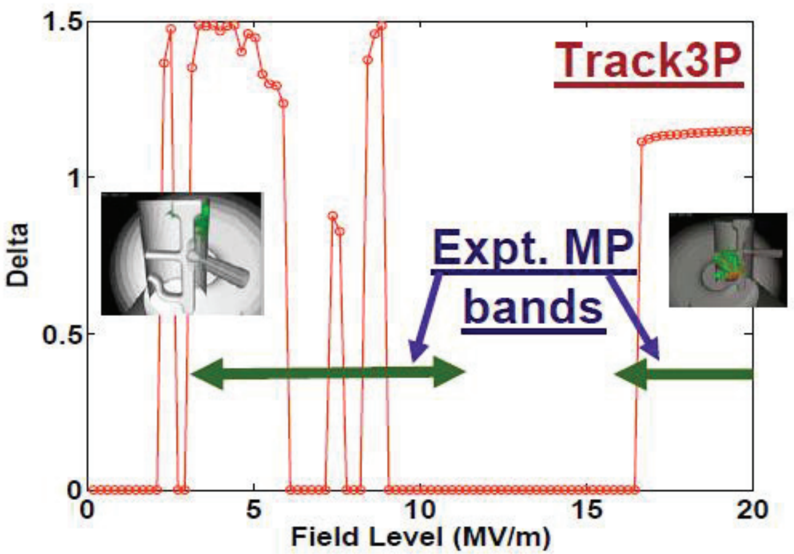

Mechanical Design

The mechanical design of a cavity follows its RF design:

- **Lorentz Force Detuning**
- **Mechanical Resonances**

$$P = \frac{\mu_0 H_s^2 - \varepsilon_0 E_s^2}{4}$$

Lorentz Force Detuning

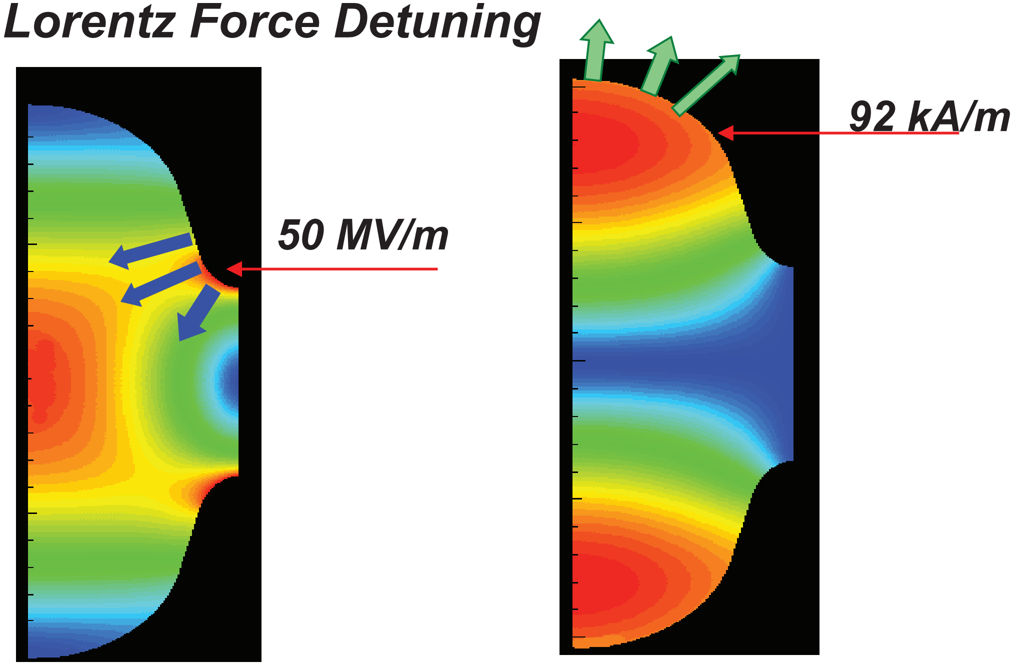

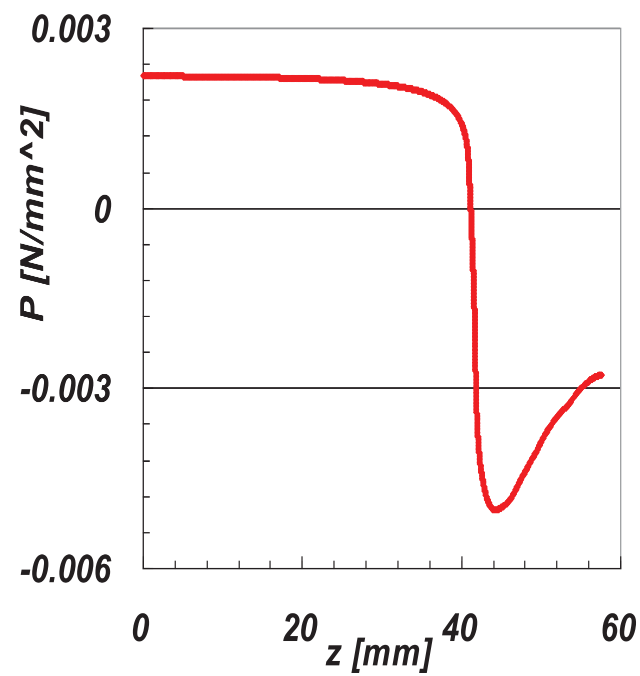

E and H at E_{acc} = 25 MV/m in TESLA inner-cup

TEM-CLASS CAVITIES

Basic Structure Geometries

Resonant Transmission Lines

- $\lambda/4$
  - Quarter-wave
  - Split-ring
  - Twin quarter-wave
  - Lollipop
- $\lambda/2$
  - Coaxial half-wave
  - Spoke
  - H-types

- **TM**
  - Elliptical
  - Reentrant

- **Other**
  - Alvarez
  - Slotted-iris

A Word on Design Tools

TEM-class cavities are essentially 3D geometries

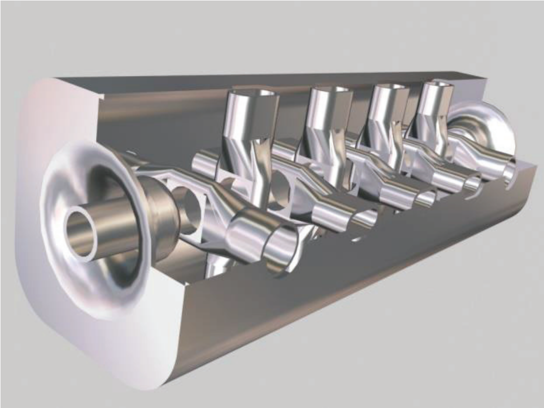

3D electromagnetic software is available

MAFIA, Microwave Studio, HFSS, etc.

3D software is usually very good at calculating frequencies

Not quite as good at calculating surface fields

Use caution, vary mesh size

Remember Electromagnetism 101

Design Tradeoffs

Number of cells

- Voltage gain
- Velocity acceptance

Frequency

- Size
- Voltage gain
- Rf losses
- Energy content, microphonics, rf control
- Acceptance, beam quality and losses

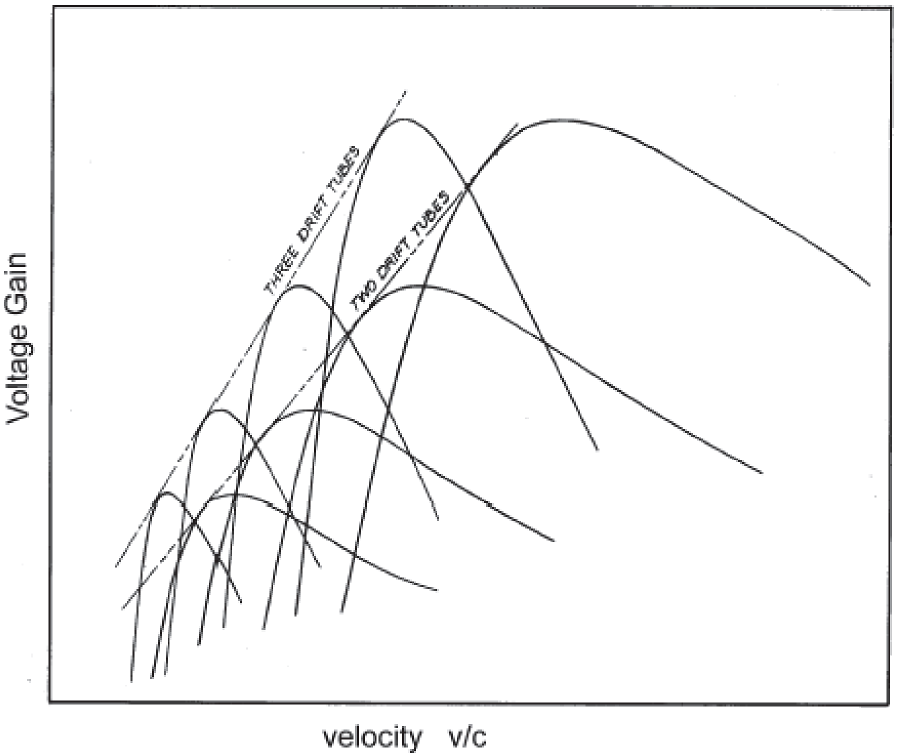

A Simple Model: Loaded Quarter-wavelength Resonant Line

If characteristic length <<λ (β<0.5), separate the problem in two parts:

- Electrostatic model of high voltage region
- Transmission line

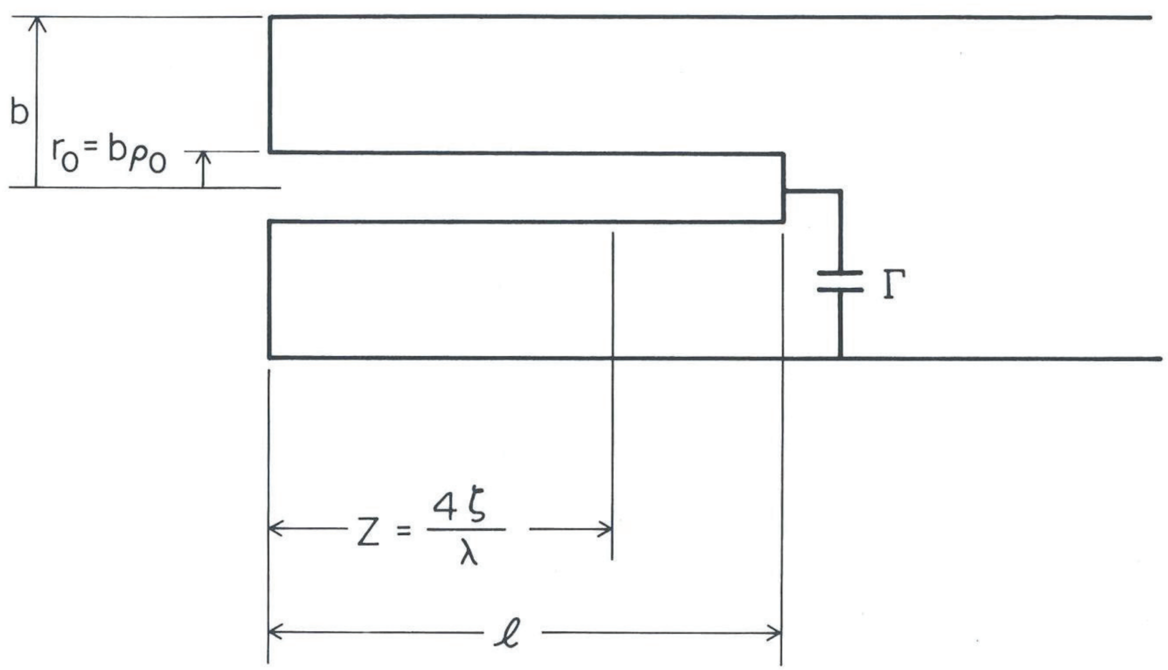

A Simple Model:
Coaxial Half-wave Resonator

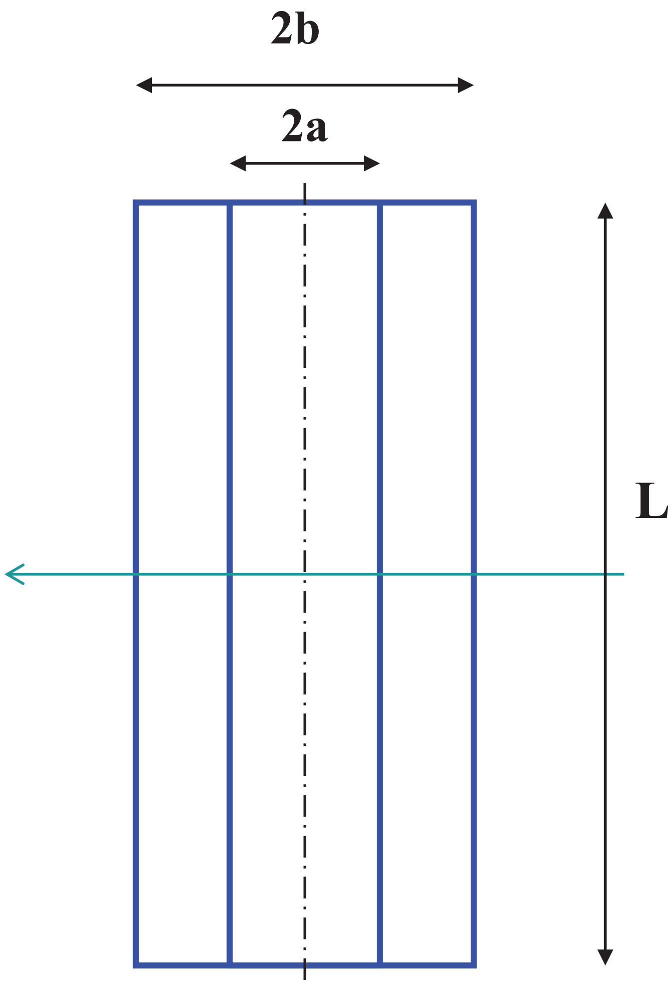

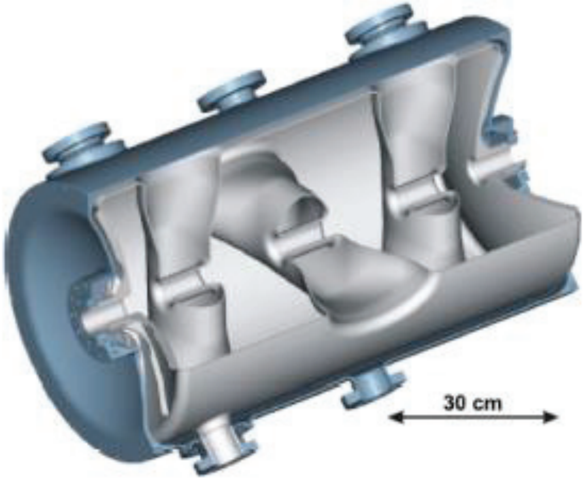

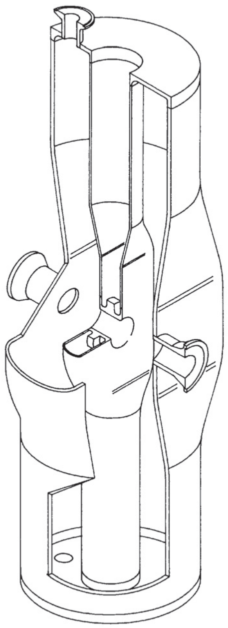

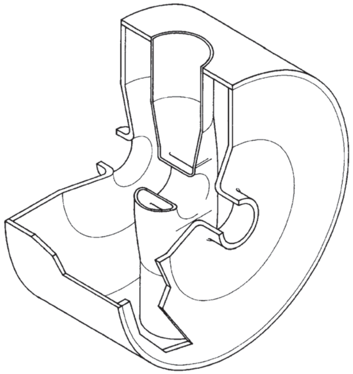

Some Real Geometries (λ/4)

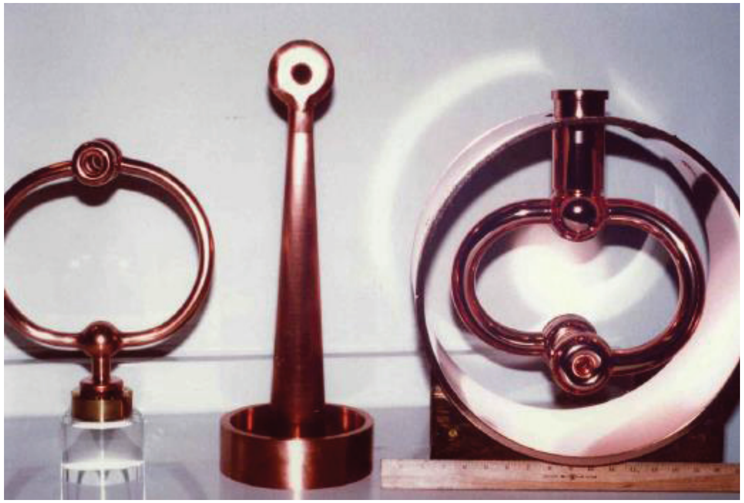

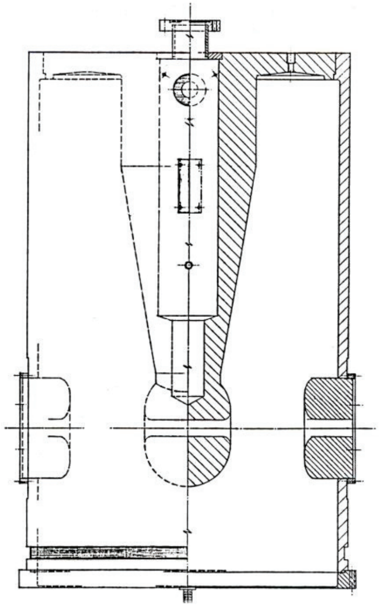

Some Real Geometries (λ/4)

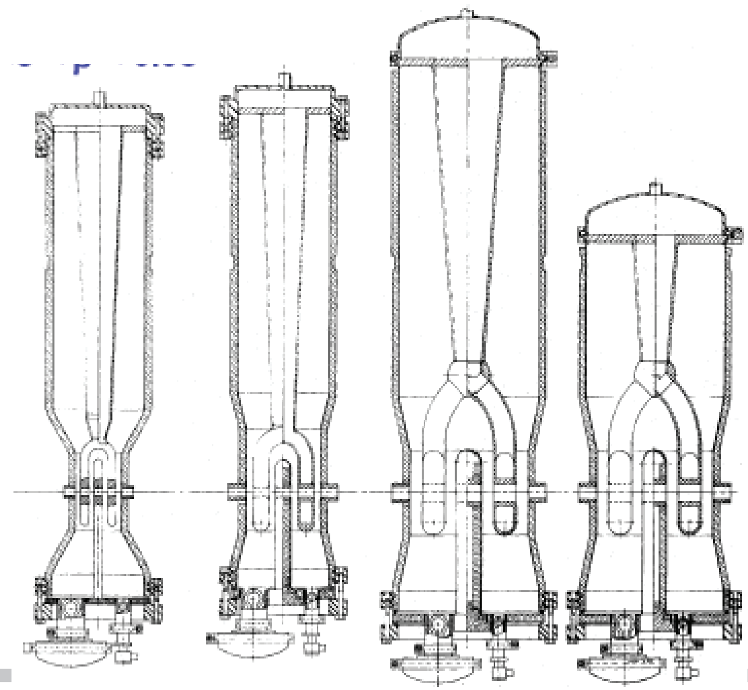

λ/4 Resonant Lines

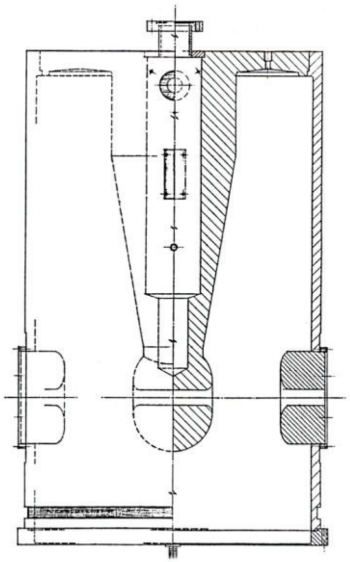

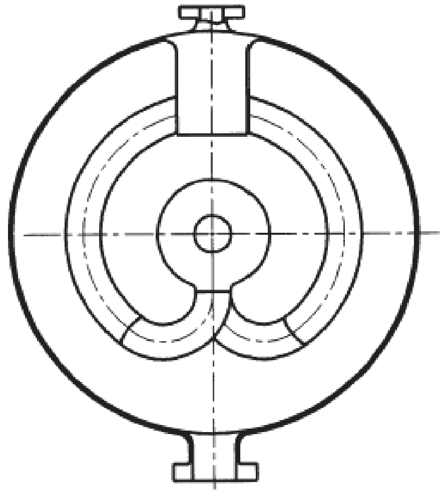

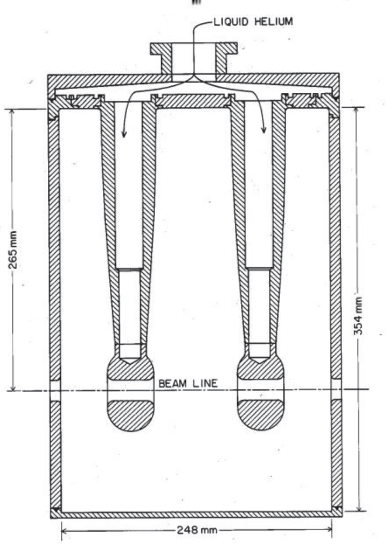

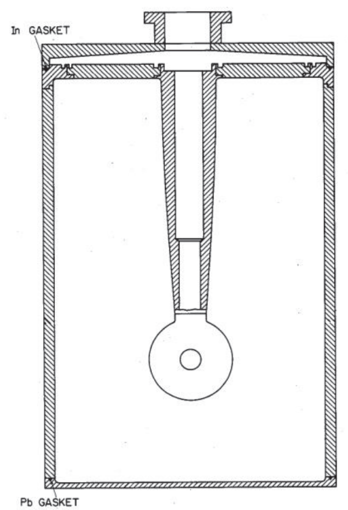

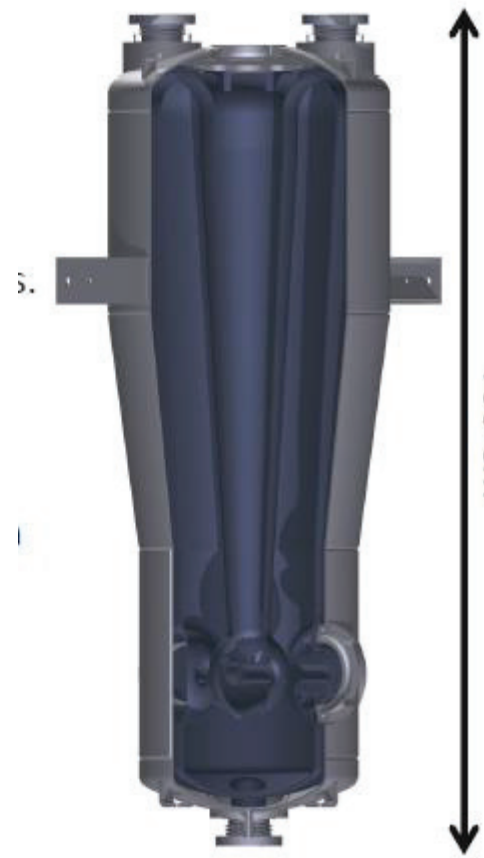

72.75 MHz, $\beta = 0.077$
Quarter-Wave Resonator

λ/2 Resonant Lines

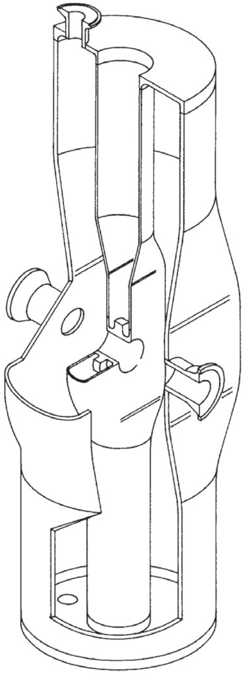

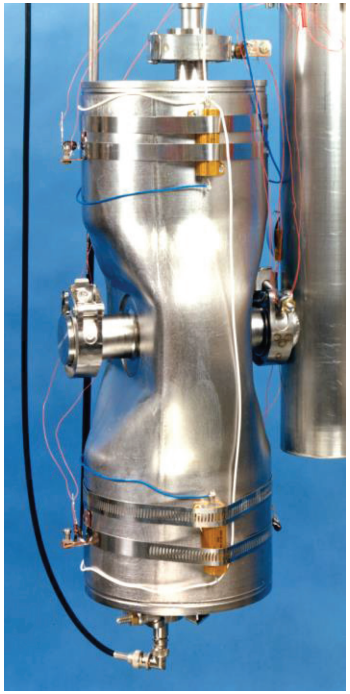

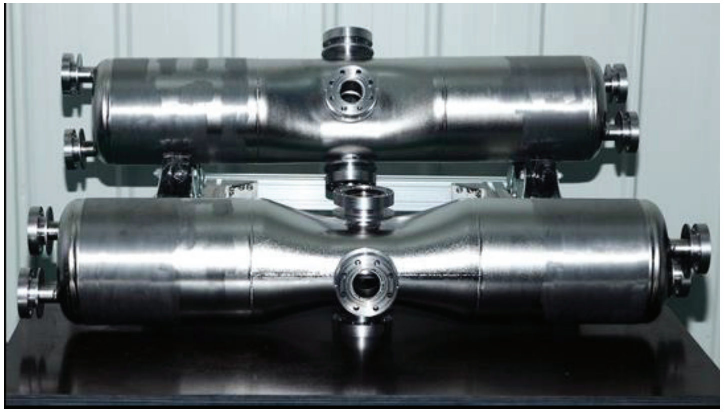

$\lambda/2$ Resonant Lines – Single-Spoke

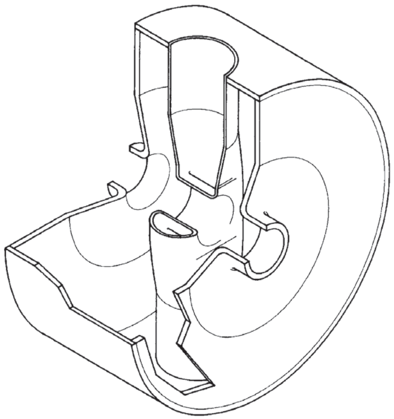

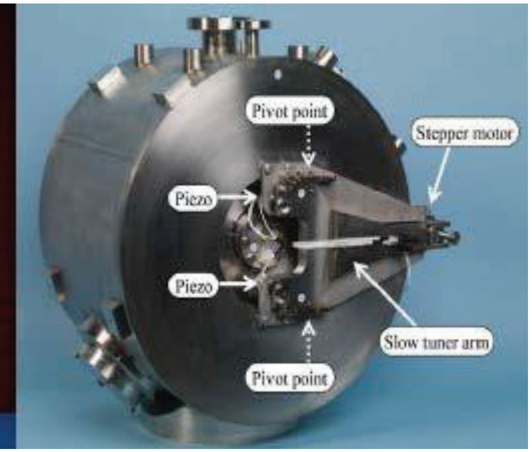

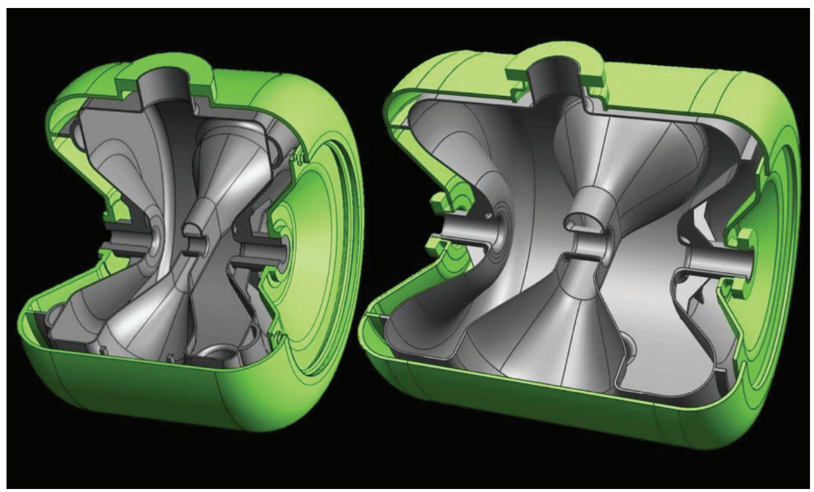

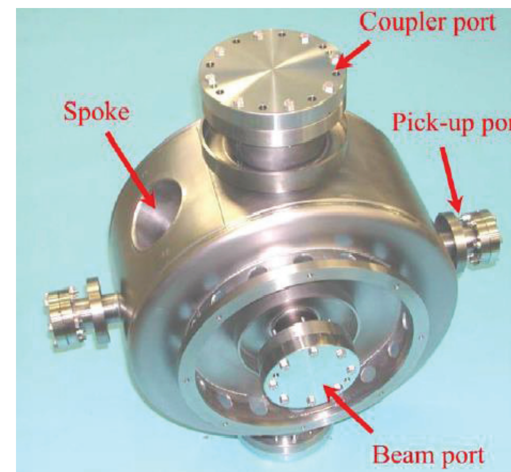

$\lambda/2$ Resonant Lines – Double and Triple-Spoke

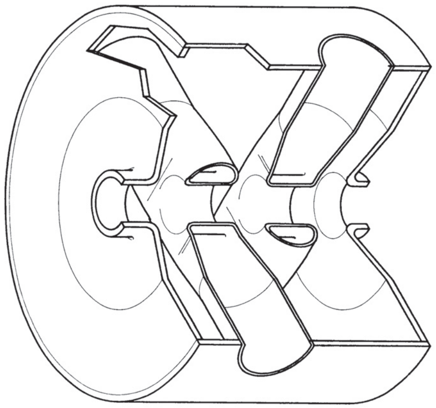

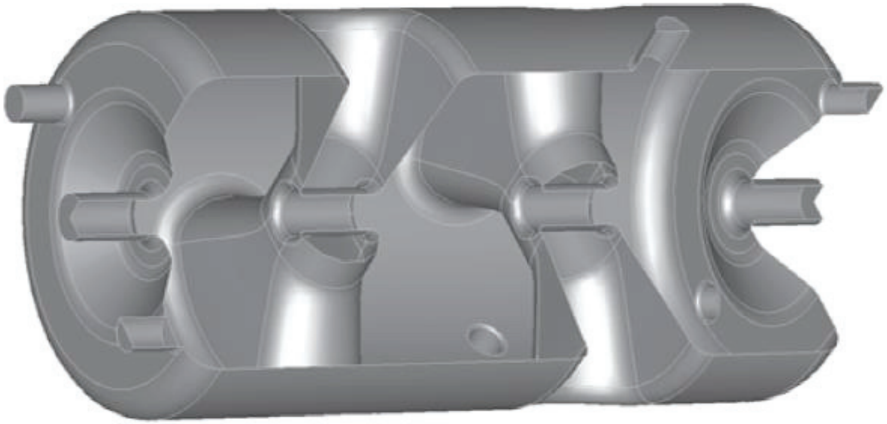

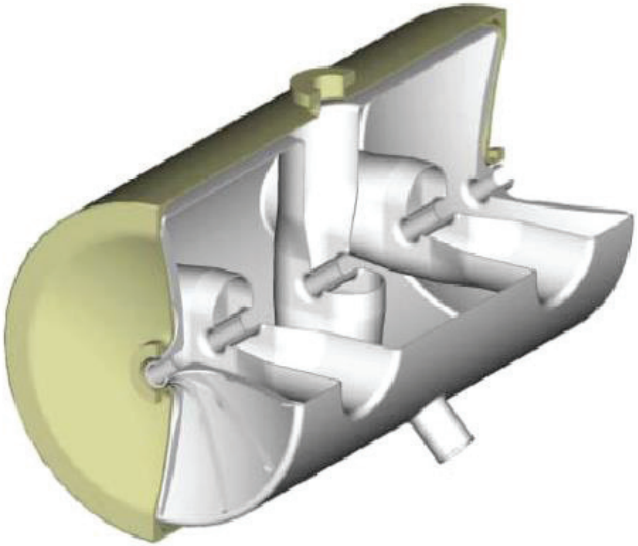

λ/2 Resonant Lines – Multi-Spoke

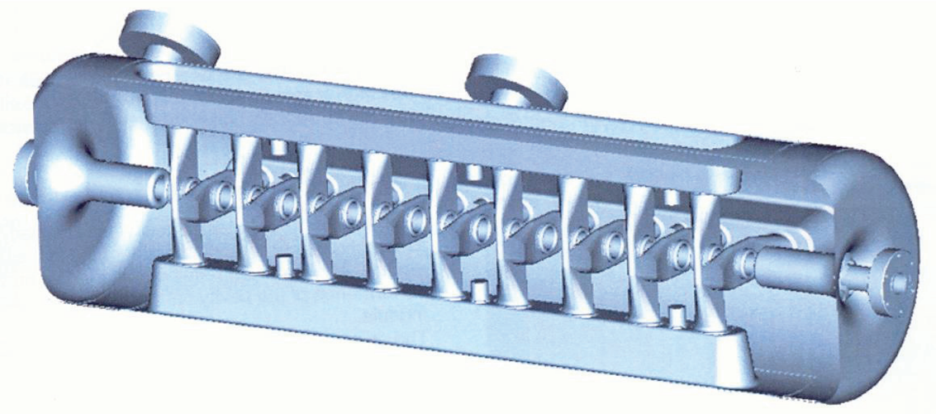

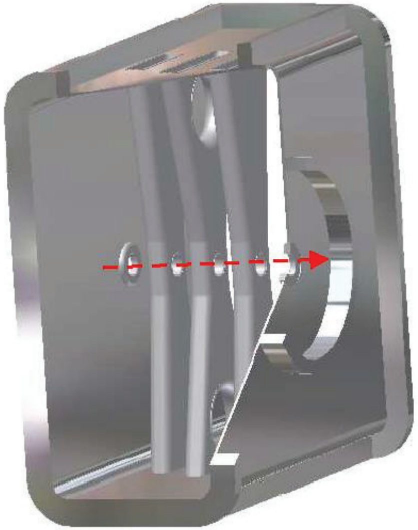

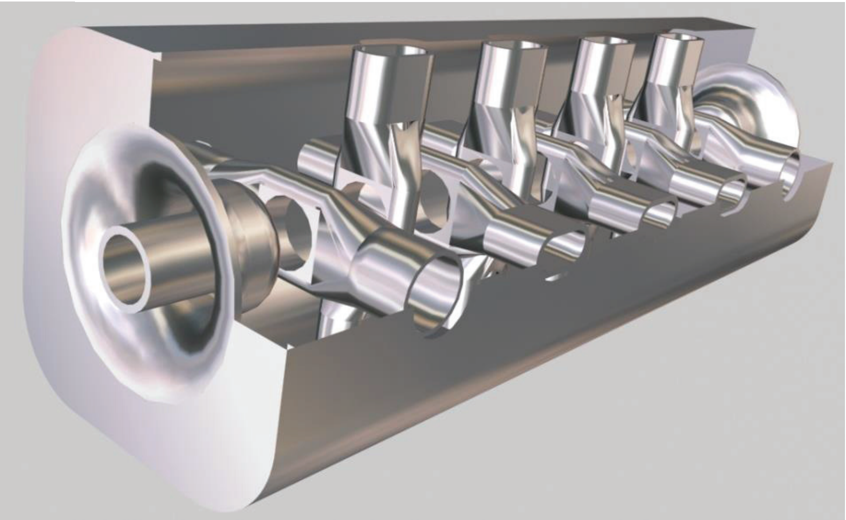

ANL extended to TEM-class SC cavities the very high-performance techniques pioneered by TESLA

Courtesy P. Ostroumov and K. Shepard

New Electromagnetic Structures
High-velocity Spoke Cavities

Double-spoke Cavities
500 MHz, β=1

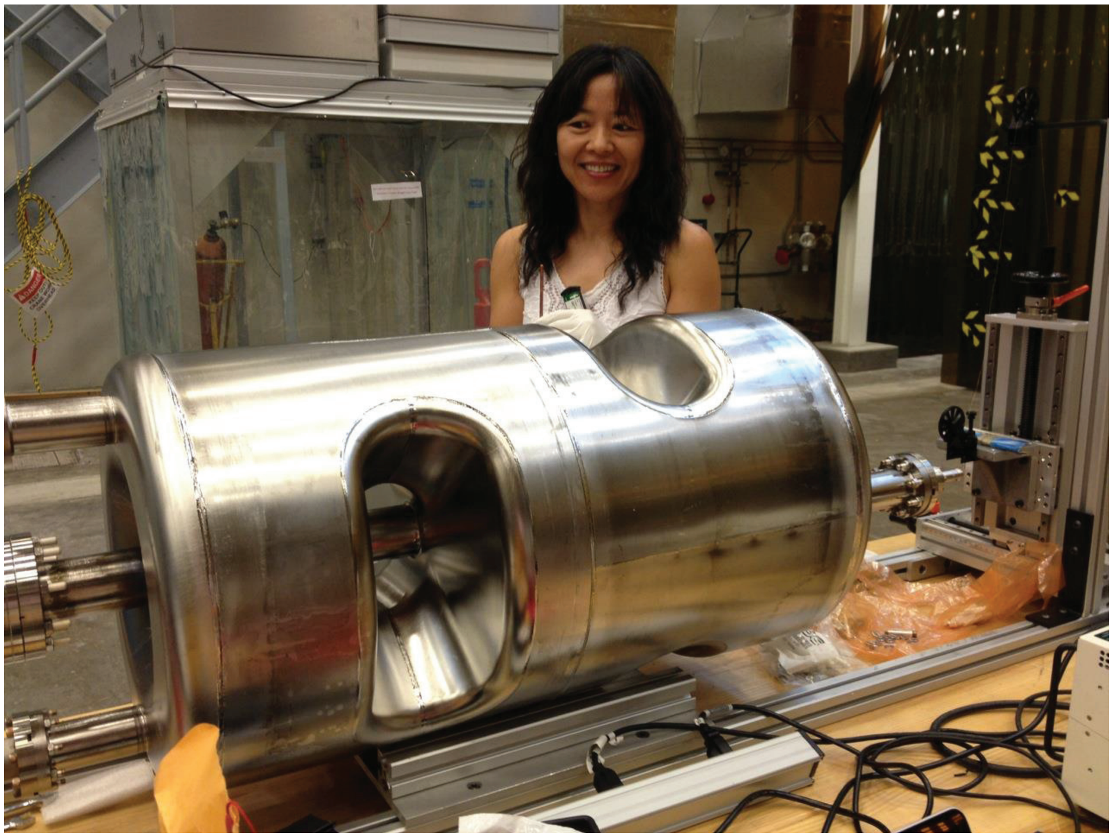

New Electromagnetic Structures
Crabbing and Deflecting Cavities

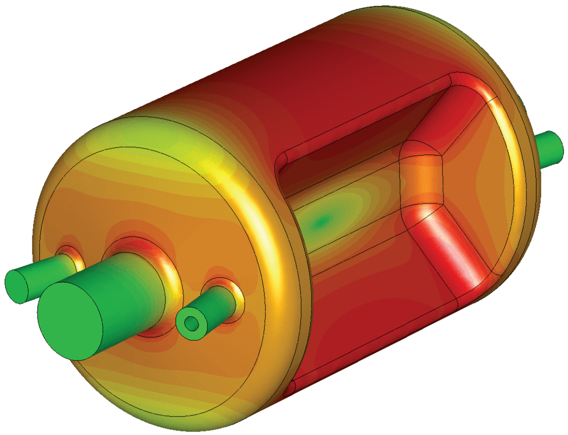

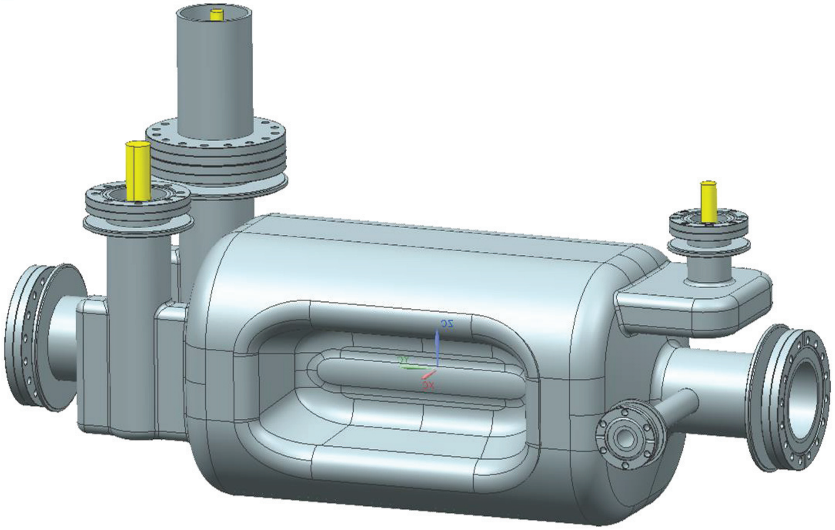

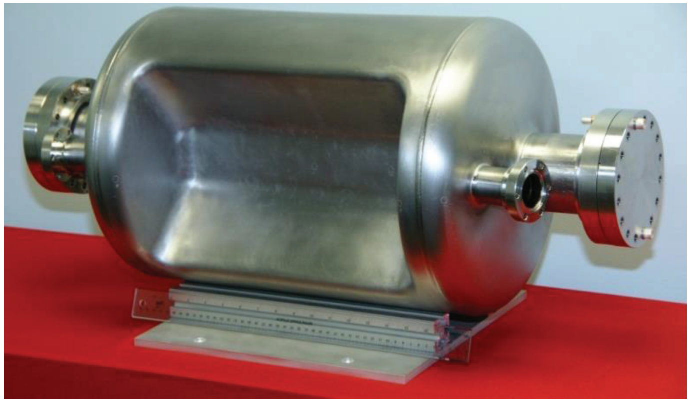

New Electromagnetic Structures
Crabbing and Deflecting Cavities

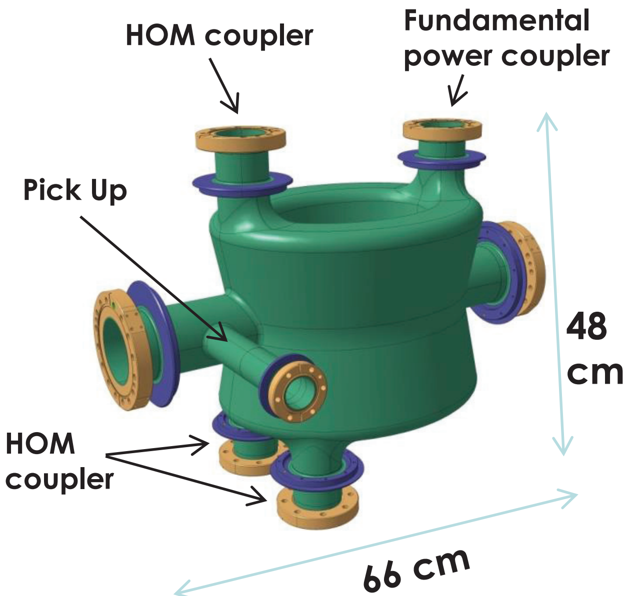

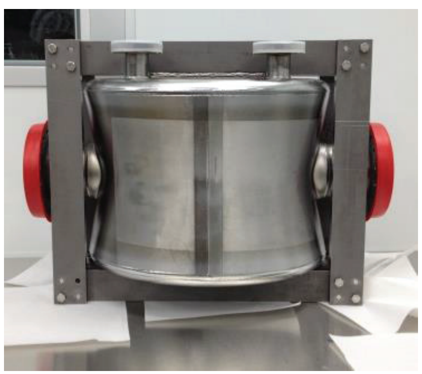

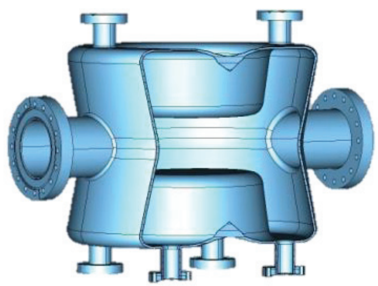

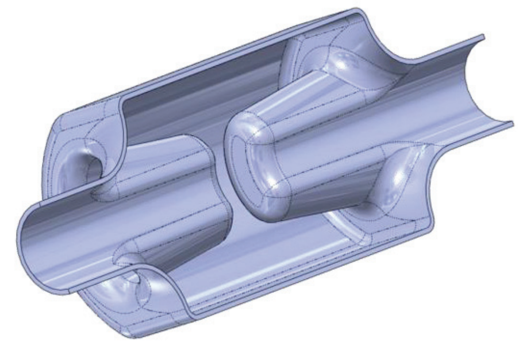

4 Rod

Parting Words

In the last 30+ years, the development of superconducting cavities has been one of the richest and most imaginative area of srf

- The field has been in perpetual evolution and progress
- New geometries are constantly being developed
- The final word has not been said

The parameter, tradeoff, and option space available to the designer is large

- The design process is not, and probably will never be, reduced to a few simple rules or recipes
- There will always be ample opportunities for imagination, originality, and common sense

SRF LIMITATIONS

Jean Delayen

Center for Accelerator Science
Old Dominion University
and
Thomas Jefferson National Accelerator Facility

Outline

- Residual resistance
- Multipacting
- Field emission
- Quench
- High-field Q-slope

The Real World

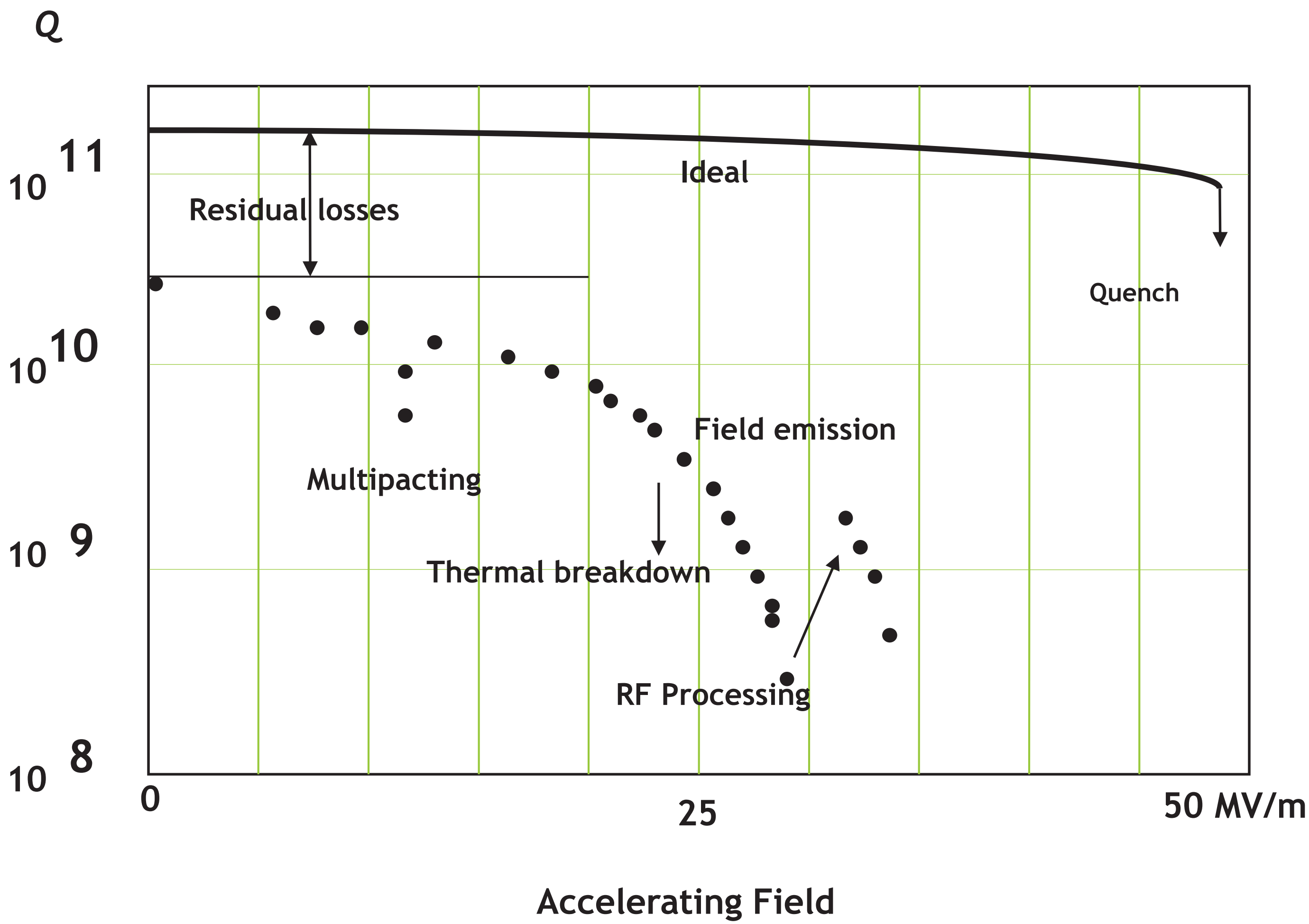

Characteristics of Residual Surface Resistance

- No strong temperature dependence
- No clear frequency dependence
- Not uniformly distributed (can be localized)
- Not reproducible
- Can be as low as 1 nΩ
- Usually between 5 and 30 nΩ
- Often reduced by UHV heat treatment above 800C

Origin of Residual Surface Resistance

- Dielectric surface contaminants (gases, chemical residues, dust, adsorbates)
- Normal conducting defects, inclusions
- Surface imperfections (cracks, scratches, delaminations)
- Trapped magnetic flux
- Hydride precipitation
- Localized electron states in the oxide (photon absorption)

R_{res} is typically 5-10 nΩ at 1-1.5 GHz

Trapped Magnetic Field

A parallel magnetic filed is expelled from a superconductor.

What about a perpendicular magnetic field?

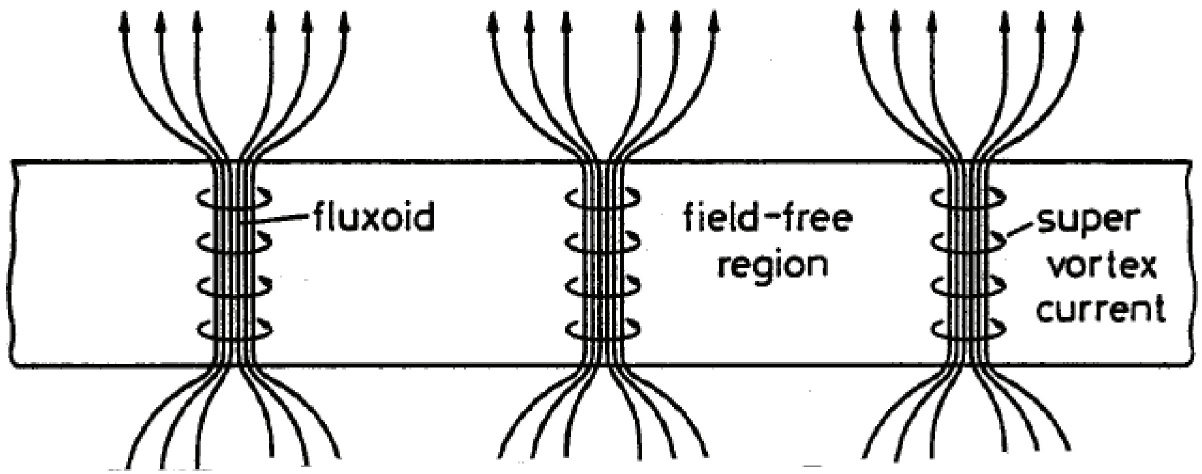

The magnetic field will be concentrated in normal cores where it is equal to the critical field.

Trapped Magnetic Field

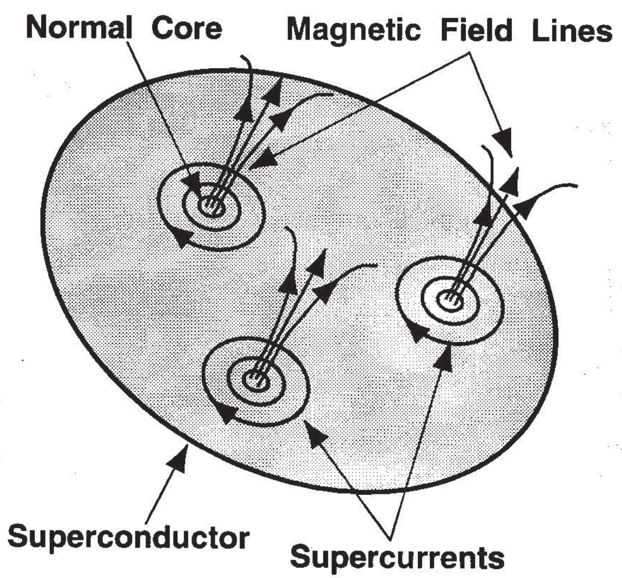

- Vortices are normal to the surface
- 100% flux trapping
- RF dissipation is due to the normal conducting core, of resistance R_n

$$R_{res} \cong R_n \frac{H_i}{H_{c2}}$$

H_i = residual DC magnetic field

• **For Nb:** $R_{res} \approx 0.3$ to 1 nΩ/mG around 1 GHz

Depends on material treatment

• While a cavity goes through the superconducting transition, the ambient magnetic filed cannot be more than a few mG.
• The earth's magnetic shield must be effectively shielded.
• Thermoelectric currents can cause trapped magnetic field, especially in cavities made of composite materials.

R_{res} Due to Hydrides (Q-Disease)

- Cavities that remain at 70-150 K for several hours (or slow cool-down, < 1 K/min) experience a sharp increase of residual resistance
- More severe in cavities which have been heavily chemically etched

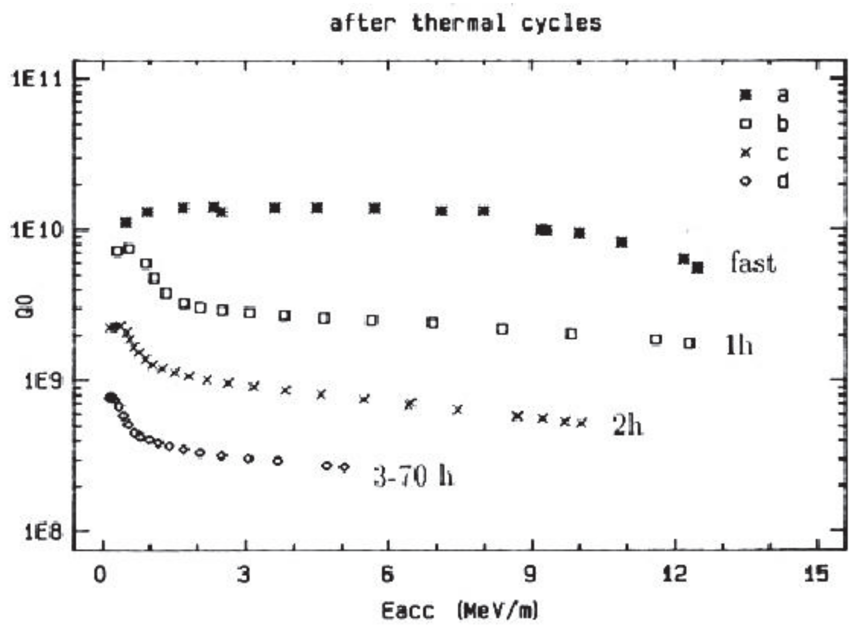

Q Disease

At room temperature, the hydrogen moves freely through niobium

At lower temperature, H precipitates to form a hydride with poor superconducting properties: Tc=2.8 K, Hc=60 G

At room temperature the required concentration to form a hydride is 10^3-10^4 ppm

At 150K it is <10ppm

Can be eliminated by baking cavity at 600-800C

Cures for Q-disease

- Fast cool-down
- Maintain acid temperature below ~ 20 °C during BCP
- “Purge” H_2 with N_2 “blanket” and cover cathode with Teflon cloth during EP
- “Degas” Nb in vacuum furnace at T > 600 °C

Multipacting

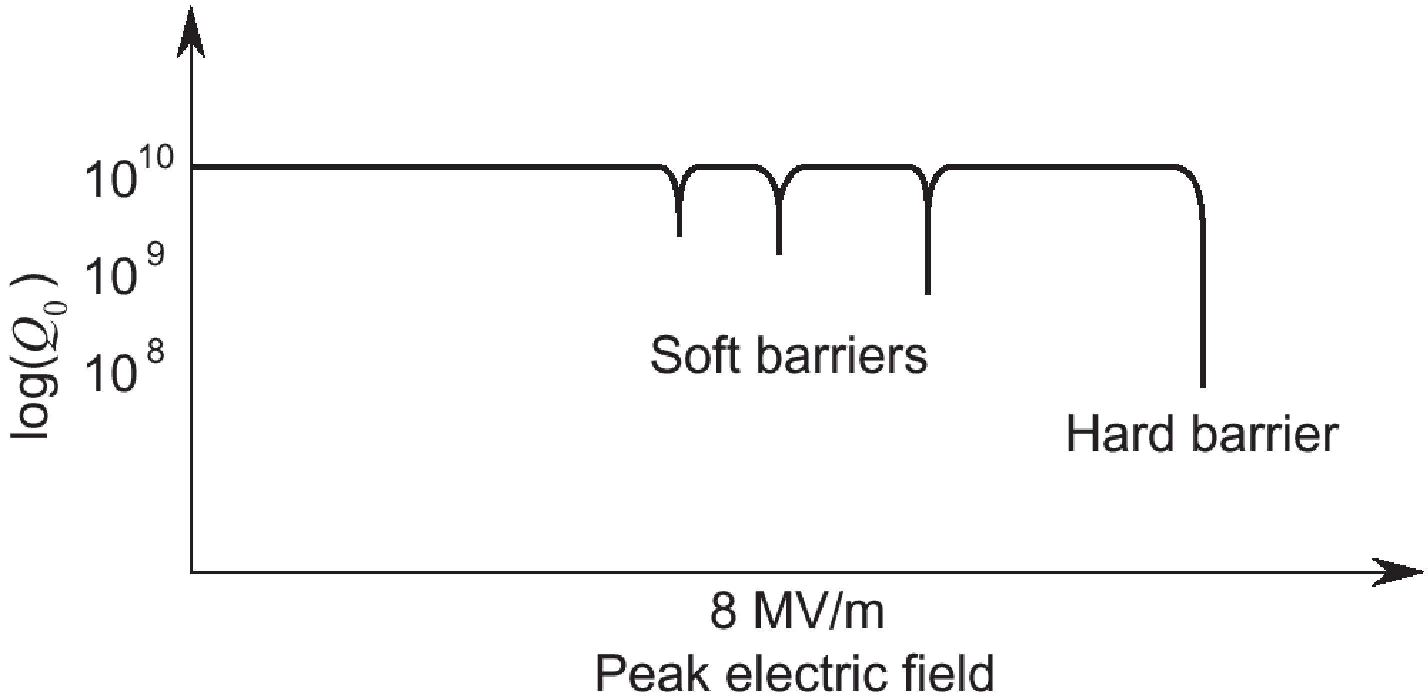

- No increase of P_t for increased P_i during MP
- Can induce quenches and trigger field emission

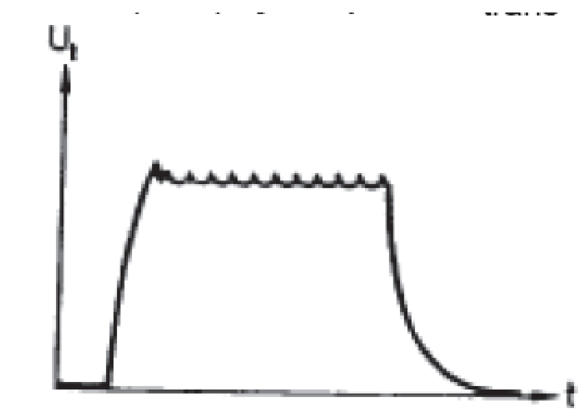

Multipacting

Multipacting is characterized by an exponential growth in the number of electrons in a cavity

Common problems of RF structures (Power couplers, NC cavities…)

Multipacting requires 2 conditions:

- Electron motion is periodic (resonance condition)
- Impact energy is such that secondary emission coefficient is >1

Secondary Emission in Niobium

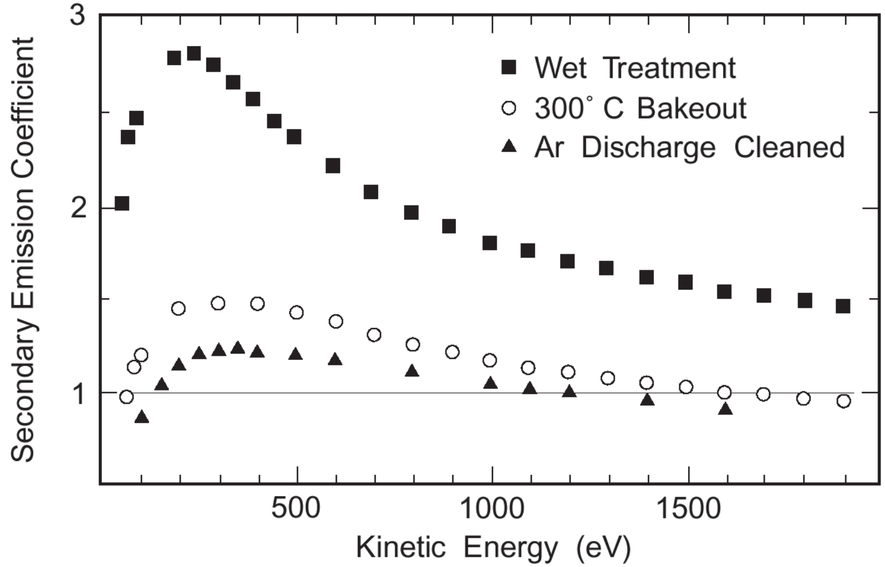

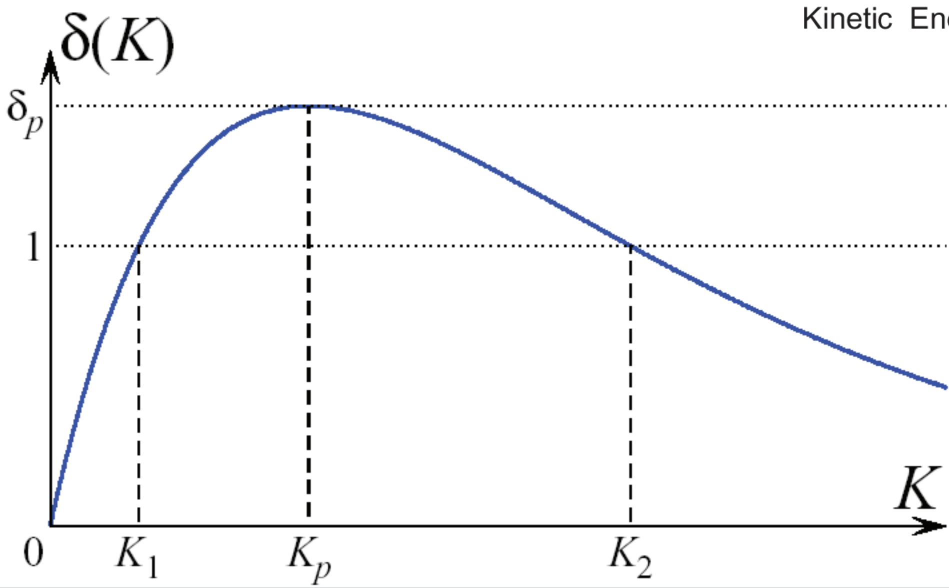

Condition	K_1	K_2
high SEY	$\sim$ 27 eV	$\gtrsim$ 2000 eV
typical SEY	$\sim$ 40 eV	$\sim$ 1000 eV
low SEY	$\sim$ 150 eV	$\sim$ 750 eV

Cures for Multipacting

- Cavity design

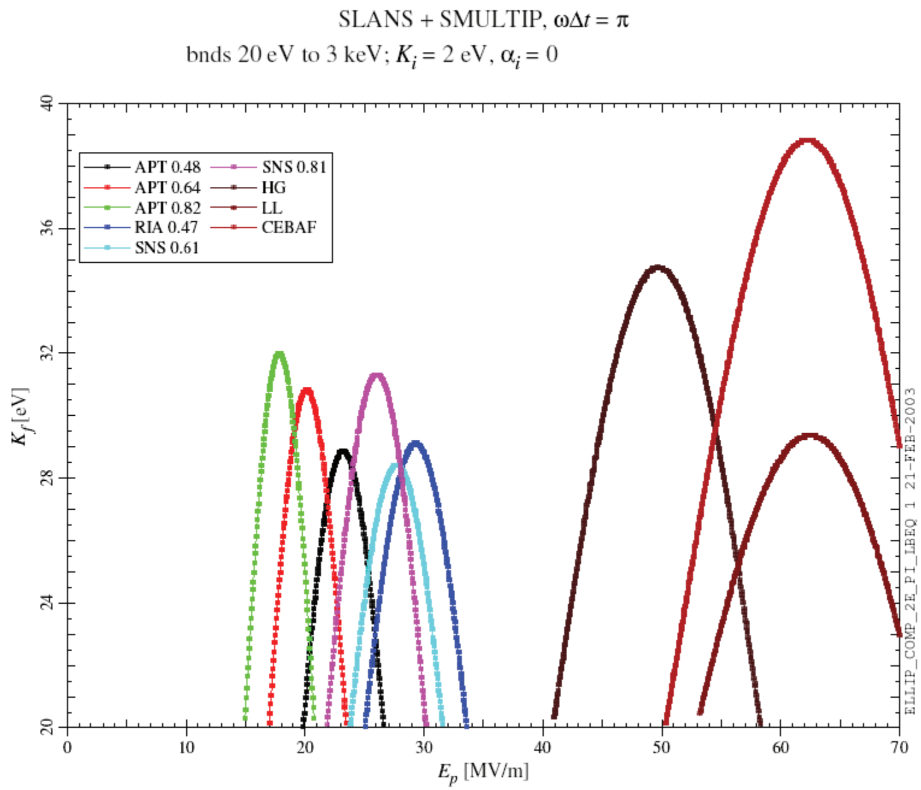

- Lower SEY: clean vacuum systems (low partial pressure of hydrocarbons, hydrogen and water), Ar discharge
- RF Processing: lower SEY by e^- bombardment (minutes to several hours)

Field Emission

- Characterized by an exponential drop of the Q_0
- Associated with production of x-rays and emission of dark current

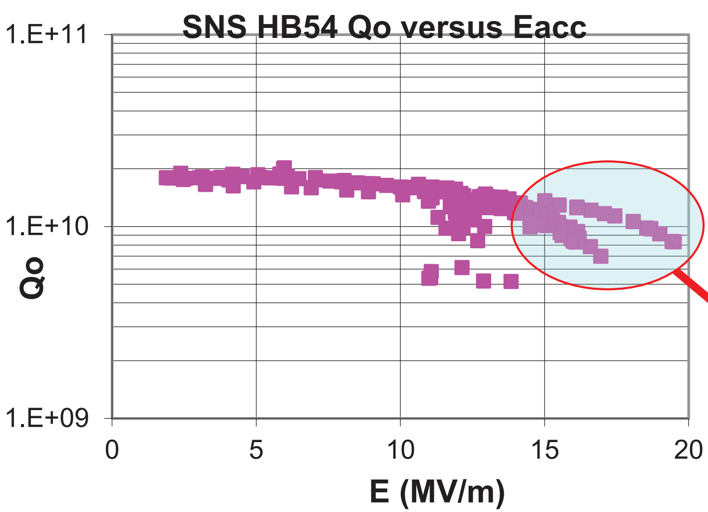

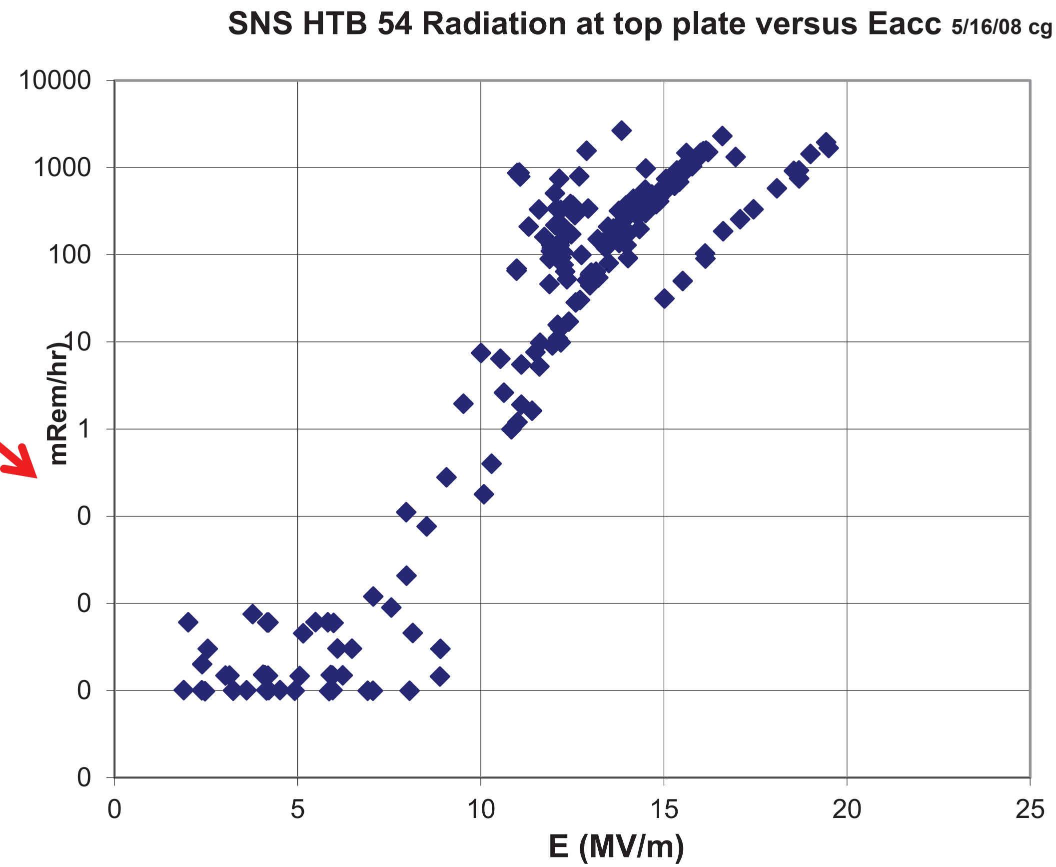

DC Field Emission from Ideal Surface

Fowler-Nordheim model

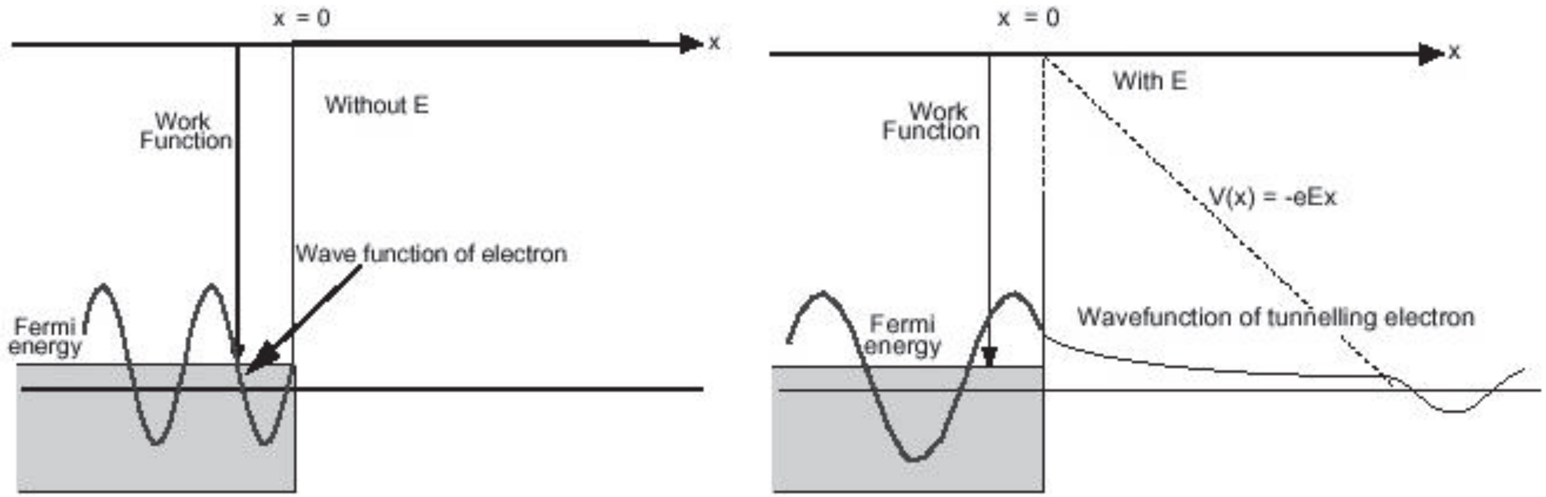

$$J = \frac{1.54\times10^{-6}E^2}{\Phi}\exp\left(-\frac{6.83\times10^{9}\Phi^{3/2}}{E}\right)$$

J : Current density (A/m^2)

E : Electric field (V/m)

Φ : Work function (eV)

Field Emission in rf Cavities

$$J = k \frac{1.54 \times 10^{-6} (\beta E)^{5/2}}{\Phi} \exp\left(-\frac{6.83 \times 10^{9} \Phi^{3/2}}{\beta E} \right)$$

β : Enhancement factor (10s to 100s)

k : Effective emitting surface

Field Emission

Surface electric field is not a fundamental limitation

- Surface fields above 100 MV/m over many cm^2 have been maintained cw in superconducting cavities (>200 MV/m for ms)

However field emission is still an important limitation

The main cause of field emission is particulate contamination

Cures for Field Emission

- **Prevention:**
  – Semiconductor grade acids and solvents
  – High-Pressure Rinsing with ultra-pure water
  – Clean-room assembly
  – Simplified procedures and components for assembly
  – Clean vacuum systems (evacuation and venting without re-contamination)
- **Post-processing:**
  – Helium processing
  – High Peak Power (HPP) processing
  – Plasma cleaning

Thermal Breakdown (Quench)

Localized heating

Hot area increases with field

At a certain field there is a thermal runaway, the field collapses

- sometimes displays a oscillator behavior
- sometimes settles at a lower value
- sometimes displays a hysteretic behavior

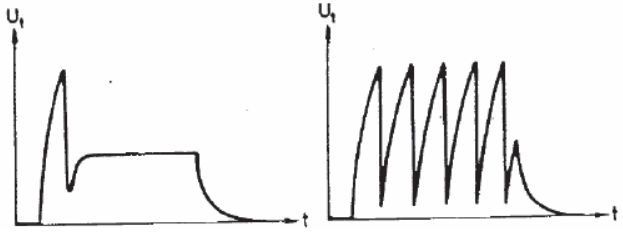

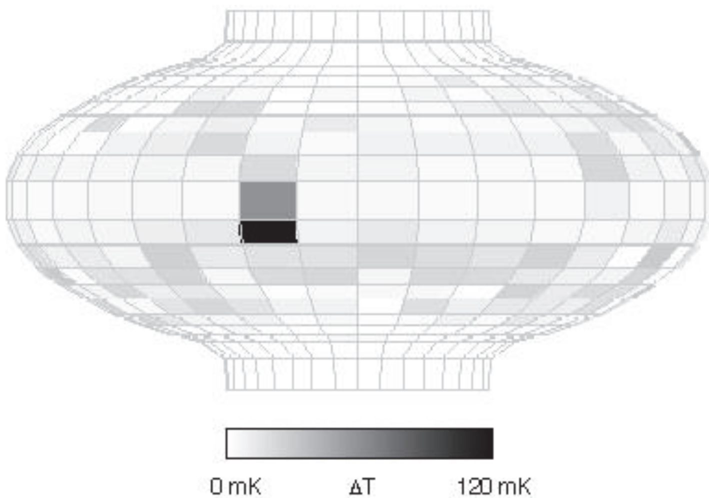

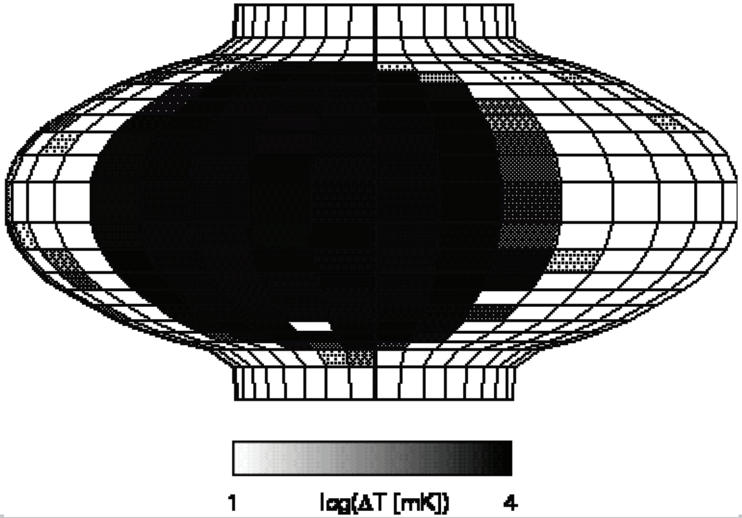

Thermal Breakdown

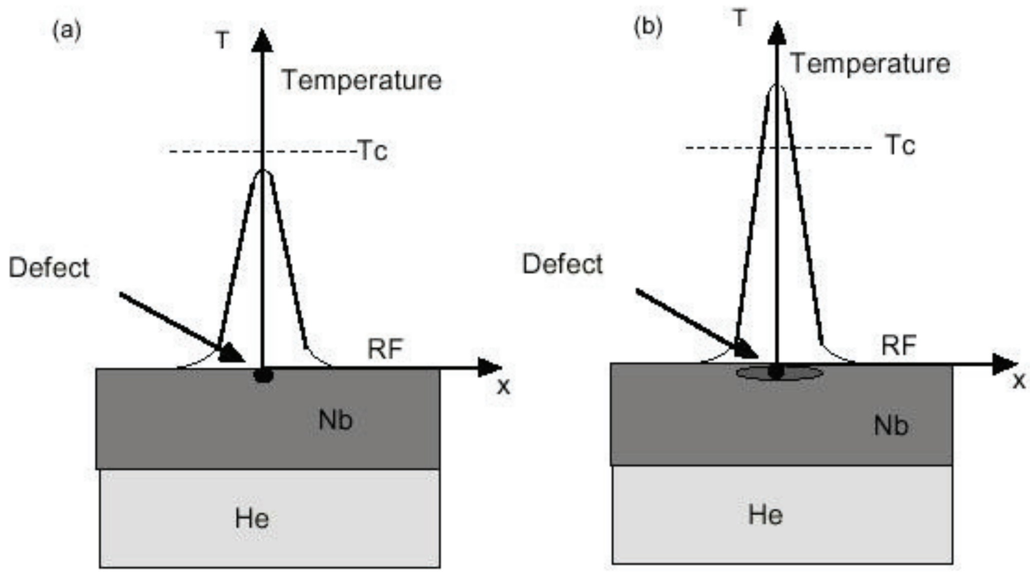

Thermal breakdown occurs when the heat generated at the hot spot is larger than that can be transferred to the helium bath causing T > T_c: "quench" of the superconducting state

Thermal Conductivity of Nb

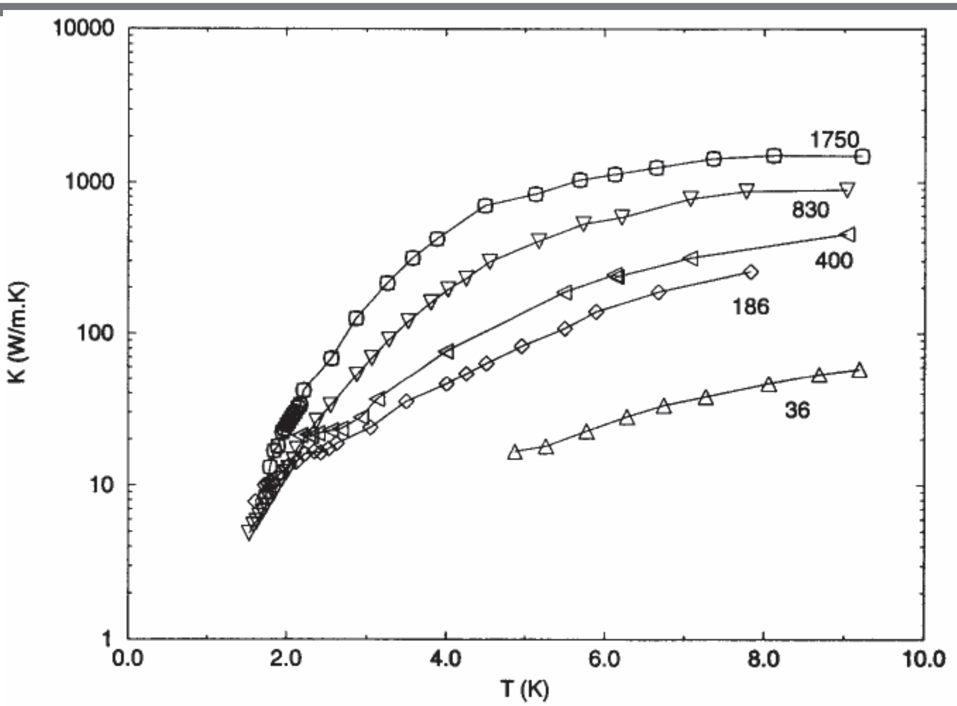

Fig. 3 The thermal conductivity of niobium as a function of temperature, for various RRR values.

RRR is the ratio of the resistivity at 300K and 4.2K

$$RRR = \frac{\rho(300K)}{\rho(4.2K)}$$

RRR is related to the thermal conductivity

For Nb: $\lambda(T = 4.2K) \approx RRR/4$ (W. m^{-1}. K^{-1})

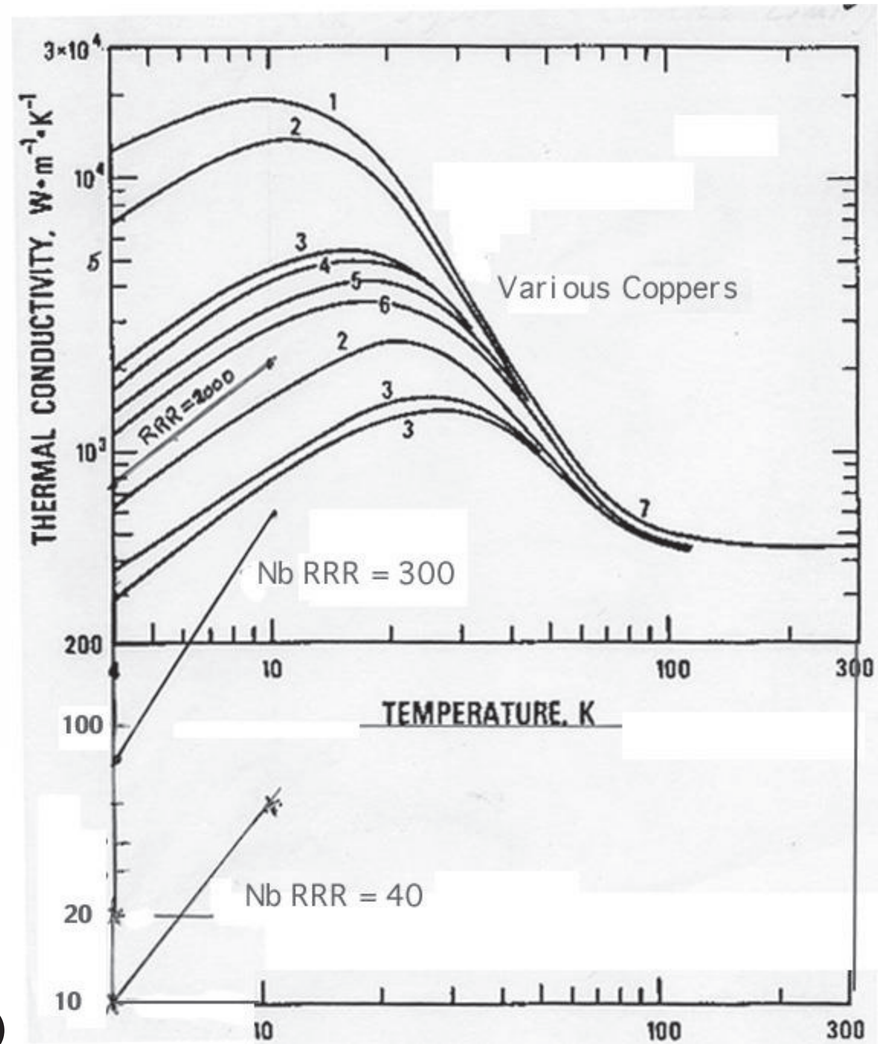

Summary on Quench

- Big improvement in Cavity fabrication and treatment
  less foreign materials found (at limitations <20MV/m only)

- Visual inspection systems are available

- Many irregularities in the cavity surface are found with this systems during and after fabrication and treatment
  pits and bumps, weld irregularities

- Often one defect limits the whole cavity

- Some correlations are found between defects and quench locations at higher fields. But often no correlation between suspicious pits and bumps and quench location

- At gradient limitations in the range >30 MV/m defects are often not identified

High-Field Q-Slope ("Q-drop")

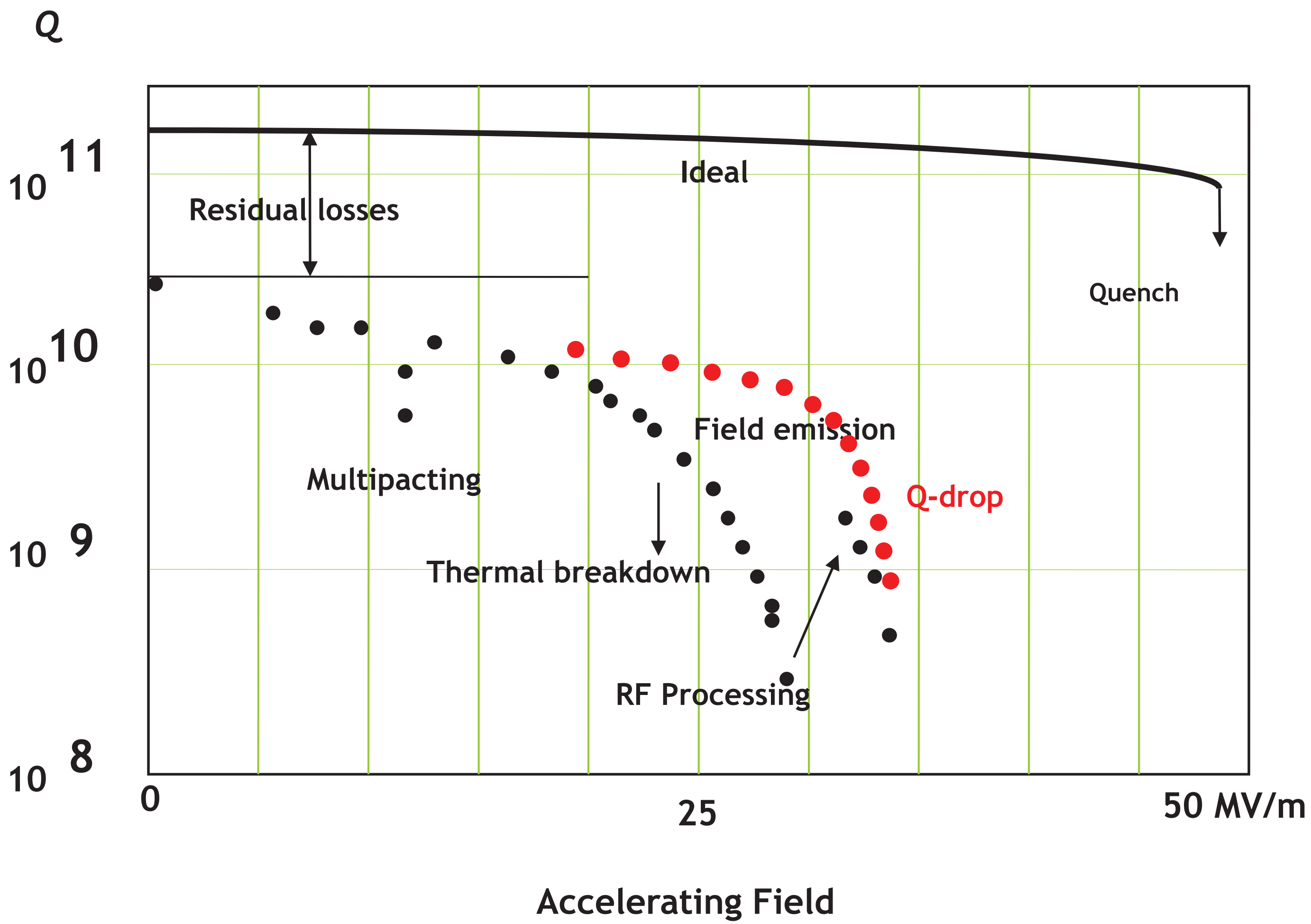

High Field Q-Drop

- Decrease of Q at high field not associated with x-rays
- Still an area of investigation
- Many models
  - Magnetic field related
  - Electric field related
- Strong indication that it is related to the concentration of oxygen at the surface
- Reduced or eliminated by mild baking around 120C

BCP leaves natural oxide + oxygen rich layer

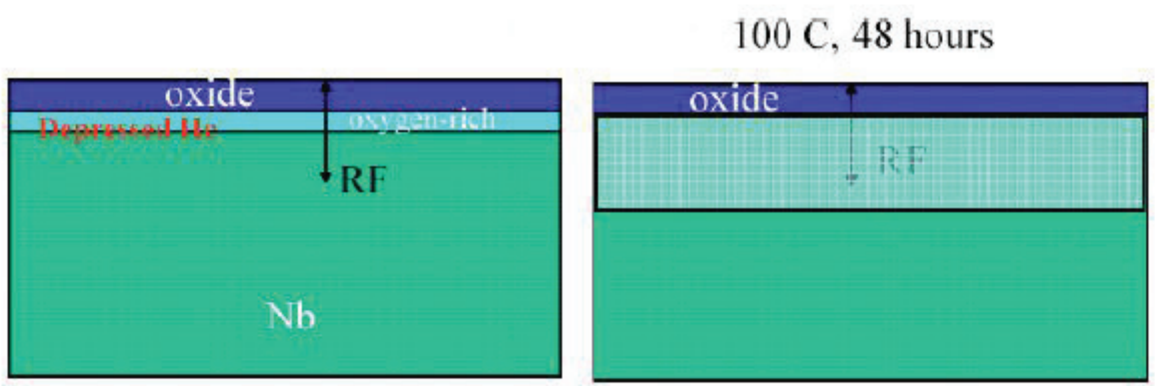

Baking dilutes oxygen rich layer

Q-drop and Baking

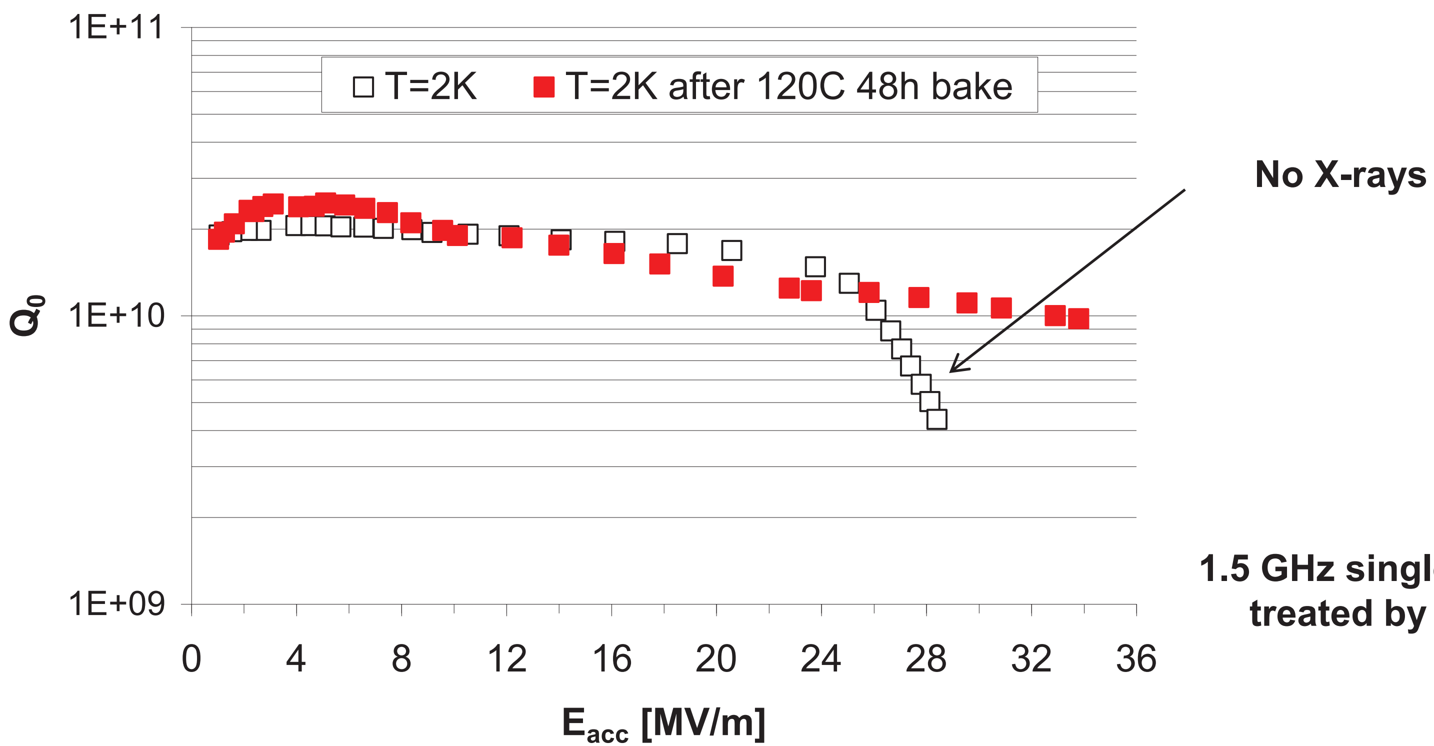

1.5 GHz single-cell, treated by EP

- The origin of the Q-drop is still unclear. Occurs for all Nb material/treatment combinations
  - The Q-drop recovers after UHV bake at 120 °C/48h for certain material/treatment combinations

Models of Q-drop & Baking

- Magnetic field enhancement
- Oxide losses
- Oxygen pollution
- Magnetic vortices

Fluxons as Source of Hot-Spots

- Motion of magnetic vortices, pinned in Nb during cool-down across $T_{c,}$ cause localized heating

- Periodic motion of vortices pushed in & out of the Nb surface by strong RF field also cause localized heating

The small, local heating due to vortex motion is amplified by R_{BCS}, causing cm-size hot-spots

Recent Developments: Impurity Doping

P. Dhakal et al, Phys Rev. ST-AB 16, 042001 (2013)

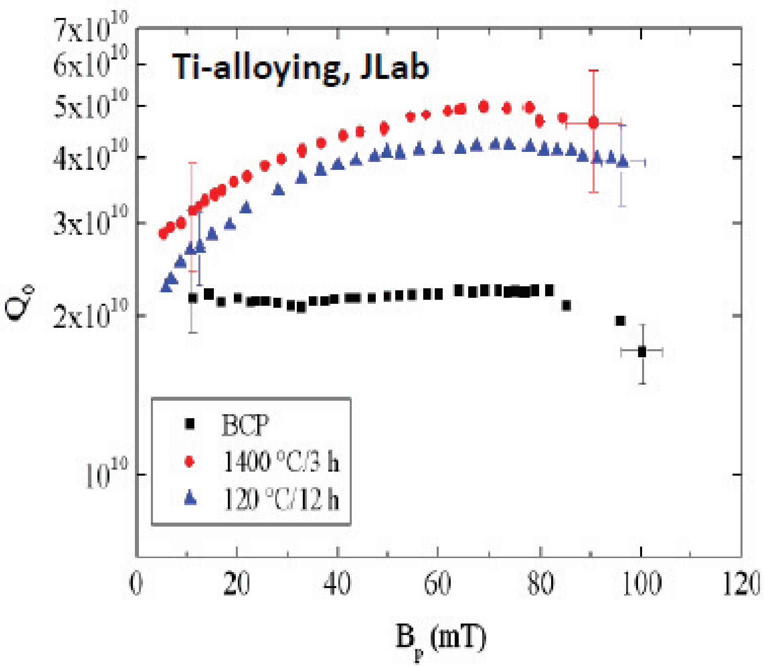

A. Grasselino et al, SUST 26, 102001 (2013)

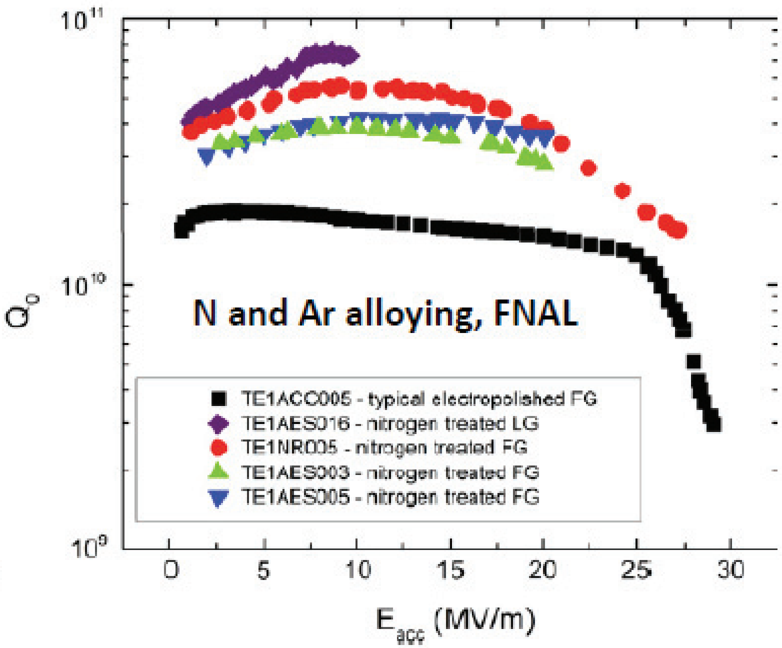

- Dirty layer due to diffusion of N or Ti into a few μm thick layer (>> λ = 40 nm) at the surface
- Decrease of $R_s(B)$ up to **$B \approx 0.5B_c$: microwave suppression of surface resistance**

Recent Developments: Nb_3Sn

Later Coatings

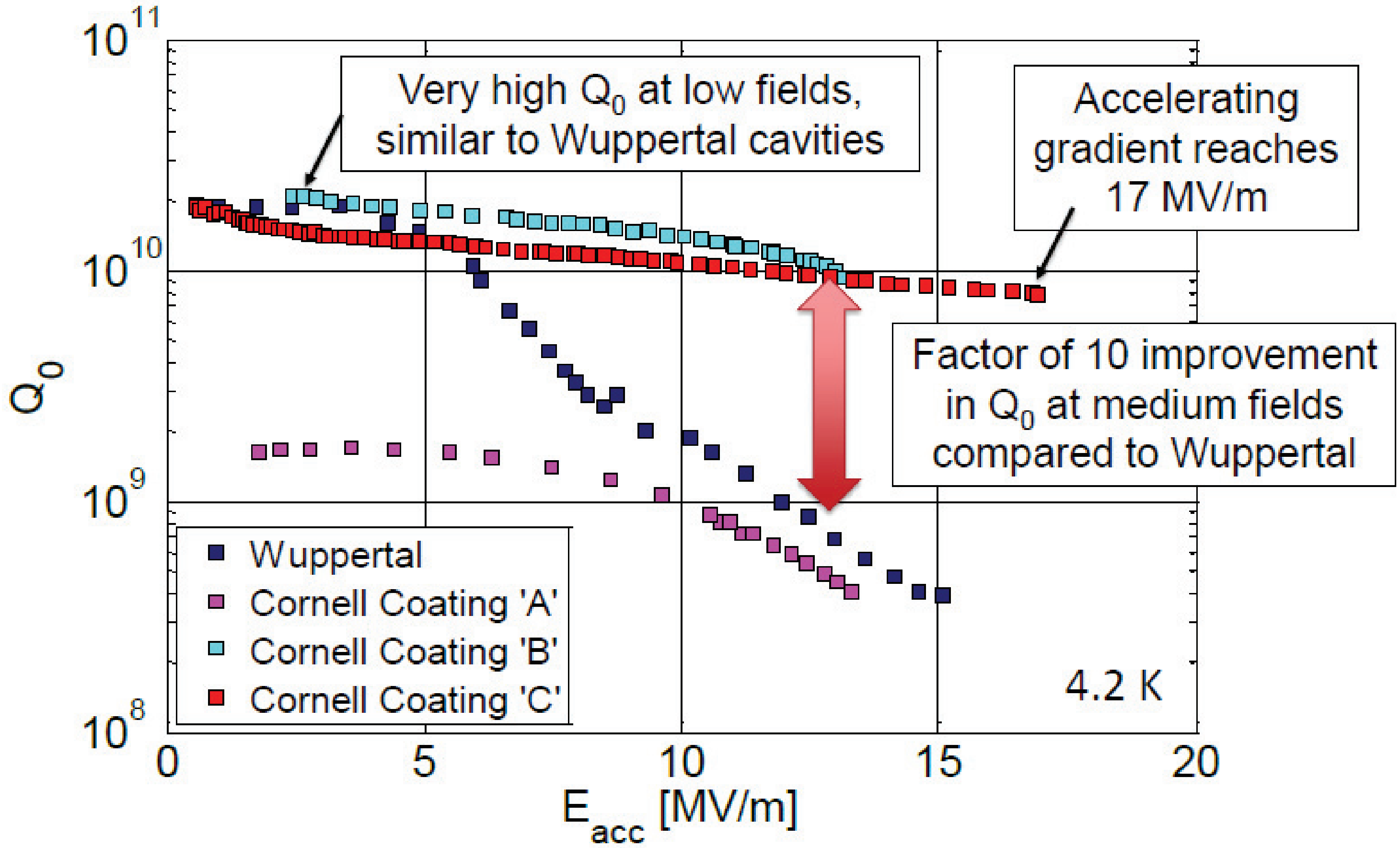

Fermilab

Parting words

SRF in now 50 years old

Much progress has been made

Many accelerators are operating successfully

But…our full understanding of the rf properties of superconductors and the fundamental limitations of srf cavities is still incomplete and new techniques are still being developed

Still many opportunities to make a difference